5-2015

IMPACT OF DIFFERENTIATION STATUS OF KIDNEY PROGENITORS IN WILMS TUMOR DEVELOPMENT

Le Huang

IMPACT OF DIFFERENTIATION STATUS OF KIDNEY PROGENITORS IN WILMS TUMOR DEVELOPMENT

by

Le Huang, M.S.

APPROVED:

_____
Vicki Huff, Ph.D. Advisory Professor

_____
Richard Behringer, Ph.D.

_____
M. John Hicks, M.D., D.D.S., Ph.D.

_____
Hui-Kuan Lin, Ph.D.

_____
Stephanie S. Watowich, Ph.D.

APPROVED:

_____
Dean, The University of Texas
Graduate School of Biomedical Sciences at Houston

IMPACT OF DIFFERENTIATION STATUS OF KIDNEY PROGENITORS IN WILMS TUMOR DEVELOPMENT

A

DISSERTATION

Presented to the Faculty of
The University of Texas
Health Science Center at Houston
and
The University of Texas
MD Anderson Cancer Center
Graduate School of Biomedical Sciences
in Partial Fulfillment

of the Requirements

for the Degree of

DOCTOR OF PHILOSOPHY

by

Le Huang, M.S.
Houston, Texas

May, 2015

DEDICATION

This thesis is dedicated to my mother, Xizhen Jiang, and my father, Yongming Huang, for their unconditional love and support.

ACKNOWLEDGMENTS

I would like to thank my supervisor, Dr. Vicki Huff, who has been tremendously supportive and encouraging throughout my graduate education. She provided me with all the education and research resources and allowed me to work on the project independently. She has always been teaching me to think critically about science and also to consider the big picture of the field. I have been fortunate to have her as a mentor with her knowledge and expertise, her passion, and her kindness.

I greatly appreciate all the committee members for their expertise, insightful advice, and dedicated service the past several years, Dr. Richard Behringer, Dr. M. John Hicks, Dr. Hui-kuan Lin, Dr. Pierre McCrea, Dr. Michelle Barton and Dr. Stephanie Watowich.

I also would like to thank current and former labmates for being very helpful and friendly, Dr. Sharada Mokkapati, Dr. Qianghua Hu, Dr. Cristy Ruteshouser, Dr.Paramahamsa Maturu, Blake Palculict. I owe a special thanks to Dr. Sharada Mokkapati, who contributed significantly to this work. Moreover, I deeply appreciate her mentorship, support, help, encouragement and friendship. Also, this work would have not been possible without Dr. Qianghua Hu's work, which built a solid foundation for this thesis work.

I am truly thankful to Genes and Development Program for providing opportunities for professional development and for being such an amazing community. Special thanks to the program coordinator Elisabeth Lindheim, the G&D program directors, and the GSBS administrative team for their strong support.

Finally, I am very grateful for my parents, Xizhen Jiang and Yongming Huang, and my many friends for their constant support and encouragement, and the wonderful times together.

This work was supported by CPRIT research training award (RP101502) and Julia Jones Matthews Cancer Research Scholarship.

IMPACT OF DIFFERENTIATION STATUS OF KIDNEY PROGENITORS IN WILMS TUMOR DEVELOPMENT

Le Huang, M.S.

Advisory Professor: Vicki Huff, Ph.D.

Wilms tumor is one of the most common solid tumors in children. It is an embryonic cancer of the kidney and is thought to arise from undifferentiated renal mesenchyme. However, the differentiation status of cells in the mesenchyme that can give rise to Wilms tumors is unknown. Gene expression analysis of a large panel of Wilms tumor patients has identified different subsets of Wilms tumors that are distinct in their clinical outcomes and gene expression signatures. These subsets express specific genes that correspond to different stages of differentiation during renal development, suggesting that Wilms tumors may arise from transformed cells at different states of differentiation. Wilms tumors are genetically heterogeneous, which can also affect the tumor biology and pathology. To test whether cells at different states of differentiation were tumorigenic, we used progenitor cell-type-specific Cre to introduce mutations of Wilms Tumor gene 1 (*Wt1*) or *β-catenin* into fetal kidney cells in a progenitor-specific manner. We found that the nephron progenitors but not the stroma progenitors were able to give rise to Wilms tumors and that the different types of mutations introduced into nephron progenitor cells resulted in Wilms tumors with differing histology and expression of developmentally regulated genes. Also, to investigate the mechanisms by which *WT1* mutations cause a predisposition to Wilms tumors, we studied the *in vivo* effects of *Wt1* ablation in different renal progenitor cells. We found that *Wt1* ablation in stroma progenitors did not affect nephrogenesis but that *Wt1* is required for nephron progenitors to undergo mesenchyme to epithelia transition.

Table of Contents

List of Illustrations

List of Tables

Abbreviations

APC – adenomatous polyposis coli protein

BMP – bone morphogenetic protein

BW – body weight

Cited1 – Cbp/p300-interacting transactivator with Glu/Asp-rich C-terminal domain 1

Cited1^{Cre} – Cited1-EGFP-Cre

CK1 – casein kinase 1

CM – cap mesenchyme

DAB – 3, 3'-diaminobenzidine

DMEM – Dulbecco's modified Eagle's medium

ERK – extracellular signal-regulated kinase

FACS – fluorescence-activated cell sorting

FBS – fetal bovine serum

Foxd1^{GCE} – Foxd1-EGFP-Cre

F-Wt1 – Foxd1$^{GCE/+}$; Wt$^{-/fl}$

GSK3 – glycogen synthase kinase 3

H&E – hematoxylin and eosin

IF – immunofluorescence

IHC – immunohistochemistry

IP – intrapertoneal injection

LRP5/6 – LDL receptor-related proteins 5 and 6

MAPK – mitogen-activated protein kinase

MET – mesenchyme to epithelial transition

MM – metanephric mesenchyme

NFAT – nuclear factor of activated T-cells

NZ – nephrogenic zone

PAS – periodic acid schiff stain

PBS – phosphate buffered saline PCP – planar cell polarity

qRT-PCR – quantitative real-time PCR

RPPA – reverse-phase protein array

RT-PCR – real-time PCR

RV – renal vesicle

SDS – sodium dodecyl sulfate

Six2^{GCE}– Six2-EGFP-Cre

S-Wt1 – Six2$^{GCE/+}$; Wt$^{-/fl}$

TCF/LEF – T-cell factor/lymphoid enhancer factor

TGFβ – transforming growth factor beta

TM – tamoxifen

WT – Wilms tumor

WT1 – Wilms Tumor Gene 1

WTX – Wilms Tumor gene on the X chromosome

Wt1-β-cat^{S} – Wt1$^{-/fl}$; β-catenin$^{e3fl/e3fl}$ or Wt1$^{+/fl}$; β-catenin$^{e3fl/e3fl}$

Wt1-Igf2 – Wt1$^{-/fl}$; H19$^{+/-m}$

Chapter 1: Introduction

1.1 Wilms tumors (WT)

Wilms tumor, also named nephroblastoma, is one of the most common solid tumors in children. It is a pediatric cancer of kidney and affects 1 in every 10,000 live births in North America (Beckwith, 1983). It was first recognized by the German surgeon Max Wilms in 1899 in a 3-year-old patient. The average age of tumor onset for Wilms tumor is 38 months old in the U.S., and the typical symptoms are growth of an abdominal mass and pain (Breslow et al., 1993). The tumors are often in one kidney, with less than 5% occurring in both kidneys (Breslow et al., 1993). Wilms tumors rarely metastasize but if they do, they metastasize mainly to the lungs, lymph nodes, bones and brain (NLM, 2015). Wilms tumor patients are usually treated with a combination of surgery and chemotherapy, and if the tumor is at an advanced stage, radiation therapy is also applied. The 5-year survival rate is approximately 90% (Smith et al., 2014). Despite the fact that 90% Wilms tumors are curable, those who survive their tumors suffer from side effects of chemotherapy and radiation therapy. Understanding the etiology of Wilms tumor will help in the development of improved treatment with fewer side effects.

Wilms tumors are usually encapsulated within a fibrotic pseudocapsule, separated from the adjacent normal kidney. The precursor lesions of WT are known as nephrogenic rests (Beckwith, 1998). Nephrogenic rests are nodules of blastemal cells, which are mesenchymal cells arrested at an early stage of differentiation during kidney development (Beckwith, 1998). Genetic studies of Wilms tumors have shown that the nephrogenic rests and Wilms tumors share the same mutations, however, additional mutations are found in Wilms tumors, suggesting a sequential progression from the nephrogenic rest to Wilms tumor (Fukuzawa et al., 2007). When second genetic mutations or oncogenic events occur within the

nephrogenic rests, the lesional cells may be transformed and clonal expansion of such cells can progress to the development of Wilms tumors.

The typical histology of Wilms tumor is triphasic, consisting of undifferentiated blastemal elements as well as differentiating epithelial and stromal elements (Beckwith and Palmer, 1978). Wilms tumors are heterogeneous, with varying degrees of each element. Abnormally differentiated elements such as myogenic, chondrogenic, osteogenic or adipogenic cells can also be found in some of the Wilms tumors. Histologically, Wilms tumors recapitulate the development of embryonic kidney (Fig. 1.1). The blastemal elements in the tumor appear like the undifferentiated metanephric mesenchyme of the developing kidney, whereas the epithelial elements resemble the differentiating epithelial structures after mesenchyme to epithelial transition, including comma-shaped body, S-shaped body, tubules and glomeruli (Beckwith, 1983). Although different histologic components are present in Wilms tumors, studies have shown that these components shared the same genetic changes, suggesting that Wilms tumor is a clonal expansion of the transformed undifferentiated mesenchymal cell that can potentially differentiate to epithelial, stromal or ectopic elements (Zhuang et al., 1997) (Guertl et al., 2006).

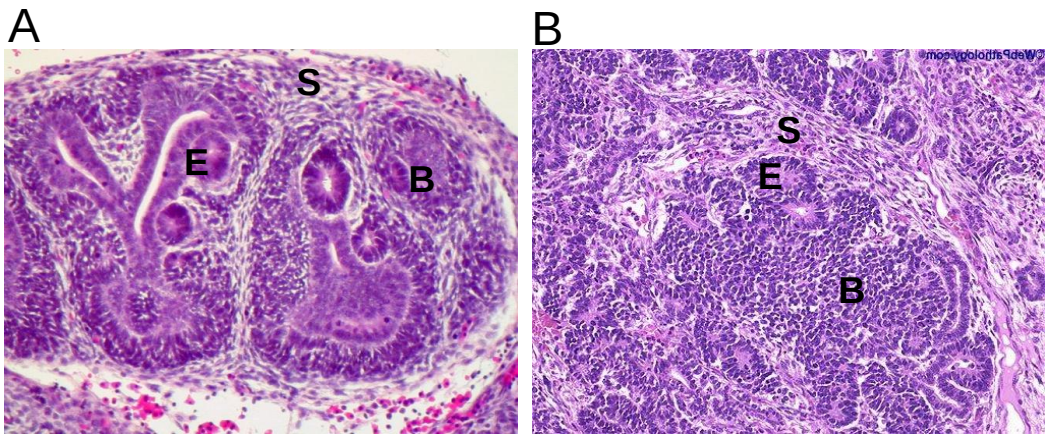

Figure 1.1 Wilms tumor histologically recapitulates fetal kidney

(A) Human fetal kidney. (B) Human Wilms tumor. B, S, and E designate blastemal, epithelial and stromal components, respectively.

Images are from website http://www.humpath.com/spip.php?article5075

1.2 Kidney development

To understand Wilms tumorigenesis, it is important to understand the process of kidney development (Fig. 1.2). Kidney development starts with the formation of the Wolffian duct and the nephrogenic cord from the intermediate mesenchyme (Davidson, 2008). The nephrogenic cord generates the pronephros, mesonephros and metanephros, with the first two degenerating during mammalian embryonic development. The Wolffian duct extends the ureteric buds to invade the metanephric mesenchyme, and at the same time, the metanephric mesenchyme signals to the ureteric buds and induces them to branch iteratively. In response, the ureteric buds stimulate the metanephric mesenchyme to differentiate. The metanephric mesenchyme first condenses around the tips of the ureteric buds to form the cap mesenchyme (CM). Then the CM undergoes mesenchyme to epithelial transition (MET) and forms the renal vesicles (RV) proximal to the ureteric buds. The resulting renal vesicles further epithelialize and connect to the ureteric buds to form the comma-shaped bodies and the S-shaped bodies. The S-shaped bodies are segmented and differentiate, together with the ureteric buds, to form the fully mature nephrons, the functional units of the kidney, which include the proximal tubules, distal tubules, loops of Henle and glomeruli (Davidson, 2008).

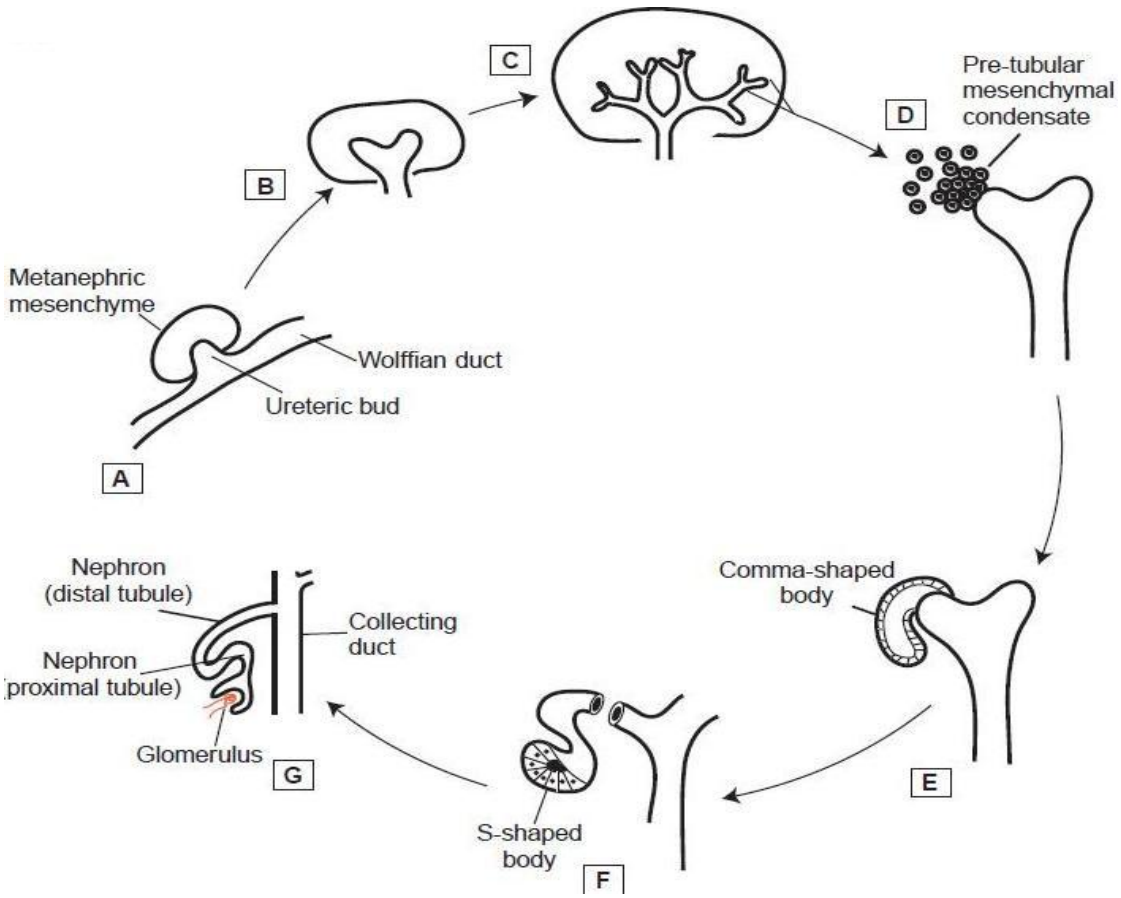

Figure 1.2 Diagram of kidney development

(A) Metanephric kidney development starts with ureteric bud (UB) invasion into metanephric mesenchyme. (B & C) UB branches repeatedly and elongates the stalk. (D) Metanephric mesenchyme condenses around the UB tip. (E & F) The mesenchyme undergoes mesenchyme to epithelial transition and differentiates to form renal vesicle, comma-shaped body and S-shaped body. (G) The S-shaped body connects to the UB and further differentiates and segments to form the nephron.

Image is from Review: Shah, M.M., Sampogna, R.V., Sakurai, H., Bush, K.T., and Nigam, S.K. (2004). Branching morphogenesis and kidney disease. Development *131*, 1449-1462.

1.3 Kidney progenitor compartments

During kidney development, there are two major types of progenitors in the undifferentiated metanephric mesenchyme: the stromal progenitor and the nephron progenitor (Fig. 1.3 A) (Mugford et al., 2009) (Self et al., 2006) (Kobayashi et al., 2014). The specification of the stromal progenitor and the nephron progenitor starts from the common Osr1-expressing precursor cells in intermediate mesenchyme and metanephric mesenchyme (MM) (Mugford et al., 2008b).

The stromal progenitors are at the periphery of the metanephric mesenchyme and surround the nephron progenitors. They specifically express FOXD1 and give rise to the interstitium, pericytes, mesangial cells, and smooth muscle cells in the kidney (Humphreys et al., 2010; Kobayashi et al., 2014).

The nephron progenitors reside in the cap mesenchyme (CM) that surrounds the tips of the ureteric buds (Fig. 1.3) (Self et al., 2006). One proposal is that the CM contains heterogeneous cell populations due to the different expression pattern of transcription factors and its spatial location surrounded by different growth factors, ligands and cell types (Hendry et al., 2011). As defined by gene expression pattern, the CM contains two subpopulations, the uninduced and the induced CM (Mugford et al., 2009). Cells within the uninduced CM express both markers CITED1 and SIX2. The $CITED1^{+}$ $SIX2^{+}$ cells have been shown to be the self-renewing population, and they resist the differentiation-inducing signals from ureteric buds (Brown et al., 2013). However, the induced CM expresses SIX2 but not CITED1 ($CITED1^{-}$ $SIX2^{+}$) and starts to differentiate and undergo MET to form RVs (Brown et al., 2013; Mugford et al., 2009). The nephron progenitors ($SIX2^{+}$ or $CITED1^{+}$) give rise to the majority of the cells in the nephrons, including epithelial cells in the glomeruli, proximal tubules, distal tubules and loop of Henle (Kobayashi et al., 2008). In situ hybridization of whole mount embryonic kidneys with transcription factors identified differences in the gene expression patterns between the uninduced CM and the induced CM

(Mugford et al., 2009). The uninduced CITED1^{+} SIX2^{+} cells express genes *Meox1* and *Dpf3*, while the induced CITED1^{-} SIX2^{+} cells express genes *Wnt4*, *Fgf8*, *Pax8*, *Lhx1* and *Pea3*, suggesting different transcription programs between the uninduced and induced CM cells (Mugford et al., 2009).

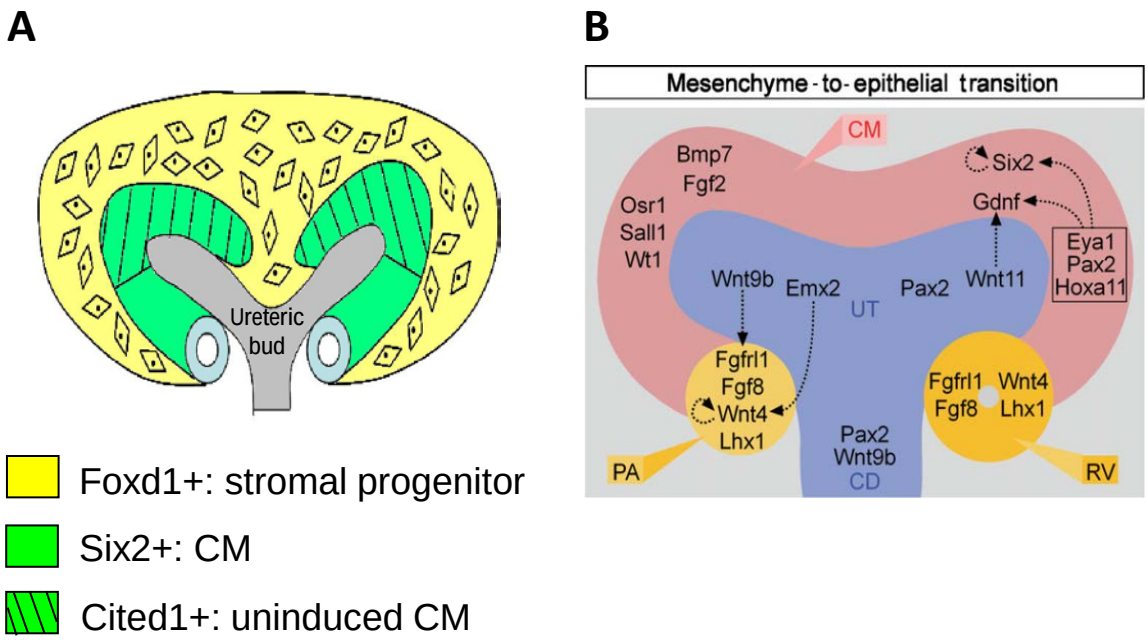

Figure 1.3 Diagram of kidney progenitor compartments in mesenchyme and interactions of proteins between CM, UB and stromal.

(A) The Foxd1+ stromal progenitors are located outside the CM and produce interstitium, pericyte and mesangial cells etc. The uninduced CM expresses both Cited1 and Six2, while the induced CM is Cited1- Six2+. The nephron progenitors in the CM give rise to the majority of the cells in the nephron.

(B) Diagram of the key genes in each compartment in the nephrogenic zone and the interactions between the compartments of CM, UB and stromal mesenchyme.

Image B is from Review: Little, M., Georgas, K., Pennisi, D., and Wilkinson, L. (2010). Kidney development: two tales of tubulogenesis. Current topics in developmental biology *90*, 193-229. Figure used with permission.

1.4 Functions of progenitor markers FOXD1, SIX2 and CITED1 in renal progenitors

Expression of FOXD1, SIX2 and CITED1 demarcates stromal or nephron progenitors, respectively. It is important to understand the roles of each marker in renal progenitors during kidney development.

Foxd1, a transcription factor, is expressed in the cortical stromal mesenchyme (Hatini et al., 1996). FOXD1 expressing cells have been shown to be the multipotent self-renewing stromal progenitors in mouse kidneys (Kobayashi et al., 2014). *Foxd1* knockout mice died immediately after birth with a phenotype of renal agenesis, demonstrating an essential role of the $FOXD1^+$ stromal mesenchyme in nephrogenesis (Hatini et al., 1996). Through paracrine signaling, *Foxd1* regulates the epithelial differentiation of the nephron mesenchyme and the growth and branching of the ureteric bud (Zhang et al., 2003).

In the CM, *Six2*, a homeobox transcription factor, is required for the maintenance of self-renewal and multipotency of the nephron progenitor in an autonomous manner (Kobayashi et al., 2008). SIX2 is expressed in both uninduced CM and induced CM, but the expression of SIX2 decreases in the RV (Mugford et al., 2009). *Six2* deletion mice died shortly after birth and showed renal hypogenesis (Self et al., 2006). *Six2* deletion caused the depletion of the nephron progenitors and the ectopic differentiation of the nephron progenitors to epithelial cells (Self et al., 2006). *Six2* activates its own expression autonomously (Brodbeck et al., 2004). To maintain the nephron progenitor, SIX2 is required for the expression of OSR1, which interacts with SIX2 through the TCF/LEF complex (Xu et al., 2014a). SIX2 and β-CATENIN compete to interact with the TCF/LEF complex in the nephron progenitors. However, SIX2 maintains the self-renewal capacity, whereas β-CATENIN promotes differentiation (Park et al., 2012).

CITED1, Cbp/p300-interacting transactivator with Glu/Asp-rich C-terminal domain 1, is a non-DNA binding transcpitional regulator. CITED1 is exclusively expressed in the nephron progenitor in the uninduced CM, and its expression decreases as the progenitor starts to

differentiate (Boyle et al., 2008). However, *Cited1* deletion does not affect kidney development, suggesting that it is not required for nephrogenesis (Boyle et al., 2007).

1.5 Signaling and interactions between kidney progenitor compartments

There are networks of intensive signaling and crosstalk between stromal progenitors, nephron progenitors and ureteric buds to orchestrate the complex molecular interactions and morphogenesis in kidneys (Fig. 1.3 B).

The metanephric mesenchyme expresses and secretes the growth factor GDNF which then binds to the GDNF receptor C-RET expressed in the cells of the ureteric buds (Patel and Dressler, 2013; Schuchardt et al., 1994). GDNF expression in the MM is controlled by transcription factors *Eya1*, *Pax2*, and *Six1* and *Six2* (Reidy and Rosenblum, 2009). The GDNF-C-RET signaling induces the outgrowth and branching of the ureteric bud through the PI-3K/AKT and ERK pathways (Tang et al., 2002). GDNF-C-RET signaling also increases the cell migration ability of ureteric buds to promote ureteric bud invasion into the metanephric mesenchyme (Tang et al., 1998).

Reciprocally, the ureteric bud sends signals to the nephron progenitors to regulate cell survival, proliferation and differentiation (Mori et al., 2003). To maintain nephron progenitor survival, FGF signaling is critical. Specifically, FGF9 secreted from the ureteric buds and FGF20 expressed in the CM are necessary and sufficient for nephron progenitors to proliferate, survive and maintain stemness (Barak et al., 2012). WNT9B derived from the ureteric buds is also required for the self-renewal and proliferation of nephron progenitors via canonical β-CATENIN signaling (Karner et al., 2011). Also, WNT9B/β-CATENIN induces early differentiation the CITED1^{+} nephron progenitors (Carroll et al., 2005). SIX2 and WNT9B/β-CATENIN coordinate the balance between the maintenance of stemness and differentiation (Karner et al., 2011). In the presence of WNT9B/β-CATENIN signaling,

nephron progenitors with high levels of SIX2 favor maintenance of self-renewal and proliferation, whereas progenitors with low expression of SIX2 are stimulated to differentiate by WNT9B/β-CATENIN (Karner et al., 2011). WNT9B activates WNT4 in differentiating cells to form renal vesicles (Carroll et al., 2005). Although activation of β-CATENIN induces differentiation, levels of this protein must be reduced and fine-tuned in order for cells to further differentiate and epithelialize (Park et al., 2007). Moreover, *in vivo* genetic studies have shown that Notch signaling can substitute for WNT signaling and induce the mesenchyme to epithelia transition of nephron progenitor (Boyle et al., 2011).

Stromal mesenchyme is also critical in regulating functions of nephron progenitors. The stromal progenitor is required for renal morphogenesis (Hum et al., 2014). Deletion of *Foxd1*, a marker for stromal progenitors, leads to failed differentiation of the nephron progenitors through DCN (Small leucine rich proteoglycan decorin)–BMP/SMAD signaling from stromal progenitors (Fetting et al., 2014). BMP-SMAD signaling primes the $CITED1^{+}SIX2^{+}$ uninduced nephron progenitors to be susceptible to induction of differentiation (Brown et al., 2013). FAT-HIPPO signaling from stromal mesenchyme cooperates with WNT9B to control the differentiation of nephron progenitors (Das et al., 2013).

Both the stromal mesenchyme and the ureteric buds send signals to nephron progenitors and coordinate the control of nephron progenitor maintenance and differentiation. However, not much is known about whether the stromal progenitors are regulated by the nephron progenitors or the ureteric buds and how they are regulated.

1.6 Pre-MM: Induction of metanephric mesenchyme

The metanephric mesenchyme (MM) is derived from the intermediate mesenchyme. There are many key transcription factors that interact to generate and define the MM. These

transcription factors, such as *Osr1*, *Eya1*, *Hox11*, *Six1* and *Pax2*, are expressed in the intermediate mesoderm and the MM, and are critical for the specification of the MM. Genetic studies have shown that loss of function of these transcription factors causes hypoplasia or kidney agenesis (Patel and Dressler, 2013).

OSR1 is expressed in the intermediate mesenchyme cells from which both metanephric stromal progenitors and nephron progenitors arise (Mugford et al., 2008b). OSR1 is required for the induction of metanephric mesenchyme from the intermediate mesenchyme (Wang et al., 2005). In the metanephric mesenchyme, OSR1 expression is restricted to the CM (SIX2+) and it works synergistically with SIX2 to maintain nephron progenitors (Mugford et al., 2008b) (Xu et al., 2014a).

EYA1 is also expressed in the intermediate mesenchyme. $EYA1^{+}$ cells in the intermediate mesenchyme give rise to the nephron forming cells. Deletion of *Eya1* results in loss of SIX2 and premature epithelialization of the nephron progenitors, indicating that *Eya1* is important in regulating nephron progenitor self-renewal (Xu et al., 2014b). $Eya1^{-/-}$ mice do not have the outgrowth of the ureteric bud and the specification of the metanephric mesenchyme, which is likely mediated through SIX1 and PAX2 (Xu et al., 1999) (Sajithlal et al., 2005).

Hox11 is a paralogous set of genes, *Hoxa11, Hoxc11* and *Hoxd11*, with redundant functions in regulating kidney development. HOXD11 has been shown to activate SIX2 in the intermediate mesenchyme and commit the intermediate mesenchyme to the MM (Mugford et al., 2008a). The triple compound mutant $Hoxa11^{-/-}Hoxc11^{-/-}Hoxd11^{-/-}$ results in a failure in the induction of MM and the outgrowth of the ureteric bud (Wellik et al., 2002). HOX11 interacts with PAX2 and EYA1 and the formed HOX-PAX-EYA complex is essential to activate *Six2* to maintain the nephron progenitor population (Gong et al., 2007).

PAX2 is expressed in the mesenchymal and ductal components of the urogenital system (Torres et al., 1995). *Pax2* and its related *Pax* gene family member, *Pax8*, are required and

sufficient for the specification of nephric lineage from the intermediate mesenchyme (Bouchard et al., 2002). *Pax2* activates *Wnt4* to induce the nephron progenitor to differentiate (Torban et al., 2006). *Pax2* deletion mice resulted in failure to develop kidneys, ureters and genital tracts (Torres et al., 1995).

1.7 Post-MM: Epithelial differentiation of nephron progenitor

In the MM, after the induction of differentiation, the nephron progenitor undergoes MET and forms the renal vesicles, where as *Wnt4, Pax8, Lef1, Lhx1* and *Fgf8* are expressed to promote epithelial differentiation (Mugford et al., 2009) (Little and McMahon, 2012). The renal vesicle is comprised of primitive epithelium with a basement membrane and a lumen, located proximal to the ureteric bud (Patel and Dressler, 2013). During morphogenesis, the renal vesicle is followed by the formation of the comma-shaped body, S-shaped body, and fully differentiated nephron (Patel and Dressler, 2013). Gene expression analysis identified a restricted expression pattern of marker genes in the renal vesicle, which correlates to the specification of glomerular, proximal and distal segments (Little and McMahon, 2012). Along the proximal-distal patterning, CADHERINs are differentially expressed, reflecting the regionalization of segmentation (Little and McMahon, 2012). CADHERIN-6 is a marker for the proximal compartment in the comma-shaped body and S-shaped body (Cho et al., 1998). E-CADHERIN is expressed in more maturely differentiated epithelium such as the proximal tubule and distal tubule (Shimazui et al., 2000). A study of the molecular mechanism of nephron patterning has shown *Notch2* null mutants lack the formation of the proximal segments, suggesting that NOTCH signaling is required for nephron segmentation (Cheng et al., 2007).

1.8 Molecular profiling of Wilms tumors showed a similar profile to the early stage of kidney development

Wilms tumor not only recapitulates the fetal kidney histologically, but it also molecularly mimics the gene expression pattern of fetal kidney. A comparison of gene expression analysis between Wilms tumors and fetal kidneys at early and late stage of development revealed that the gene expression profile of Wilms tumor was similar to that of the committed metanephric mesenchyme in the transition of mesenchyme to epithelia (Li et al., 2002). The overexpressed genes shared by both Wilms tumor and the metanephric mesenchyme included *Pax2, Eya1, HBF2, Hoxa11, Six1, Meox1* and *Sall2*, which play an important role on the survival, proliferation and function of the mesenchyme cells (Li et al., 2002). Further analysis of transcription profile of specific cellular components in Wilms tumors, e.g. the blastemal, epithelial and stromal, demonstrated that all these components expressed genes that are highly expressed in metanephric mesenchyme at the earliest stage of renal development (Maschietto et al., 2008). Tumors also expressed genes expressed at a late stage of differentiation. However, tumor blastema had the least in common with the expression profile at a later stage of differentiation, while the tumor epithelial and stromal elements showed higher commonality with it (Maschietto et al., 2008). These molecular profiling results indicate that Wilms tumor arises from cells arrested at an early metanephric mesenchymal stage during kidney development.

1.9 Wilms tumor genetics: *WT1*, *β-CATENIN*, *WTX*, and *IGF2*

Mutations of a few genes have been identified in Wilms tumors, such as *Wilms Tumor Gene 1* (*WT1*), *β-CATENIN* (*CTNNB1*), *Wilms Tumor gene on the X chromosome* (*WTX*) (Ruteshouser et al., 2008), *IGF2* (Ogawa et al., 1993), *DROSHA*, *DICER1* (Wu et al., 2013) and *TP53* (Bardeesy et al., 1994; Huff, 2007).

WT1 is found mutated in 20% of tumors. The mutations included deletion, truncation or missense mutations, which resulted in the loss of functional WT1 (Ruteshouser et al., 2008). *WT1* mutations are associated with mixed triphasic histology in Wilms tumors (Gadd et al., 2012). *WT1* is a transcription factor with four Kruppel type zinc finger domains and regulates the expression of genes involved in cell differentiation, survival and proliferation (Mrowka and Schedl, 2000). One of its isoforms also regulates mRNA processing (Hohenstein and Hastie, 2006). *Wt1* knock-out mice lacked the development of kidneys and died at mid-gestation due to defects in the development of cardiovasculature (Kreidberg et al., 1993).

70% of Wilms tumors exhibited loss of imprinting of *IGF2*, resulting in biallelic expression of *IGF2* (Steenman et al., 1994). The *H19-Imprinting Control Region* (*ICR*) region on the maternal allele transcriptionally represses the expression of *IGF2* on the same allele. Normally *IGF2* is expressed from the paternal allele but not the maternal one. However, deletion of *H19-ICR* region on the maternal allele results in biallelic *Igf2* expression (Leighton et al., 1995). IGF2 is a fetal mitogen that promotes proliferation of mesenchymal cells in kidney development.

β-CATENIN activation mutations occur in 15% of Wilms tumors and are frequently found associated with *WT1* mutations (Maiti et al., 2000). Studies have found a sequential occurrence of genetic alterations during the progression from nephrogenic rest to tumor (Fukuzawa et al., 2007). In the same individual, the nephrogenic rests carried only *WT1* mutation, but the tumor had the same *WT1* mutation and an additional β-catenin mutation (Fukuzawa et al., 2007). This result suggests that a *WT1* mutation in nephrogenic rests is essential but not sufficient for cell transformation, and when a second mutation such as β-CATENIN stabilization occurs, the nephrogenic rest becomes tumorigenic (Fukuzawa et al., 2007).

WTX, a gene on the X chromosome, is found mutated in 20% of Wilms tumors (Ruteshouser et al., 2008). WTX has been shown to negatively regulate WNT/β-CATENIN signaling (Major et al., 2007). Mutant mice with germ-line knock-out of *Wtx* died after birth and had malformation in the mesenchyme derived tissues (Moisan et al., 2011). *Wtx* deletion in the mesenchyme progenitors resulted in changed fate of the lineage restricted cells and delayed differentiation due to increased WNT/β-CATENIN signaling (Moisan et al., 2011).

DICER1 syndrome patients who have germ-line *DICER* null mutations are predisposed to Wilms tumors. Very recently, genes involved in the micro RNA biogenesis pathway were found to be associated with 15% Wilms tumors (Torrezan et al., 2014). These genes include *DROSHA* (12%) (Torrezan et al., 2014), *DICER1* (2.6%) (Wu et al., 2013) and some other micro RNA processing genes, suggesting a role of micro RNA biogenesis in Wilms tumor development (Torrezan et al., 2014).

1.10 Wilms tumor mouse models

Three different genetic mouse models of Wilms tumors have been generated so far. Our lab has generated the first one by ablating *Wt1* somatically and mosaically in the background of bi-allelic *Igf2* expression (Hu et al., 2010). In this model, a tamoxifen inducible *Cre-ER*^{TM} was used to ablate *Wt1* mosaically and somatically at E11.5, an early stage of kidney development (*Ub*^{Cre}*-Wt1-Igf2*). The *Wt1* was ablated by CRE in a non-specific manner in kidney cells. This mouse model of Wilms tumor had typical triphasic histology, mimicking the triphasic histology of human Wilms tumors. Developmentally, *Wt1* ablation only blocked mesenchyme differentiation (Hu et al., 2010). The tumors with *Wt1* ablation and *Igf2* upregulation had increased ERK signaling, corresponding to a subset of human WTs with elevated ERK1/2 phosphorylation (Hu et al., 2010).

A second genetic mouse model of Wilms tumor had stabilized β-CATENIN with or without the activation of K-RAS in kidney epithelial cells (Clark et al., 2011). This study applied a metanephric mesenchyme specific tamoxifen inducible *Cre*, *Cited1*^{CreERT2}, and activated the CRE postnatally to stabilize β-CATENIN by deleting exon 3 of *Ctnnb1*. In addition to targeting the mesenchyme, they also used a proximal tubule specific *Cre* transgene *γGT-Cre* to activate *β-catenin* and *K-Ras*. With both methods, mutant mice developed primitive epithelial Wilms tumors. Moreover, the activation of both *β-catenin* and *K-Ras* synergistically caused metastasis of Wilms tumors to the lungs. Molecularly, the mouse primary Wilms tumors showed increased ERK and PI3K/AKT signaling (Clark et al., 2011).

Very recently, the overexpression of *Lin28* with *Wt1-Cre* induction in the intermediate mesenchyme derivatives led to the development of Wilms tumors (Urbach et al., 2014). *Lin28* is an RNA-binding protein and is important in the maintenance of stem cell proliferation and self-renewal (Urbach et al., 2014). The tumors with *Lin28* overexpression displayed a phenotype of being arrested at an early differentiation stage in the cap mesenchyme. It has been shown that in the mouse Wilms tumors *Lin28* acted through the microRNA *Let7* signal transduction pathway (Urbach et al., 2014). However, *Lin28* overexpression in stromal progenitors (*Foxd1-Cre*), nephron progenitors (*Six2-Cre*) or ureteric buds (*Chd16-Cre*), did not induce Wilms tumors (Urbach et al., 2014). Microarray and IHC analysis showed that *Lin28B* but not *Lin28A* was expressed in human Wilms tumors and the expression levels of *Lin 28B* was significantly associated with increased severity of tumor progression (Urbach et al., 2014).

These mouse Wilms tumor models provided useful tools to study the mechanisms of Wilms tumor development *in vivo*; however, in these tumor models the genetic alterations were introduced randomly into developing kidney cells, or post-natal kidney cells, or pre-

metanephric mesenchme cells. It is still not clear what types of cells in the metanephric kidney, or at what differentiation state during renal development, initiate the development of Wilms tumors. These are the questions that our study specifically addressed.

1.11 Cell Origins of Wilms tumors

A study of global gene expression array with a large panel of human Wilms tumors has identified 5 subsets of Wilms tumors (Table 1) (Gadd et al., 2012). These subsets are different in gene expression profiles, histological features, and clinical outcomes (Gadd et al., 2012). For example, Subset 1 is characterized by differentiated epithelial histology and a gene expression signature corresponding to terminal epithelial differentiation. Clinically, patients within this subset had no tumor relapses. On the other hand, Subsets 2-4 are characterized by triphasic histology with undifferentiated blastemal cells mixed with epithelial and stromal cells, and these tumors had gene expression signatures corresponding to early stage of the mesonephric mesenchyme and renal interstitium. Moreover, 10-50% of these patients had tumor recurrences. These data suggested that the different Wilms tumor subsets arise from cells at different stages of mesenchyme differentiation (Gadd et al., 2012). Therefore, we hypothesized that the differentiation status of the initially mutated cell impacts the formation of different types of Wilms tumors. Addressing this hypothesis will help us to understand how the different types of Wilms tumors occur and potentially help us to develop improved therapy accordingly.

Table 1. Identification of human WT subsets based on gene expression array

	Relapse	Histology	Signature genes
Subset 1 (S1)	0/11	Epithelial differentiated	After MET and in terminally differentiated epithelium e.g. NOTCH signaling, HOXA11, MEIS2
Subset 2 (S2)	2/23	Triphasic, muscle differentiation elements	Very early mesonephric mesenchyme and renal interstitium e.g. NFAT and TGFB signaling, TWIST1, DLK1, WIF1, MYH3, TTN, ACTA1
Subset 3 (S3)	7/21	Similar to S2, less muscle differentiation	NFAT, TGFB and RAS signaling
Subset 4 (S4)	6/11	Similar to S2	Similar to S2
Subset 5 (S5)	50/158	Triphasic, mostly blastema predominant	Early metanephric mesenchyme e.g. SIX1, PAX2, EYA1, HOXA11

Previously, our lab generated a mouse model of Wilms tumor by using a ubiquitous *Cre* to somatically and mosaically ablate *Wt1* at E11.5 in the background of *Igf2* over-expression (Hu et al., 2010). In this model, *Wt1* ablation is essential for the development of mouse Wilms tumors. However, it is unclear what cell types were targeted with *Wt1* ablation and consequently gave rise to tumors. At E11.5, WT1 is expressed in the metanephric mesenchyme mainly composed of stromal progenitors and nephron progenitors. In this mouse model, when *Wt1* is ablated randomly with the ubiquitous *Cre*, the stromal progenitors or the nephron progenitors could have been targeted and serve as promising candidates for the tumor initiating cells. To find out the cell origins of Wilms tumors, we applied the same approach of generating the mouse tumor model by using *Cre-Loxp* system, but we used progenitor cell-type specific tamoxifen-inducible *Cre* to introduce genetic mutations into specific cellular compartment (stromal progenitor or nephron progenitor) in the metanephric mesenchyme.

1.12 Targeting kidney progenitors with the cell-type specific *Cre*

The abilities of self-renewal and multipotency in progenitor cells make them a promising candidate as tumor initiation cells. To determine whether the kidney progenitors are the primary targets for cell transformation, progenitor specific tamoxifen-inducible Cre^{ER} alleles were used. $Foxd1^{GCE}$ was used to target the stromal progenitor and $Six2^{GCE}$ or $Cited1^{Cre}$ was used to target the nephron progenitor. Since *Wt1* loss-of-function and *β-catenin* activating mutations are often found in Wilms tumors, it is clinically and molecularly relevant to introduce these genetic mutations to the mouse and generate mouse Wilms tumors. The *Cre-LoxP* system was applied to induce *Wt1* ablation or β-CATENIN stabilization in kidney stromal progenitor or nephron progenitor.

$Foxd1^{GCE}$ (stomal progenitor specific) and $Six2^{GCE}$ (nephron progenitor specific) knock-in alleles replace endogenous exon 1 at the initiation codon of *Foxd1* or *Six2*, respectively,

with a gene cassette of *GFP* and tamoxifen inducible *Cre* (*GCE*) (Fig. 1.4 A). The *Foxd1*$^{GCE/GCE}$ and *Six2*$^{GCE/GCE}$ mutant homozygote mice die soon after birth, but the heterozygotes are viable and phenotypically normal (Hatini et al., 1996) (Self et al., 2006). The *Cited1*^{Cre} is a *BAC* transgene in which GFP-CRE expression is under the transcriptional control of 190 kb genomic sequence 5' of the *Cited1* gene (Fig. 1.4 A) (Boyle et al., 2008). All three *Cre* lines have been shown to express the CRE recombinase where endogenous FOXD1, SIX2 or CITED1 proteins are normally expressed in the fetal kidney. Therefore, with the inducible CRE, we could introduce *Wt1* ablation or β-CATENIN stabilization in a progenitor cell type-specific manner to study cell origins of Wilms tumors.

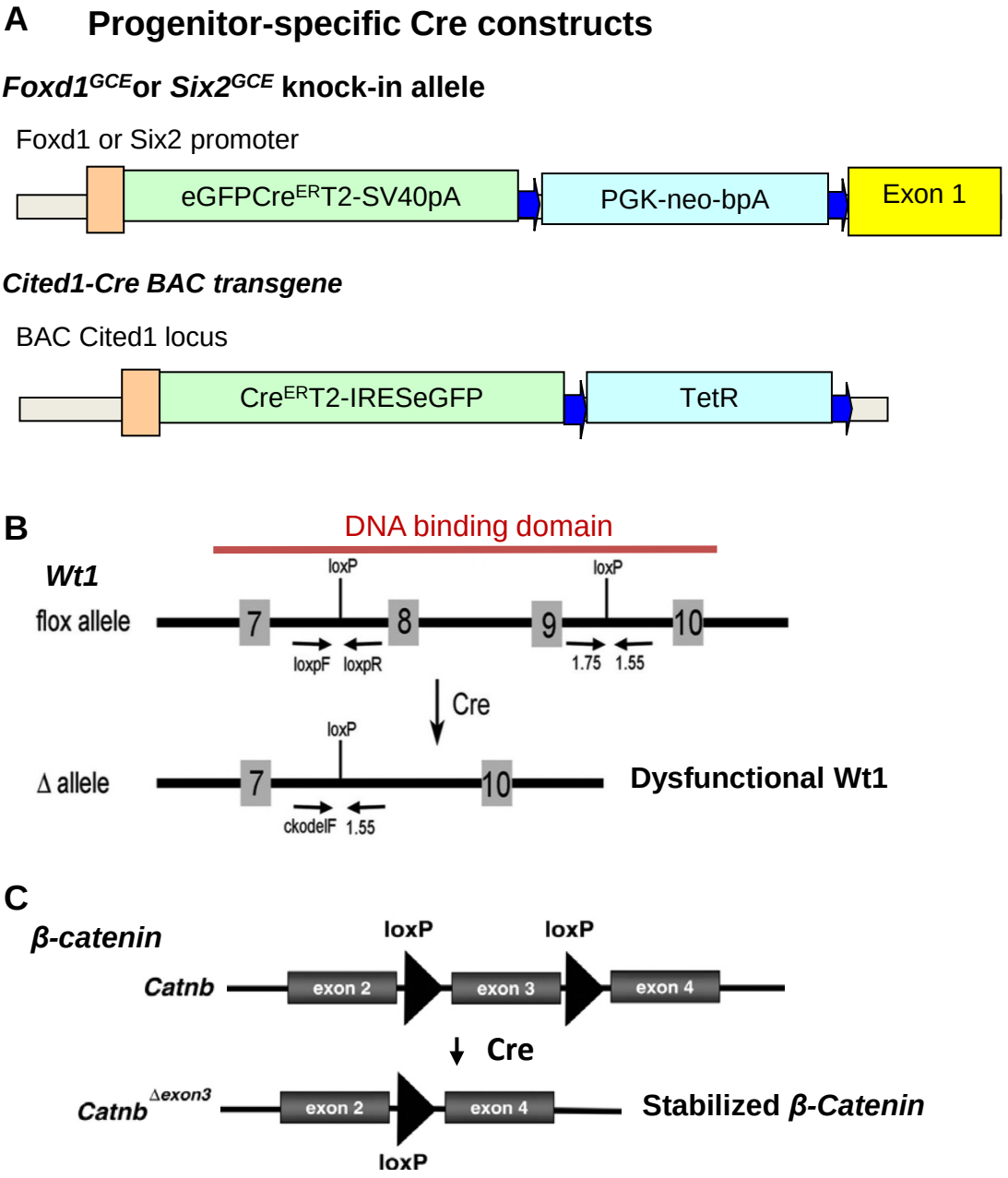

Figure 1.4 Diagram of progenitor-specific *Cre* alleles and *Wt1* and *β-catenin* flox alleles.

(A)The construct of *Foxd1*^{GCE}or *Six2*^{GCE} knock-in alleles. (B) Constructs of *Wt1*^{fl} and *Wt1*$^{\Delta}$ alleles. (C)The construct of *β-catenin*^{e3fl} *and β-catenin*$^{e3\Delta}$ alleles.

Image B is from Gao, F., Maiti, S., Alam, N., Zhang, Z., Deng, J.M., Behringer, R.R., Lecureuil, C., Guillou, F., and Huff, V. (2006). The Wilms tumor gene, Wt1, is required for Sox9 expression and maintenance of tubular architecture in the developing testis. Proceedings of the National Academy of Sciences of the United States of America *103*, 11987-11992. (Copyright (2006) National Academy of Sciences, U.S.A.) Image C is from Mucenski, M.L., Nation, J.M., Thitoff, A.R., Besnard, V., Xu, Y., Wert, S.E., Harada, N., Taketo, M.M., Stahlman, M.T., and Whitsett, J.A. (2005). Beta-catenin regulates differentiation of respiratory epithelial cells in vivo. American journal of physiology Lung cellular and molecular physiology *289*, L971-979. Figures used with permission.

1.13 *Wt1* in kidney development and Wilms tumor

1.13.1 *Wt1* is a transcription factor

Wt1 is a transcription factor and RNA binding protein. The human *WT1* gene is about 50 kb in size, encoding a 3 kb mRNA with 10 exons (Call et al., 1990). The WT1 protein has four Kruppel-type zinc fingers at the carboxyl terminus, which are involved in DNA binding (Call et al., 1990). Exons 8-9 encode the second and third DNA binding domains which are critical for *Wt1* functions. To disrupt *Wt1* function, *loxP* sites were inserted flanking exons 8-9 and, in the presence of CRE recombinase, the in-frame deletion of Exons 8-9 results in truncated, inactive *Wt1* (Fig. 1.4 B) (Gao et al., 2006).

WT1 has many isoforms due to alternative translational start sites, alternative splicing and RNA editing (reviewed in (Hohenstein and Hastie, 2006)). Alternative splicing results in the inclusion or exclusion of exon5 and of 3 amino acids (lysine-threonine-serine, KTS) at the 3 prime end of exon 9 (Hohenstein and Hastie, 2006). The KTS- isoform binds to DNA with a high affinity and functions as a transcription factor (Hohenstein and Hastie, 2006). The KTS+ Wt1 isoform has a low DNA binding affinity, but interacts with RNA preferentially (Hohenstein and Hastie, 2006). These various isoforms remain in relative proportion in fetal kidney (Hohenstein and Hastie, 2006).

WT1 can transcriptionally activate or repress downstream target genes, depending on the cellular context and interacting proteins. Some of the downstream targets include *Egfr* (Englert et al., 1995), *Igf2* (Drummond et al., 1992), *Pax2* (Ryan et al., 1995), *Wnt4* (Sim et al., 2002) and *Amphiregulin* (Lee et al., 1999), which are all important in kidney development. A systematic genome-wide study was carried out to identify *Wt1* targets controlling cell function and differentiation of nephron progenitors (Hartwig et al., 2010). This study analyzed embryonic kidneys at E18.5 and used the approaches of chromatin immunoprecipitation and mouse promoter microarray. The defined targets associated with renal agenesis are WNT inhibitor *Cxxc5*, MAP kinase signaling effector *Erk1*, epigenetic

regulators such as *Rest* and *Jmdj3*, and proteins involved in TGFβ/BMP signaling (Hartwig et al., 2010).

1.13.2 *WT1* is a tumor suppressor in Wilms tumors

WT1 is defined as a tumor suppressor in Wilms tumors given that loss of function of *WT1* predisposes patients to Wilms tumor development. Predisposition to Wilms tumor is observed in four congenital syndromes, WAGR, Denys-Drash, Beckwith-Wiedemann and Frasier syndromes, most of which have genitourinary defects (Mrowka and Schedl, 2000), and all of which involve alterations of chromosome 11p13-15. Germ-line *WT1* mutations are associated with bilateral tumors and an early age at diagnosis, but there is no difference in overall survival between patients with and without *WT1* mutations (Discenza and Pelletier, 2004).

However, many Wilms tumors with wild type *WT1* overexpress WT1. High expression of wild type *WT1* in Wilms tumor result in the arrest of undifferentiated mesenchymal cells at early differentiation and suggests that factors controlling the WT1 expression are preserved in tumors. WT1 is also overexpressed in most acute myelogenous leukemia, acute lymphoblastic leukemia, chronic myelogenous leukemia (CML), and myelodysplastic syndrome (MDS) (Rosenfeld et al., 2003). In breast cancer, *WT1* has been implicated as an oncogene since its high expression is associated with poor prognosis (Miyoshi et al., 2002). *WT1* plays different roles in tumor development of different kinds of cancers.

1.13.3 *Wt1* is required for nephrogenesis

WT1 plays an essential role in kidney development. *Wt1* has been shown to have different functions at different stages of kidney development (Elizabeth, 2014). In the developing kidney, *Wt1* is weakly expressed in the intermediate mesoderm and metanephric mesenchyme (Armstrong et al., 1993). The expression of WT1 increases in the proximal

segment of the comma-shaped body and S-shaped body, the precursor of glomerular podocytes (Grubb et al., 1994). Then its expression is restricted to the podocytes of nephrons (Grubb et al., 1994).

Wt1 is required for cell survival in the intermediate mesoderm, as *Wt1* knock-out in mice led to cell apoptosis in the intermediate mesoderm and the metanephric mesenchyme, resulting in disruption in urogenital development (Kreidberg et al., 1993). In the metanephric mesenchyme, *Wt1* is essential for the mesenchyme to epithelial transition (Hu et al., 2010). Conditional ablation of *Wt1* in the metanephric mesenchyme at E11.5 resulted in lack of condensation of the mesenchyme around the ureteric bud tips, expansion of the mesenchymal region, and blocked mesenchyme to epithelia transition (Hu et al., 2010). The expanded mesenchyme caused by *Wt1* deletion arrested before the MET makes the mesenchymal cells at the pre-MET stage a very likely candidate for tumor development (Elizabeth, 2014). In the metanephric mesenchyme, *Wt1* transcriptionally activates the expression of *Wnt4* and thus stimulates epithelial differentiation (Sim et al., 2002). In the mature nephron, *Wt1* is highly expressed in the podocytes, and reduced expression of *Wt1* causes the accumulation of matrix in the basement membrane, thus leading to crescentic glomerulonephritis or mesangial sclerosis (Guo et al., 2002).

Wt1 is expressed in the metanephric mesenchyme including stromal progenitors and nephron progenitors and it regulates cell apoptosis, survival and MET during kidney development. However, its specific function in each renal progenitor cell type remains unclear. Using the progenitor-specific *Cre* to ablate *Wt1* in the mouse, we can dissect out its *in vivo* effects on nephrogenesis in either stromal progenitor or nephron progenitor and this knowledge would help us understand the mechanisms by which *Wt1* mutations predispose to the development of Wilms tumors.

1.14 WNT/β-CATENIN in kidney development and Wilms tumor

1.14.1 WNT/β-CATENIN signaling

The WNT/β-CATENIN signal transduction pathway is critical in embryogenesis and is often associated with cancer development. WNT proteins are a family of secreted glycolipoproteins that interact with the receptors of the FRIZZLED proteins and the LDL receptor-related proteins 5 and 6 LRP5/6) (MacDonald et al., 2009). The WNT ligands act through β-CATENIN dependent (canonical) pathways or β-CATENIN independent (non-canonical) pathways. The non-canonical pathways include the Planar Cell Polarity (PCP) pathway and the WNT/Ca^{2+} pathway (Komiya and Habas, 2008).

In the canonical pathway, β-CATENIN is the mediator of WNT ligand induced signaling. Without WNTs, β-CATENIN is susceptible to protein degradation by the APC complex composed of the scaffolding protein AXIN, the tumor suppressor adenomatous polyposis coli protein (APC), casein kinase 1 (CK1), and glycogen synthase kinase 3 (GSK3) (reviewed in (MacDonald et al., 2009)). Initially β-CATENIN binds to AXIN, then β-CATENIN is phosphorylated by CK1 at Ser45 in *β-catenin* exon 3, and is subsequently phosphorylated by GSK3 at Ser33, Ser37 and Ser41 (reviewed in (Voronkov and Krauss, 2013)). CK1 and GSK3 also phosphorylate APC, and phosphorylated APC has a higher affinity for β-CATENIN, resulting in the transfer of β-CATENIN to APC from AXIN. The N-terminal phosphorylated β-CATENIN in the APC complex is exposed to ubiquitinase β-TrCP and subjected to proteasomal degradation (reviewed in (Voronkov and Krauss, 2013)). WNT ligands, such as WNT9 and WNT4, bind to the receptor complex LRP5/6-Frizzled and the complex recruits the scaffold proteins DISHEVELLED and AXIN, thus inhibiting AXIN-mediated β-CATENIN phosphorylation and the subsequent β-CATENIN degradation (reviewed in (Voronkov and Krauss, 2013)). Thus, β-CATENIN is stabilized and accumulates in the cytoplasm. The accumulated β-CATENIN is translocated to the nucleus where it

interacts with transcription repressor complex the TCF/LEF, activating the expression of downstream targets (reviewed in (MacDonald et al., 2009)). With the genetic in-frame deletion of exon3 (Fig. 1.4 C), *β-catenin* is not susceptible to phosphorylation and is therefore stabilized, thus activating downstream oncogenic events (Harada et al., 1999).

1.14.2 WNT/β-CATENIN in renal progenitors

β-CATENIN signaling is critical in nephron progenitors. Deletion of *β-catenin* in nephron progenitors using the *Six2-Cre* transgene led to failed formation of renal vesicles and no expression of induction markers in renal vesicles such as *Fgf8*, *Wnt4*, *Pax8* and *Lhx1* (Park et al., 2007). β-CATENIN activation stimulated nephron progenitors to go through MET and ectopically express markers of renal vesicles (Park et al., 2007). Thus, β-CATENIN is necessary and sufficient to initiate MET induction in nephron progenitors. However, a constant high level of β-CATENIN activity in nephron progenitors did not result in complete epithelial differentiation such as the formation of E-CADHERIN expressing epithelium (Park et al., 2007). Therefore, transient activation of *β-catenin* is required to induce differentiation of nephron progenitor to renal vesicle stage, but to further epithelialize, β-CATENIN activity has to be reduced and fine-tuned (Park et al., 2007). β-CATENIN is activated by WNT9B from the ureteric bud and WNT9B activates WNT4 in the induced nephron progenitor to increase β-CATENIN signaling (Karner et al., 2011). β-CATENIN acts through the *Tcf/Lef* transcriptional program to maintain the survival, proliferation and early differentiation of nephron progenitors (Schmidt-Ott and Barasch, 2008). To promote the differentiation of the nephron progenitor, nuclear β-CATENIN is increased by stromal cells in the niche through FAT4-HIPPO signaling (Das et al., 2013). SIX2 counteracts β-CATENIN initiated differentiation signals via TCF/LEF complex to maintain nephron progenitor self-renewal (Park et al., 2012).

For the stromal progenitors, β-CATENIN has been shown to be expressed in the cell membrane (Das et al., 2013) and is likely involved in cell-cell adhesion junctions. Conditional deletion of *β-catenin* using *Foxd1-Cre* did not show any abnormality in nephron induction or ureteric bud branching, however, the mutants had slightly thicker cortices and failed development of the medulla (Yu et al., 2009). *Wnt2b* is expressed in the stromal mesenchyme, but *Wnt2/Wnt2b* double knock out mice did not show abnormal phenotype in the kidney (Goss et al., 2009). These results suggested that WNT/β-CATENIN did not seem to be essential for the functions of stromal progenitors, but the specific roles of WNT/β-CATENIN signaling in the stromal progenitors still remains to be investigated.

1.14.3 WNT/β-CATENIN in Wilms tumors

High activity of β-CATENIN is associated with numerous cancers. *β-catenin* stabilization mutations or nuclear accumulation of β-CATENIN is often found in Wilms tumors with stromal histology and ectopic mesenchymal elements such as myogenesis or chondrogenesis (Fukuzawa et al., 2009). Wilms tumors with *β-catenin* mutations showed high expressions of *β-catenin* targets *PITX2* and *APCDD1*, *Wnt/β-catenin* extracellular inhibitors, muscle-related genes and oncogenes in retinoic acid and *RAS* pathways (Zirn et al., 2006). In Wilms tumors, *β-CATENIN* stabilization mutations are frequently associated with *WT1* loss of function mutations (Maiti et al., 2000). Another genetic study of Wilms tumors also found *β-CATENIN* stabilization mutations were detected only in *WT1* mutated Wilms tumors (Li et al., 2004). These tumors also expressed high level of genes such as β-CATENIN/TCF targets, WNT inhibitors, myogenic differentiation factors and TGF-β signaling (Li et al., 2004).

Summary

Wilms Tumor is thought to arise from the undifferentiated metanephric mesenchyme, and the observation of distinctive subsets of tumors suggests that each subset arises from cells at different stages of differentiation (Gadd et al., 2012). In this thesis, by using mouse genetic models, we applied progenitor-specific Cre^{ER} to somatically and mosaically introduce *Wt1* ablation in the context of *Igf2* biallelic expression or *β-catenin* activation into stromal progenitors and nephron progenitors. We investigated whether Wilms tumors could arise from fetal kidney cells at distinct differentiation statuses and whether specific kidney progenitor populations could produce different types of Wilms tumors with respect to tumor initiation, growth and pathology. We also studied the impact of different types of gene mutations on the development of Wilms tumors. Moreover, with the same approach, we studied the effects of *Wt1* ablation on kidney development to understand how *Wt1* ablation predisposes to malignant transformation. These results could provide insights into the cell origins of Wilms tumor and the mechanisms of tumor initiation and development and also help us to understand the functions of *Wt1* in stromal progenitors and nephron progenitors. Potentially the mouse model studies will help us to develop improved therapies that target different types of tumors specifically and trigger the most effective responses according to the tumor cell origins or tumor types.

Chapter 2: Materials and Methods

2.1 Mice

The mice were housed and handled according to the guidelines of The University of Texas MD Anderson Cancer Center Institutional and Animal Care and Use Committee. All of the mice were maintained on a C57BL/6J x 129/SvEv mixed genetic background. Littermates of the mutant mice were used as controls. The mice were genotyped via standard PCR analysis of genomic DNA isolated from the tails as described previously (Gao et al., 2006; Harada et al., 1999; Hayashi and McMahon, 2002; Leighton et al., 1995).

Foxd1$^{GCE/+}$, *Six2*$^{GCE/+}$, *Cited1*^{Cre}, *R26*$^{tdTomato/tdTomato}$, *Wt1*$^{+/-}$, *Wt1*$^{fl/fl}$, *β-catenin*$^{e3fl/e3fl}$, and *H19*$^{-/-}$ mice described previously (Humphreys et al., 2010) (Kobayashi et al., 2008) (Boyle et al., 2008) (Kreidberg et al., 1993) (Gao et al., 2006) (Harada et al., 1999) (Leighton et al., 1995) were used in this study. We bred the *Foxd1*$^{GCE/+}$ or *Six2*$^{GCE/+}$ or *Cited1*^{Cre} with *Wt1*$^{+/-}$ mice to generate *Foxd1*$^{GCE/+}$; *Wt1*$^{+/-}$ or *Six2*$^{GCE/+}$; *Wt1*$^{+/-}$ or *Cited1*^{Cre}; *Wt1*$^{+/-}$ male mice. *Wt1*$^{fl/fl}$ mice were bred with *β-catenin*$^{e3fl/e3fl}$ or *H19*$^{-/-}$ or *R26*$^{tdTomato/tdTomato}$ or *R26*$^{βgal/βgal}$ mice for a few generations to generate females that were *Wt1*$^{fl/fl}$; *β-catenin*$^{e3fl/e3fl}$ or *Wt1*$^{fl/fl}$; *H19*$^{-/-}$ or *Wt1*$^{fl/fl}$; *R26*$^{tdTomato/tdTomato}$ or *Wt1*$^{fl/fl}$; *R26*$^{βgal/βgal}$.

2.1.1 *β-gal* reporter analysis of *Foxd1*^{GCE} and *Six2*^{GCE} mice

Tamoxifen was dissolved in corn oil and injected at E11.5 or E14.5 intraperitoneally into pregnant mice (*R26*$^{βgal/βgal}$) mated with *Foxd1*$^{GCE/+}$ or *Six2*$^{GCE/+}$ male mice. Kidneys (*Cre*$^{+}$; *R26*$^{βgal/+}$) were analyzed at E14.5 and E19.5 with littermates (*R26*$^{βgal/+}$) as controls. When tamoxifen was injected at E11.5, kidney sections at E14.5 showed that both *Foxd1*^{GCE} and *Six2*^{GCE} Cre alleles were effective to induce recombination (Fig. 3.2, A and C). However, when tamoxifen injection time was at E14.5, kidney sections at E19.5 showed that only *Six2*^{GCE} but not *Foxd1*^{GCE} was efficient in inducing recombination (Fig. 3.2, B and D). This

result provided us information on the conditions of tamoxifen injection time for the mouse tumor cohort generation. To target progenitor cells effectively, tamoxifen was administered at E11.5 for *Foxd1*^{GCE} cohort generation, but at E11.5 or E14.5 for *Six2*^{GCE} cohort generation.

2.1.2 tdTOMATO reporter analysis of *Foxd1*^{GCE}, *Six2*^{GCE} and *Cited1*^{Cre} mice

To analyze the efficiency of the Cre, *Foxd1*$^{GCE/+}$, *Six2*$^{GCE/+}$ or *Cited1*$^{Cre/+}$ mice were crossed with *tdTomato* reporter mice (*R26*$^{tdTomato/tdTomato}$) expressing the *loxP-Stop-loxP tdTomato* transgene. *Cre*$^{+}$; *R26*$^{tdTomato/+}$ embryos were induced with tamoxifen (1 or 3 mg / 40g body weight) at E11.5 or E14.5 during mid-gestation. CITED1 expression does not become robust until E14.5, therefore we selected E14.5 and E17.5 as the time point for tamoxifen induction in *Cited1*^{Cre} mice. Embryonic kidney sections were prepared for histology analysis at E19.5.

2.1.3 Generation of the mouse tumor cohorts with progenitors targeted

To generate the tumor cohorts, *Cre*$^{+}$*; Wt1*$^{+/-}$ males were bred with females *Wt1*$^{fl/fl}$*;H19*$^{-/-}$ (Fig. 2.1 A) or *Wt1*$^{fl/fl}$*; β-catenin*$^{ex3fl/fl}$ (Fig. 2.1 B) or *β-catenin*$^{ex3fl/ex3fl}$ (Fig. 2.1 C). Pregnant mice were injected with tamoxifen (0.5, 1 or 3 mg / 40g BW) intraperitoneally to activate the inducible CRE in fetal kidney progenitors (Table 3). For *Foxd1*^{GCE}, tamoxifen was administered at E11.5. For *Six2*^{GCE}, tamoxifen was administered at E11.5 or E14.5. The *Cited1*^{Cre} transgene is expressed in the liver at E14.5 but not at E17.5, and β-CATENIN activation in the CITED1^{+} liver progenitors at E14.5 led to the development of hepatocellular carcinoma and hepatoblastoma in 90% of mutants at early ages (Mokkapati et al., 2014). To avoid this competing phenotype and cause of death for our Wilms tumor study, E17.5 was selected as the time point for tamoxifen injection for the *Cited1*^{Cre}*-Wt1-β-catenin* cohort

generation. *Wt1* ablation by *Cited1*^{Cre} and *Igf2* up-regulation did not result in a detectable liver phenotype with tamoxifen injection at E14.5, therefore we injected tamoxifen at E14.5 for *Cited1*^{Cre}*-Wt1-Igf2* cohort generation. Mutant mice *Cre*$^{+}$*; Wt1*$^{+/fl}$ or *Wt1*$^{-/fl}$ or *Wt1*$^{+/+}$*; β-catenin*$^{exon3+/fl}$ or *Cre*$^{+}$*; Wt1*$^{-/fl}$*; H19*$^{+/-m}$ were monitored for tumor development.

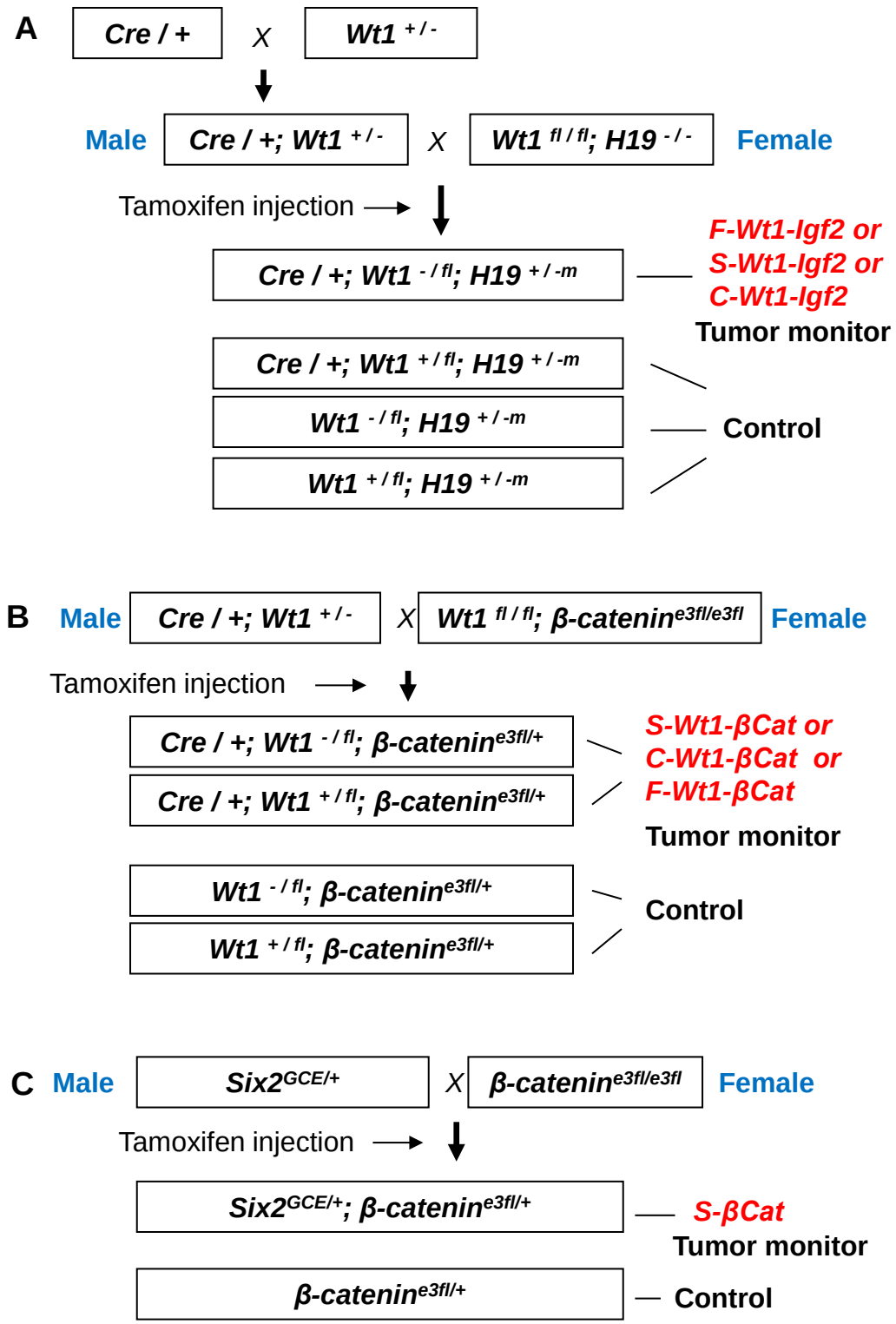

Figure 2.1 Schematic diagram of mouse crosses for cohort generation

2.2 Histological, immunohistochemical, and Western blot analysis

Tumor and kidney tissue specimens were fixed in 4% paraformaldehyde, embedded in paraffin, and cut into 5-μm sections. Hematoxylin and Eosin (H&E), immunohistochemical and immunofluorescent staining and Western blot analysis of proteins were performed as described previously (Hu et al., 2010). Antibodies specific for WT1 (sc-192, Santa Cruz Biotechnology) (1:100), KI67 (ab15580, Abcam) (1:200), pHH3 (06-570, Upstate Biotechnology) (1:200), β-CATENIN (610154 BD Biosciences) (1:200), DLK1 (sc-8624 Santa Cruz Biotechnology) (1:100), CITED1 (9219 FisherScientific) (1:100), SIX2 (11562-1-AP, Proteintech) (1:100), PAX2 (PRB-276P Covance) (1:200), NCAM (C9672 Sigma) (1:200), E-CADHERIN (3195, Cell Signaling Technology) (1:200), K-CADHERIN (ab79005, Abcam) (1:200), VIMENTIN (V2258 Sigma) (1:100), COLLAGEN IV (AB756P Chemicon) (1:100), CYCLIN D1 (sc-753 Santa Cruz Biotechnology) (1:100), C-MYC (9E10 Santa Cruz Biotechnology) (1:100), ERK 1/2 (4377, Cell Signaling Technology) (1:100), pERK 1/2 (4376, Cell Signaling Technology) (1:100), and pAKT (4051S Cell Signaling Technology) (1:100) were used.

2.3 β-gal staining

Freshly dissected kidneys or slides made from OCT-embedded frozen tissues were fixed in fixation buffer (0.2% glutaraldehyde, 2% formalin, 5 mM EGTA, 2 mM $MgCl_2$ in 0.1 M phosphate buffer) for 30 min to 1 hour at room temperature. Samples were rinsed in rinse buffer (0.1% sodium deoxycholate, 0.2% NP40, 2 mM $MgCl_2$ in 0.1 M phosphate buffer). Then samples were stained at 4^{o}C overnight in staining solution (1 mg/ml X-gal, 5 mM K ferricyanide and 5 mM ferrocyanide in rinse buffer). After staining, tissues or slides were rinsed and postfixed in 4% paraformaldehyde. Slides were counterstained with eosin for histological analysis.

2.4 Kidney rudiment culture

Pregnant mice were injected intraperitoneally at E11.5 with tamoxifen at a dose of 3mg/40g body weight. Kidney rudiments were dissected out of embryos at E12.5 or E13.5. Mutant and control rudiments were cultured on a trans-well plate (Transwell) with media containing 1μM 4-OH-TM (Sigma-Aldrich), 10% fetal bovine serum (Sigma-Aldrich) and DMEM (Sigma-Aldrich 10-017-CV) at 37^{o}C as described previously (Hu et al., 2010). During culture, live imaging pictures of the rudiments were taken every day with an inverted microscope (Olympus IX71). After culturing for 3 days, the cultured rudiments were rinsed in PBS and fixed in methanol for whole-mount immunofluorescence staining (Hu et al., 2010).

2.5 Reverse-phase protein array

Protein was extracted from murine tumors and normal kidney tissues and the concentration of the protein extracts were calculated with Bradford assay (Bio-Rad). The samples were analyzed by reverse-phase protein arrays (RPPA) analysis as described previously (Hu et al., 2010). RPPA is a high-throughput method to detect protein expression with 135 antibodies against common onco-proteins and tumor suppressors (mdanderson.org). Briefly, protein samples were denatured by SDS buffer, loaded on nitrocellulose-coated slides, and probed with antibodies. The signals from binding interaction were detected by DAB colorimetric reaction.

2.6 Fluorescence-activated cell sorting analysis (FACS)

We administered 1 or 3 mg (per 40g body weight) of tamoxifen to pregnant mice in utero at E11.5, E14.5 or E17.5. Single-cell suspensions from fetal kidneys harvested at E15.5 or E19.5 from *Foxd1*$^{GCE/+}$*; R26*$^{tdTomato/+}$, *Six2*$^{GCE/+}$*; R26*$^{tdTomato/+}$ and *Cited1*$^{Cre/+}$*; R26*$^{tdTomato/+}$ embryos were prepared as previously described (Kobayashi et al., 2008). Briefly, kidney tissues were trypsinized at 37^{o}C for 3-5 minutes and mechanically disintegrated into single

cells by repeated pipetting up and down in DMEM with 10% FBS. The cell suspensions were washed with PBS containing 2% FBS and filtered through 70 μm pore filter (BD Falcon). Cells expressing tdTomato were isolated by using a BD FACS Aria high-speed digital cell sorter (BD Biosciences). Cell suspensions from littermate kidneys without *Cre* served as negative controls.

2.7 Quantitative real-time PCR

Tumor or kidney tissue specimens or isolated tdTomato-positive cells were flash-frozen in liquid nitrogen. RNA was extracted from specimens or cell pellets using the RNAqueous-4PCR kit (Ambion AM1914). The concentration of RNA was determined using the Nanodrop spectrophotometer (Nanodrop ND-1000). RNA was then converted to cDNA using reverse transcription reagents (Applied Biosystems). Real-time (RT)-PCR was performed using SYBR Green PCR Master Mix (Applied Biosystems) with a 7900HT sequence detection system (Applied Biosystems).

2.8 Statistical analysis

The Student *t*-test or analysis of variance was used to analyze RT-PCR results. Results were presented as mean value with standard deviation. P-values less than 0.05 were considered statistically significant.

2.9 qRT-PCR Primers

Gene	**5' to 3'**	
Eya1-F	CATAGCCGACTGAGTGGTAGT	(Basta et al., 2014)
Eya1-R	GCTCTGTTTTAACTTCGGTGCC	
Osr1-F	TACTCTTTCCTTCAGGCAGTGA	
Osr1-R	GATCGAGGCAAGTGCATGG	
Hoxa11-F	TTTGATGAGCGTGGTCCCTG	PrimerBank ID 6754226a1
Hoxa11-R	AGGAGTAGGAGTATGTCATTGGG	
Pax2-F	AAGCCCGGAGTGATTGGTG	
Pax2-R	CAGGCGAACATAGTCGGGTT	
Wnt4-F	AGACGTGCGAGAAACTCAAAG	
Wnt4-R	GGAACTGGTATTGGCACTCCT	
CyclinD1-F	GCGTACCCTGACACCAATCTC	PrimerBank ID 6680868a1
CyclinD1-R	CTCCTCTTCGCACTTCTGCTC	
Jag1-F	CCTCGGGTCAGTTTGAGCTG	PrimerBank ID 7305197a1
Jag1-R	CCTTGAGGCACACTTTGAAGTA	
E-cadherin-F	ACTGTGAAGGGACGGTCAAC	
E-cadherin-R	GGAGCAGCAGGATCAGAATC	
Titin-F	TCAAGGAGGAAGCGTCCAAAG	PrimerBank ID 19388004a1
Titin-R	GACTTCTTCGGATGCCTGTGA	
Actin a1-F	CCCAAAGCTAACCGGGAGAAG	PrimerBank ID 33563240a1
Actin a1-R	CCAGAATCCAACACGATGCC	
Axin2-F	TGACTCTCCTTCCAGATCCCA	
Axin2-R	TGCCCACACTAGGCTGACA	
Wif1-F	TCTGGAGCATCCTACCTTGC	PrimerBank ID 6755999a1

Wif1-R	ATGAGCACTCTAGCCTGATGG	
Cyclin E-F	GTGGCTCCGACCTTTCAGTC	
Cyclin E-R	CACAGTCTTGTCAATCTTGGCA	
Cxxc4-F	CTGCCCGCAGAATCATTCCT	
Cxxc4-R	CAGACGCCACAGTTGATGAG	
Pitx2-F	ACCCCGGCTATTCGTACAAC	PrimerBank ID 1724116a1
Pitx2-R	GAGGACAGGGGATTGACGTTC	
Dlk1-F	AGTGCGAAACCTGGGTGTC	PrimerBank ID 12838136a1
Dlk1-R	GCCTCCTTGTTGAAAGTGGTCA	
Hmga2-F	GAGCCCTCTCCTAAGAGACCC	PrimerBank ID 30017353a1
Hmga2-R	TTGGCCGTTTTTCTCCAATGG	
Dkk2-F	CTGATGCGGGTCAAGGATTCA	PrimerBank ID 31560347a1
Dkk2-R	CTCCCCTCCTAGAGAGGACTT	
NCAM-F	ACCACCGTCACCACTAACTCT	
NCAM-R	TGGGGCAATACTGGAGGTCA	
Pax8-F	ATGCCTCACAACTCGATCAGA	
Pax8-R	ACAATGCGTTGACGTACAACTT	
Stim1-F	TGACAGGGACTGTACTGAAGATG	
Stim1-R	TATGCCGAGTCAAGAGAGGAG	
Nfat4-F	CAAGATGGAAGACCTCATTGG	
Nfat4-R	GGGAGGAACTTCAAGGACAA	
CD15-F	TGGTACTACGCGTGTTCGAC	
CD15-R	CCAGGGCTTTGCCAGTTA	
CD248-F	CAACGGGCTGCTATGGATTG	
CD248-R	GCAGAGGTAGCCATCGACAG	

Synaptopodin-F	GGAAAGTGATGACAGCCAGTG	
Synaptopodin-R	TTTTCGGTGAAGCTTGTGCT	
Dnmt1-F	AAGAATGGTGTTGTCTACCGAC	
Dnmt1-R	CATCCAGGTTGCTCCCCTTG	
Sall1-F	CTCAACATTTCCAATCCGACCC	
Sall1-R	GGCATCCTTGCTCTTAGTGGG	
Meox2-F	TGTCCTACCCCGAACTCTCC	
Meox2-R	GTGCCAGTTGCTTTGCAGA	
Pax3-F	TTTCACCTCAGGTAATGGGACT	
Pax3-R	GAACGTCCAAGGCTTACTTTGT	

(Spandidos et al., 2010)

Chapter 3: Results

Part I: Impact of differentiation state and genetic context on the development of mouse Wilms tumors

3.1 Expression of the progenitor-specific *Cre* alleles as determined by GFP reporter expression

To determine what cells in the undifferentiated renal mesenchyme are able to generate Wilms tumors, we used progenitor-specific tamoxifen-inducible *Cre* (stromal progenitor *Foxd1*^{GCE} and nephron progenitor *Six2*^{GCE} and *Cited1*^{Cre}) to introduce gene mutations somatically and mosaically into specific cellular compartments of the mouse fetal kidneys.

The expression of CRE and GFP (*Cre-Gfp*) are both driven by the same promoter. We examined the *Cre-Gfp* cassette expression driven by the progenitor-specific gene promoter at E14.5 by assessing the GFP expression. The *Foxd1*^{GCE}*-Gfp* cassette was expressed in the stromal progenitors surrounding the cap mesenchyme (Fig. 3.1B). The *Six2*^{GCE}*-Gfp* cassette was expressed in the uninduced and induced cap mesenchyme in a bracket pattern (Fig. 3.1D). The *Cited1*^{Cre}*-Gfp* cassette was expressed only in the uninduced cap mesenchyme (Fig. 3.1, E and F).

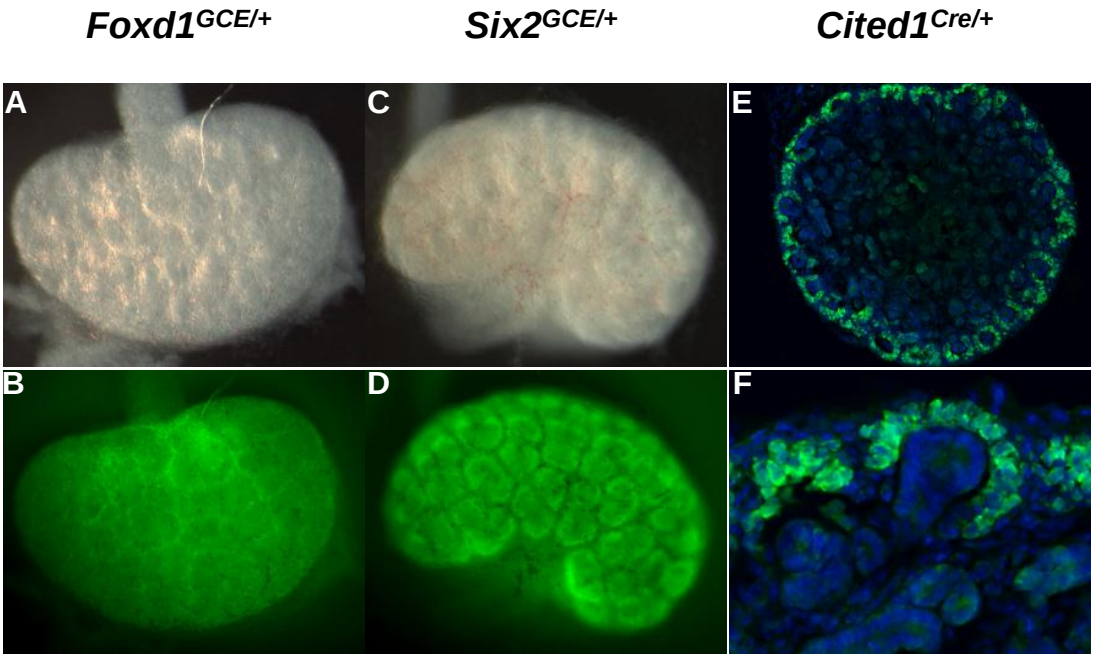

Figure 3.1 Cre-GFP expression under the control of progenitor-specific gene promoter.

Kidneys from *Foxd1*$^{GCE/+}$ (A and B), *Six2*$^{GCE/+}$ (C and D) and *Cited1*$^{Cre/+}$ (E and F) at E14.5. (A and C) Bright field images of whole kidneys. (B) GFP image of kidney from *Foxd1*$^{GCE/+}$ embryo showed that Foxd1-Cre-GFP was expressed in the stromal progenitors surrounding the cap mesenchyme. (D) GFP image of kidney from *Six2*$^{GCE/+}$ embryo showed that Six2-Cre-GFP was expressed in the uninduced and induced cap mesenchyme. (E-F) Anti-GFP antibody staining of kidney sections from *Cited1*$^{Cre/+}$ embryo showed that Cited1-Cre-GFP was expressed in the uninduced cap mesenchyme. Dapi staining shows the nuclear staining of cells.

3.2 Validation of the fate mapping of the progenitor-specific Cre alleles

We then confirmed the cell fate of the progenitors expressing specific CRE using a *β-gal* reporter construct. As reported previously, the stromal progenitors ($FOXD1^{+}$) generated interstitial cells, pericytes and mesangial cells (Fig. 3.2, A and B). The nephron progenitors ($SIX2^{+}$) gave rise to epithelial cells including comma-shaped bodies, S-shaped bodies, podocytes, glomeruli, proximal tubules and distal tubules (Fig. 3.2, C and D). These results confirmed the cell lineage of $Foxd1^{GCE/+}$ labeled stromal progenitors and $Six2^{GCE/+}$ marked nephron progenitors in the mixed genetic background of our mouse strains.

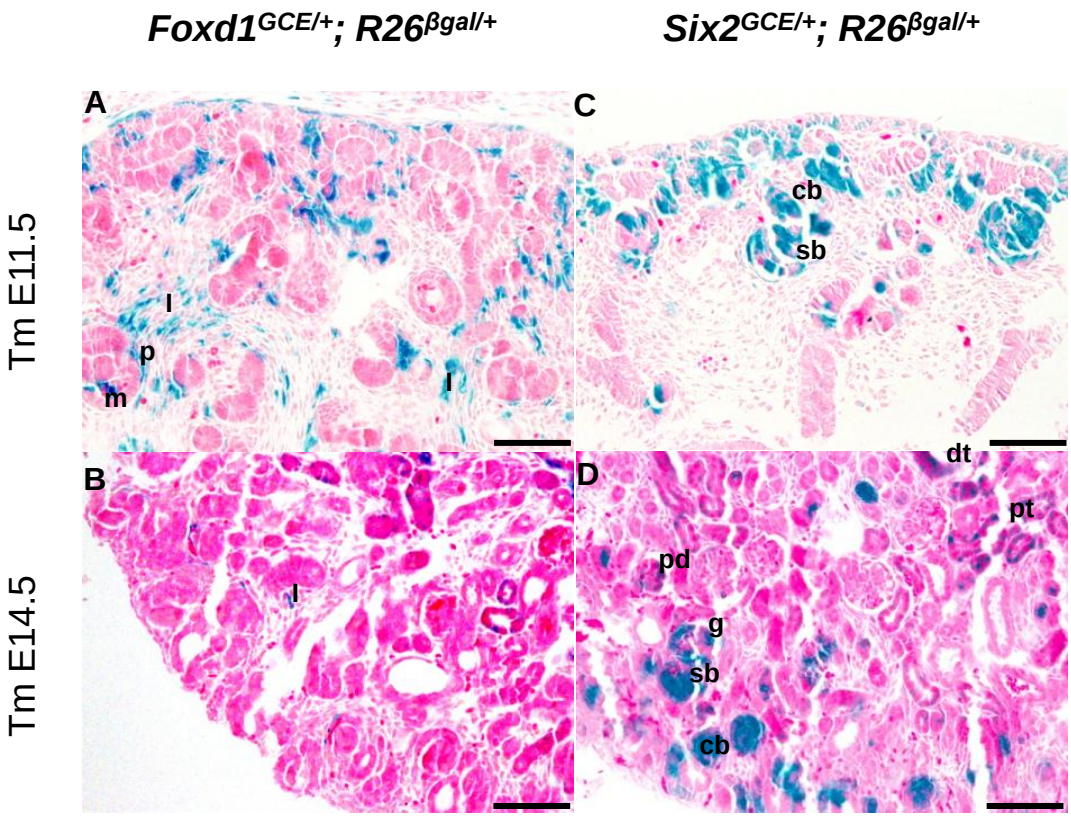

Figure 3.2 Lineage tracing of the stromal (Foxd1⁺) progenitors and nephron (Six2⁺) progenitors.

β-gal staining of kidney sections from *Foxd1$^{GCE/+}$; R26$^{βgal/+}$* (A and B) and *Six2$^{GCE/+}$; R26$^{βgal/+}$* (C and D). Kidney sections at E14.5 (A) and E19.5 (B) showed that β-gal labeled cells derived from Foxd1^{GCE} included interstitial cells (I), pericytes (p) and mesangial cells (m).
Kidney sections at E14.5 (C) and E19.5 (D) showed that β-gal labeled cells derived from Six2^{GCE} were in comma-shaped bodies (cb), S-shaped bodies (sb), podocytes (pd), glomeruli (g), proximal tubules (pt) and distal tubules (dt). Tm: tamoxifen. Scale bars: 100 μm.

3.3 Estimation of the efficiency of the progenitor-specific CRE

The efficiency of the progenitor-specific CRE recombinase was analyzed at E19.5 by using the fluorescent protein reporter, tdTOMATO. Similar results were observed using the tdTOMATO reporter and β-gal staining. With tamoxifen injection at E11.5, tdTOMATO induced by *Foxd1*^{GCE} was expressed in stromal progenitors, interstitial cells and pericytes (Fig. 3.3 A). *Six2*^{GCE} was efficient in recombination when tamoxifen injection was at either E11.5 or 14.5 (Fig. 3.3 B and C). *Six2*^{GCE} induced tdTOMATO was expressed in nephron progenitors, renal vesicles, comma-shaped bodies, S-shaped bodies and tubules (Fig. 3.3 B and C). *Cited1*$^{Cre/+}$ was also efficient in recombination with tamoxifen injection at either E14.5 or 17.5 (Fig. 3.3 D and E). *Cited1*^{Cre} induced tdTOMATO expression was mainly in nephron progenitors and early stage of epithelial differentiation structures (Fig. 3.3 B and C), due to the short time window between tamoxifen injection and reporter expression analysis.

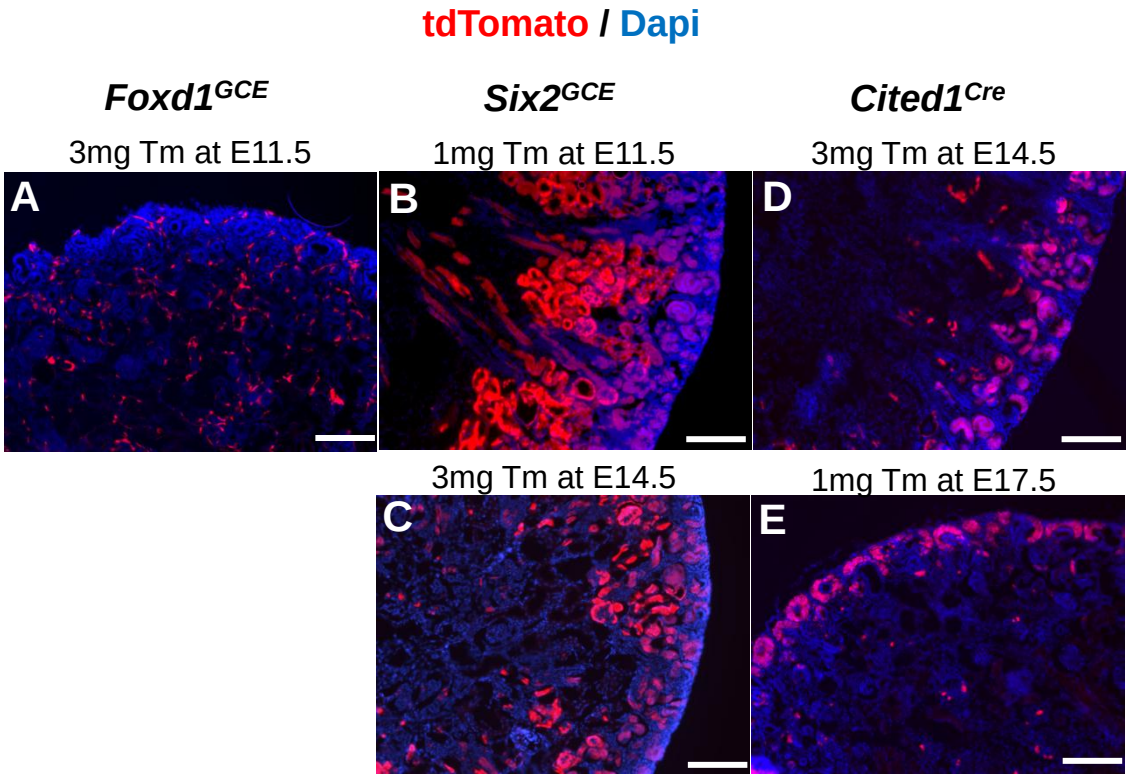

Figure 3.3 TdTomato reporter showing efficient recombination and specific cell fate from *Foxd1*^{GCE}, *Six2*^{GCE} and *Cited1*^{Cre}.

tdTomato reporter imaging of kidney sections at E19.5 from *Foxd1*$^{GCE/+}$ (A), *Six2*$^{GCE/+}$ (B and C) and *Cited1*^{Cre} (D and E) after tamoxifen (Tm) injection with indicated conditions. Scale bars: 200 μm.

To quantitatively assess the frequency of recombination by the CRE recombinase, we counted the percentage of tdTOMATO labeled cells in the whole kidneys from *Cre*$^{+}$*; R26*$^{tdTomato/+}$ embryos by FACS assay. Single-cell suspensions from fetal kidneys harvested at E15.5 or E19.5 were sorted for tdTOMATO expression (Table 2). tdTOMATO^{+} cells were easily distinguished and separated from the tdTOMATO^{-} cells as shown in a representative FACS sorting plot (Fig. 3.4 A). FACS analysis at E19.5 showed that about 7% of cells were labeled with tdTOMATO by *Foxd1*^{GCE}, 30-34% by *Six2*^{GCE}, and 5-7% by *Cited1*^{Cre} (Table 2 and Fig. 3.4B). With *Cited1*^{Cre}, tamoxifen injection at E14.5 or E17.5 did not seem to affect the frequency of tdTOMATO^{+} cells (6.8% and 5.1% respectively), although the frequency was slightly higher when tamoxifen injection was earlier (Table 2 and Fig. 3.4 B). We also compared the percentage of tdTOMATO^{+} cells when analyzed at different time points with the same conditions of tamoxifen administration. For *Foxd1*^{GCE} and *Six2*^{GCE}, tdTOMATO^{+} cells were assessed at E15.5 and E19.5, and a very similar percentage of tdTOMATO expressing cells were detected (7.1% vs. 7% and 33.7% vs. 30.2%) (Table 2 and Fig. 3.4 B). Altogether, efficient recombination was achieved with the tamoxifen injection conditions we used in this study for *Foxd1*^{GCE}*, Six2*^{GCE} and *Cited1*^{Cre}.

Table 2. Conditions of Tamoxifen injection used to quantify the Cre efficiency and percentages of tdTomato^{+} cells targeted by progenitor-specific Cre

Cre	Time point of Tm injection	Tm dosage	FACS	tdTomato^{+} cells %
Foxd1^{GCE}	E11.5	3 mg	E15.5	7.1
			E19.5	7.0
Six2^{GCE}	E11.5	1 mg	E15.5	33.7
			E19.5	30.2
	E14.5	3 mg	E19.5	30.0
Cited1^{Cre}	E14.5	1 mg	E19.5	6.8
	E17.5	1 mg	E19.5	5.1

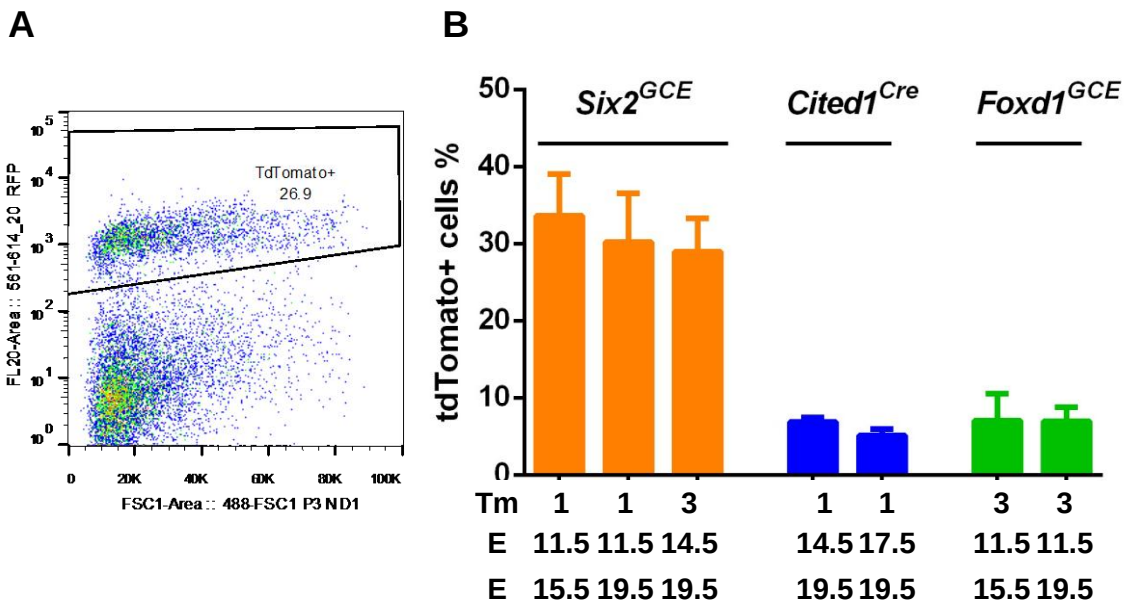

Figure 3.4 FACS analysis of embryonic kidney cell suspension for tdTomato⁺ cells.

(A) Representative dot-plot of tdTomato⁺ cells from single cell suspension of *Cited1*^{Cre}; *R26*$^{tdTomato/+}$ kidney at E19.5 after 3 mg/40g BW Tm treatment at E14.5. (B) FACS analysis for tdTomato⁺ cells showing efficient targeting of stromal progenitor by *Foxd1*^{GCE} and of nephron progenitor by *Six2*^{GCE} or *Cited1*^{Cre}. In the table below the bar graph, the 1st row shows the amount of mg of tamoxifen injected per 40g body weight, the 2nd row shows the injection time and the 3rd row shows the harvest time.

3.4 Mutated renal stromal progenitors did not result in Wilms tumor

To investigate the cell origin of Wilms tumors in mouse, we used progenitor-specific *Cre* and the *Cre-Loxp* system to mosaically and somatically introduce genetic lesions into stromal progenitors or nephron progenitors. The genes we genetically engineered are commonly found mutated in human Wilms tumors, such as *Wt1*, *Igf2* and *β-catenin* (reviewed in (Huff, 2007)). Based on the strong association of mutations in each of these genes found in human Wilms tumors, we combined the genetic mutations into different groups in our mouse models: *Wt1* ablation with *Igf2* up-regulation (*Wt1-Igf2*), *β-catenin* stabilization with ($Wt1^{-/fl}$-β-cat^{S}) or without *Wt1* ablation ($Wt1^{+/fl}$-β-cat^{S}), and *β-catenin* stabilization only (β-cat^{S}).

We found that the nephron progenitors but not the stromal progenitors were susceptible to Wilms tumor development. With the stromal progenitors targeted by $Foxd1^{GCE}$, none of the combinations of mutations, *F-Wt1-Igf2*, $F\text{-}Wt1^{-/fl}$-β-cat^{S} or $F\text{-}Wt1^{+/fl}$-β-cat^{S}, resulted in Wilms tumors in the mutant mice (Table 3).

Table 3. Summary of mutant mouse cohorts

Designation	Genotype	Tamoxifen (mg/40gBW)	Tumor mice / Mutant mice
F-Wt1-Igf2	*Foxd1^{GCE}, Wt1$^{-/fl}$, H19$^{+/-m}$*	3 at E11.5	0 / 9
F-Wt1$^{-/fl}$-β-cat^{S}	*Foxd1^{GCE}, Wt1$^{-/fl}$, β-cat$^{e3+/fl}$*	3 at E11.5	0 / 17
F-Wt1$^{+/fl}$-β-cat^{S}	*Foxd1^{GCE}, Wt1$^{+/fl}$, β-cat$^{e3+/fl}$*	3 at E11.5	0 / 11
S-Wt1-Igf2	*Six2^{GCE}, Wt1$^{-/fl}$, H19$^{+/-m}$*	1 at E11.5	0 / 27
S-Wt1$^{-/fl}$-β-cat^{S}	*Six2^{GCE}, Wt1$^{-/fl}$, β-cat$^{e3+/fl}$*	3 at E14.5	8 / 11
S-Wt1$^{+/fl}$-β-cat^{S}	*Six2^{GCE}, Wt1$^{+/fl}$, β-cat$^{e3+/fl}$*	3 at E14.5	6 / 12
S-β-cat^{S}	*Six2^{GCE}, β-cat$^{e3+/fl}$*	3 at E14.5	2 / 5
C-Wt1-Igf2	*Cited1^{Cre}, Wt1$^{-/fl}$, H19$^{+/-m}$*	1 at E14.5	9 / 18
C-Wt1$^{-/fl}$-β-cat^{S}	*Cited1^{Cre}, Wt1$^{-/fl}$, β-cat$^{e3+/fl}$*	0.5 at E17.5	9 / 20
C-Wt1$^{+/fl}$-β-cat^{S}	*Cited1^{Cre}, Wt1$^{+/fl}$, β-cat$^{e3+/fl}$*	0.5 at E17.5	3 / 7

3.5 Nephron progenitors targeted with *Wt1-β-cat*^{s} mutations by *Cited1*^{Cre} or *Six2*^{GCE} gave rise to Wilms tumors

In contrast to the stromal progenitors, nephron progenitors (*Six2*^{GCE} or *Cited1*^{Cre}), targeted with β-CATENIN stabilization with (*S/C-Wt1*$^{-/fl}$*-β-cat*^{S}) or without *Wt1* ablation (*S/C-Wt1*$^{+/fl}$*-β-cat*^{S}) led to the development of Wilms tumors in mice (Table 3). A small cohort of mice with β-CATENIN stabilization only (*β-cat*^{S}) by *Six2*^{GCE} (*S-β-cat*^{S}) was also generated and the mutant mice also developed Wilms tumors (Table 3). Both unilateral and bilateral tumors were observed and the tumors were frequently associated with kidney cysts filled with blood fluid (Fig. 3.5 A-a & b). The *S/C-Wt1*$^{-/fl}$*-β-cat*^{S} and *S/C-Wt1*$^{+/fl}$*-β-cat*^{S} mutant cohorts had a significantly decreased survival compared to the control mice (Fig. 3.5 B and C). The *Wt1*$^{-/fl}$*-β-cat*^{S} mutants showed a slightly reduced overall life span compared to the *Wt1*$^{+/fl}$*-β-cat*^{S} mutants, but there was no significant difference (Fig. 3.5 B and C).

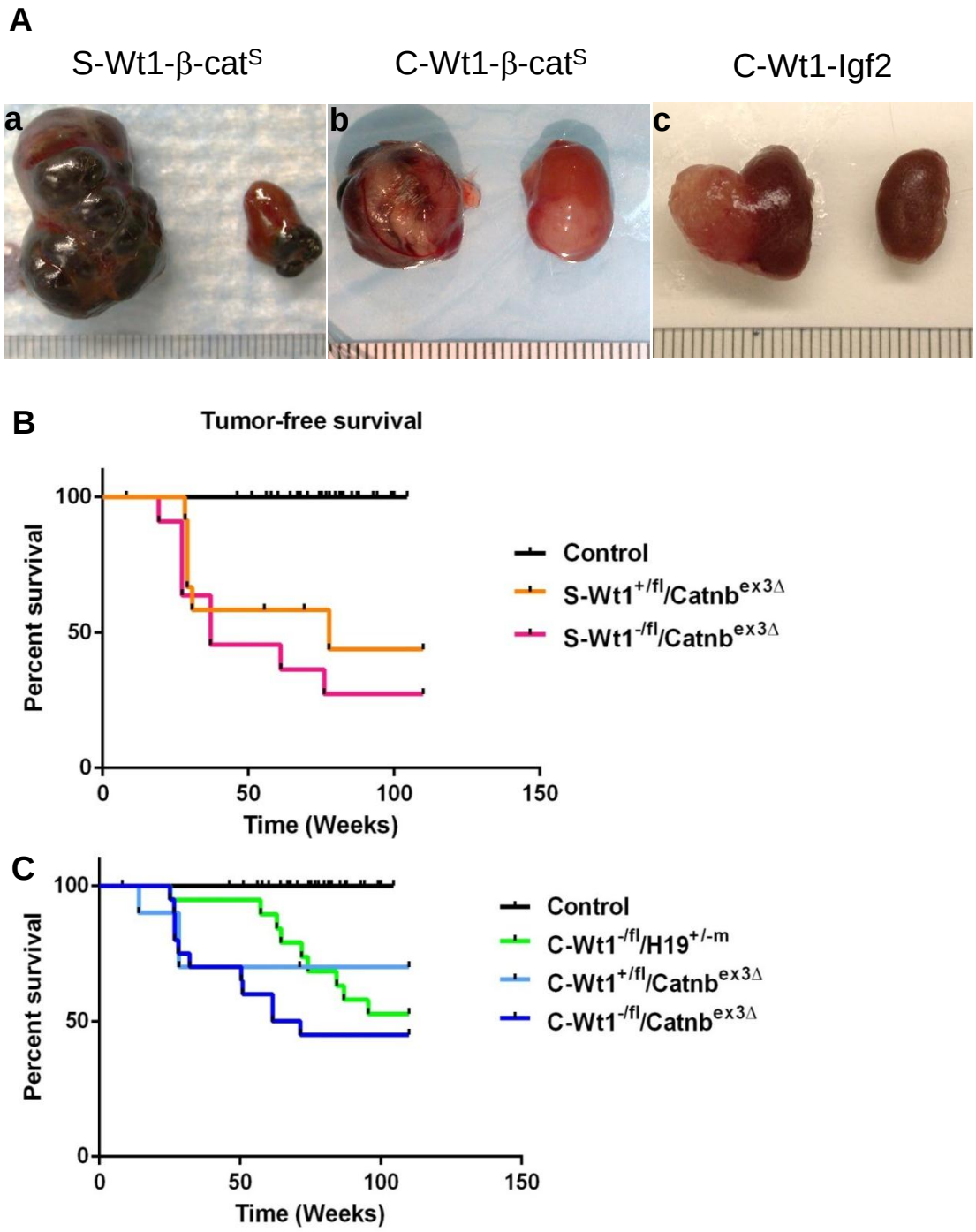

Figure 3.5 Development of WT from nephron progenitors.
(A) Gross appearance of tumors from Six2^{GCE} mutants (a), Cited1^{Cre} mutants (b and c) of the indicated genotypes. (B and C) Kaplan-Meier tumor-free survival curve showing the incidence of mouse WTs in Six2^{GCE} and Cited1^{Cre} mutant mice with β-catenin stabilization with and without Wt1 ablation (*S-Wt1*$^{-/fl}$-β-cat^{s}, *S-Wt1*$^{+/fl}$- β-cat^{s}, *C-Wt1*$^{-/fl}$- β-cat^{s}, and *C-Wt1*$^{+/fl}$- β-cat^{s}) and Wt1 ablation and IGF2 upregulation (C-Wt1-Igf2) in comparison to control mice.

To confirm that the tumors carried the mutations due to somatic recombination of the floxed allele(s) the mice carried, we examined the recombination status of the floxed alleles of *β-catenin* (*β-cat*^{ex3fl} to *β-cat*$^{ex3\Delta}$) and *Wt1* (*Wt1*^{fl} to *Wt1*$^{\Delta}$) in tumors. PCR analysis detected the recombined *β-cat*$^{ex3\Delta}$ in all *S/C-Wt1*$^{-/fl}$*-β-cat*^{S}*, S/C-Wt1*$^{+/fl}$*-β-cat*^{S} and *S-β-cat*^{S} tumors (Fig. 3.6A). Interestingly, 50% of the tumors from *S/C-Wt1*$^{-/fl}$*-β-cat*^{S} and *S/C-Wt1*$^{+/fl}$*-β-cat*^{S} mice had incomplete recombination of the *Wt1*^{fl} to *Wt1*$^{\Delta}$ allele (Fig. 3.6B). These results and the observation of tumor development in *S-β-cat*^{S} tumors with wild-type *Wt1* (*Wt1*$^{+/+}$) suggested that β-CATENIN stabilization in nephron progenitors was sufficient to generate tumors and that *Wt1* ablation was not required for the development of mouse Wilms tumors once *β-catenin* was stabilized. *β-cat*^{S} tumors with or without *Wt1* ablation (*Wt1*$^{-/\Delta}$, *Wt1*$^{-/fl}$, *Wt1*$^{+/\Delta}$, *Wt1*$^{+/fl}$ and *Wt1*$^{+/+}$) showed very similar phenotypes, histology and gene expression profile as shown below, therefore *Wt1* dosage did not seem to play a role in the tumor development if β-CATENIN was stabilized. So we collectively designated the *S-Wt1*$^{-/fl}$*-β-cat*^{S} and *S-Wt1*$^{+/fl}$*-β-cat*^{S} tumors as *S-Wt1-β-cat*^{S} tumors, and the *C-Wt1*$^{-/fl}$*-β-cat*^{S} and *C-Wt1*$^{+/fl}$*-β-cat*^{S} tumors as *C-Wt1-β-cat*^{S} tumors.

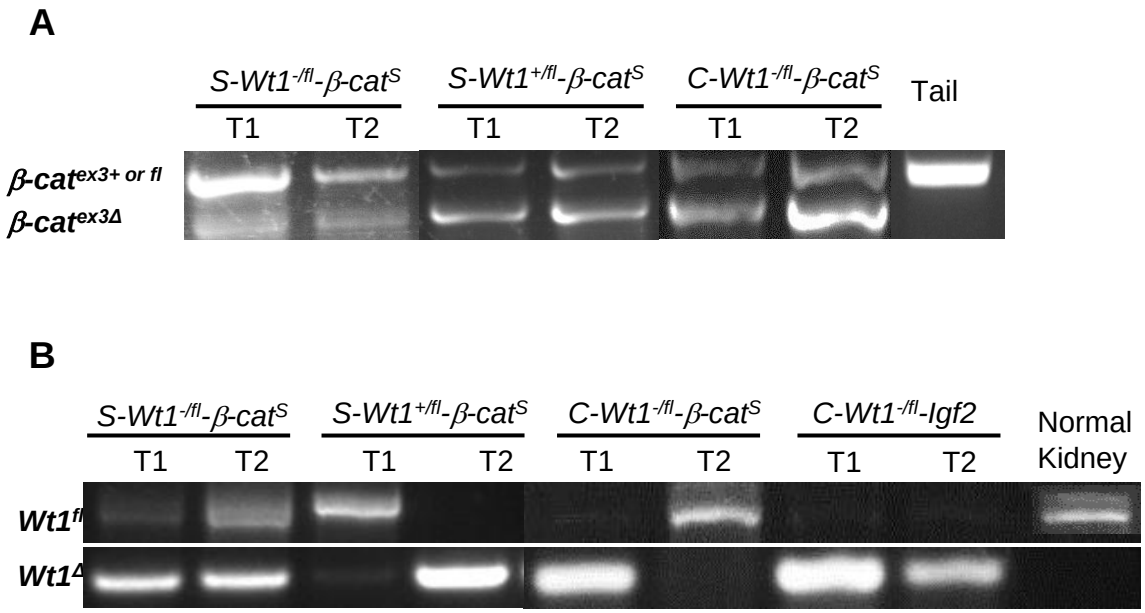

Figure 3.6 PCR detection of *β-cat*$^{ex3\Delta}$ and *Wt1*$^{\Delta}$ in tumors

PCR analysis confirming the presence of gene mutations of the *β-cat*$^{ex3\Delta}$ in S/C-Wt1$^{-/fl}$-β-cat^{S} and S/C-Wt1$^{+/fl}$-β-cat^{S} tumors, and the *Wt1*$^{\Delta}$ in C-Wt1-Igf2 tumors. (A) PCR analysis of DNA from tumors for *β-catenin* wild type or floxed allele, and exon3 deleted allele (*β-cat*$^{ex3+}$ or *β-cat*^{ex3fl}, & *β-cat*$^{ex3\Delta}$). (B) PCR analysis of DNA from tumors showing *Wt1*^{fl} and *Wt1*$^{\Delta}$.

3.6 Nephron progenitors targeted with *Wt1-Igf2* mutations by *Cited1^{Cre}* but not by *Six2^{GCE}* generated Wilms tumors

Although *Six2^{GCE}* targeted nephron progenitors and *Cited1^{Cre}* targeted un-induced nephron progenitors, interestingly, the *Six2^{GCE}, Wt1$^{-/fl}$, H19$^{+/-m}$* (*S-Wt1-Igf2*) mutants did not develop tumors but the *Cited1^{Cre}, Wt1$^{-/fl}$, H19$^{+/-m}$* (*C-Wt1-Igf2*) mutants did (Table 3). The *C-Wt1-Igf2* mutants developed circumscribed unilateral tumors at the periphery of the kidney (Fig. 3.5 A-c). PCR analysis detected the recombined *Wt1$^{\Delta}$* in all *C-Wt1-Igf2* tumors (Fig. 3.6B). The *C-Wt1-Igf2* mutant cohort had a significantly decreased survival compared to the control mice (Fig. 3.5 C).

3.7 In nephron progenitors, different sets of mutations resulted in Wilms tumors with different histologies

With the same set of genetic alterations in nephron progenitors targeted with different *Cre* alleles, *S-Wt1-β-cat^{S}* tumors and *C-Wt1-β-cat^{S}* tumors showed very similar histology (Fig. 3.7 C-F). These tumors presented with an epithelial histology, mainly composed of epithelial elements surrounded by blastemal and stromal elements (Fig. 3.7 A-F). In the tumors, the primitive epithelial cells formed rudimentary tubules (Fig. 3.7 A, C and E), and the more differentiated epithelial cells possessed well-formed tubular structures with cuboidal cells or tall columnar cells (Fig. 3.7 B, D and F). Many of the tubular structures had luminal esophilic material resembling protein casts. The *S-β-cat^{S}* tumors with wild-type *Wt1* also had a very similar histology to *S-Wt1-β-cat^{S}* and *C-Wt1-β-cat^{S}* tumors with varying degree of *Wt1* gene dosage (Fig. 3.7 A-F).

By contrast, with the same nephron progenitor cell origin as *S/C-Wt1-β-cat^{S}* tumors, the *C-Wt1-Igf2* tumors were characterized by a triphasic histology comprised of undifferentiated blastemal nodules, differentiating epithelial tubules, and stromal cells as did the *Ub^{Cre}-Wt1-Igf2* tumors in previously published model with a Ubiquitous *Cre-ER^{TM}* (Fig. 3.7 G-H).

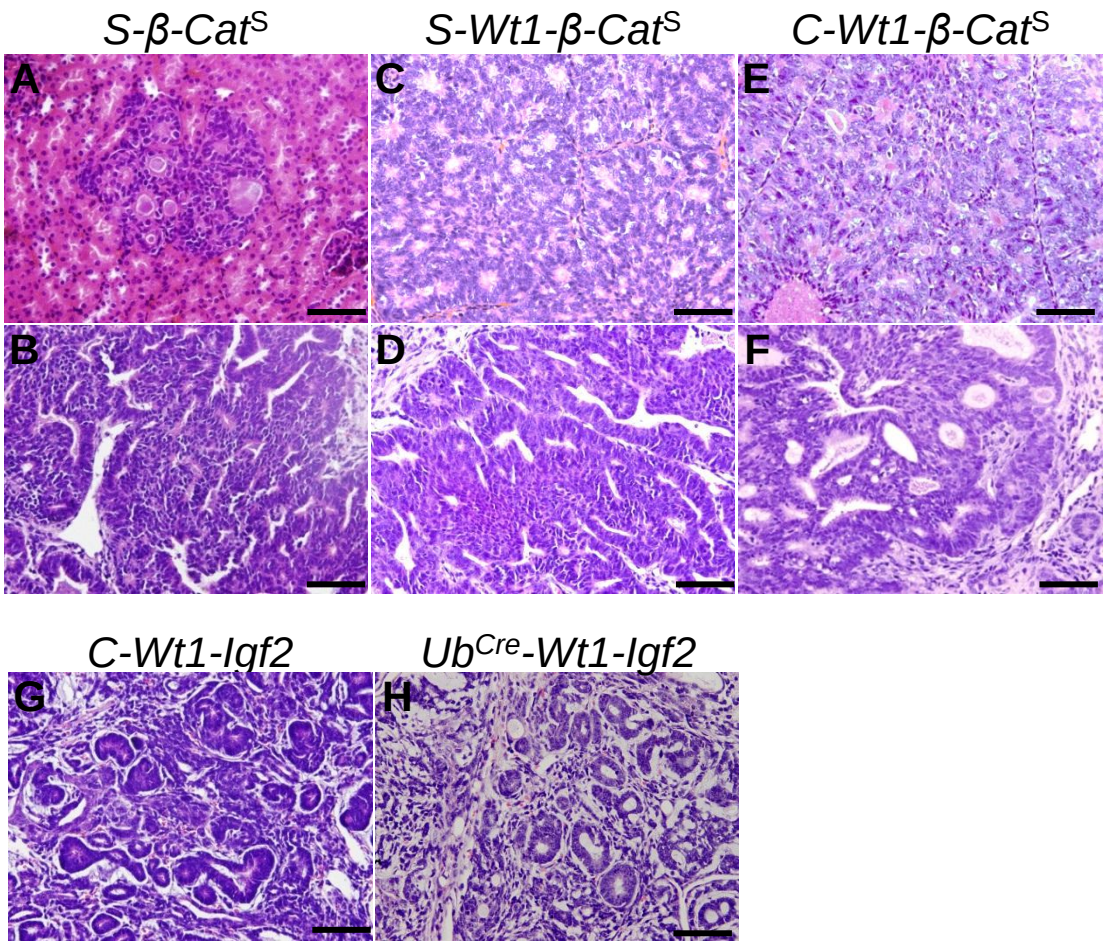

Figure 3.7 Histology of WTs from Six2^{GCE} and Cited1^{Cre} mutant mice.

H&E staining of WT sections of S-β-cat^S, S-Wt1-β-cat^S, C-Wt1-β-cat^S, and C-Wt1-Igf2 mice. The S-β-cat^S (A&B), S-Wt1-β-cat^S (C&D), and C-Wt1-β-cat^S (E&F) tumors had a very similar epithelial histology. Rosettes lack of nuclear concentration at the center were present in S-β-cat^S (A), S-Wt1-β-cat^S (C), and C-Wt1-β-cat^S (E) tumors. Predominant tubules with cuboidal or columnar cells were present in S-β-cat^S (B), S-Wt1-β-cate^S (D), C-Wt1-β-cat^S (F) tumors. By contrast, C-Wt1-Igf2 (G) tumors had a triphasic histology with blastema, epithelia and stromal elements. (H) Triphasic histology of Ub^{Cre}-Wt1-Igf2 tumors. Scale bars: 100 µm.

3.8 *S/C-Wt1-β-cat*^{S} and *C-Wt1-Igf2* mouse tumors were proliferative

To characterize the proliferation profile of the tumors, Ki67 IHC staining was performed. The *S-Wt1-β-cat*^{S}, *C-Wt1-β-cat*^{S} and *C-Wt1-Igf2* tumors displayed the tumors cells were actively proliferating as assessed by Ki67 staining. However, the *S-Wt1-β-cat*^{S} and *C-Wt1-β-cat*^{S} tumors had proliferative cells mostly in their epithelial elements (Fig. 3.8) whereas the *C-Wt1-Igf2* tumors had a high proportion of proliferative cells in the blastemal and epithelial elements and some in the stromal (Fig. 3.8).

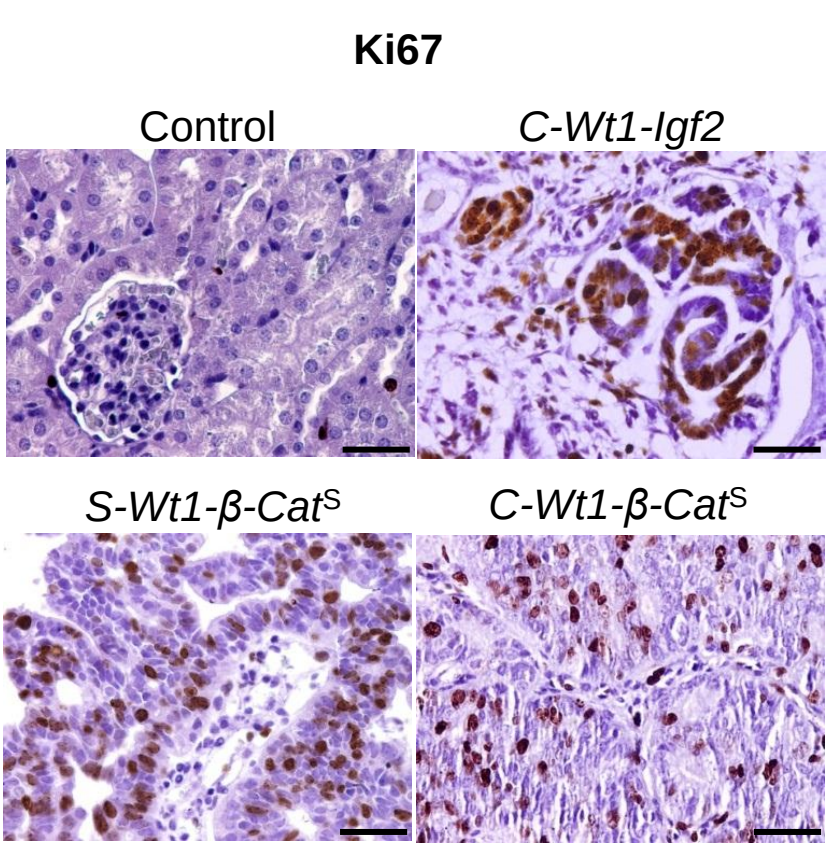

Figure 3.8 WTs from Six2^{GCE} and Cited1^{Cre} mutant mice were highly proliferative.

Ki67 IHC staining of tumor sections from control , S-Wt1-β-cat^{S}, C-Wt1-β-cat^{S}, and C-Wt1-Igf2 tumors. Scale bars: 50 µm.

3.9 *Wt1-β-cat*^{S} and *Wt1-Igf2* tumors showed different RNA expression of epithelial differentiation markers

Different subsets of human Wilms tumors had various expression profiles of developmentally regulated genes (Gadd et al., 2012). One subset histologically and molecularly corresponded to a differentiated epithelial stage of renal mesenchyme, while certain other subsets showed a histology and gene expression profile arrested at an early stage of renal mesenchyme (Gadd et al., 2012). In our mouse models, the *S/C-Wt1-β-cat*^{S} tumors showed an epithelial histology whereas the *C-Wt1-Igf2* tumors had a less differentiated blastemal predominant histology. Therefore to examine whether, with the same nephron progenitor cell origin (SIX2^{+} or CITED1^{+}), *S/C-Wt1-β-cat*^{S} tumors and *C-Wt1-Igf2* tumors had different expression of developmentally regulated genes, we characterized the gene/protein expressions of various differentiation stage markers in the tumors with qRT-PCR and IHC assays.

Detection of RNA expression in these tumors using qRT-PCR demonstrated that the *S/C-Wt1-β-cat*^{S} and *S-β-cat*^{S} tumors had very low expression of the early mesenchyme markers such as *Eya1*, *Osr1*, *Hoxa11*, and *Pax2*, which are essential for the function and survival of the undifferentiated metanephric mesenchyme (Fig. 3.9). Compared to the *S/C-Wt1-β-cat*^{S} and *S-β-cat*^{S} tumors, *C-Wt1-Igf2* tumors had a significantly higher expression of these markers at early stage of renal mesenchyme differentiation (Fig. 3.9).

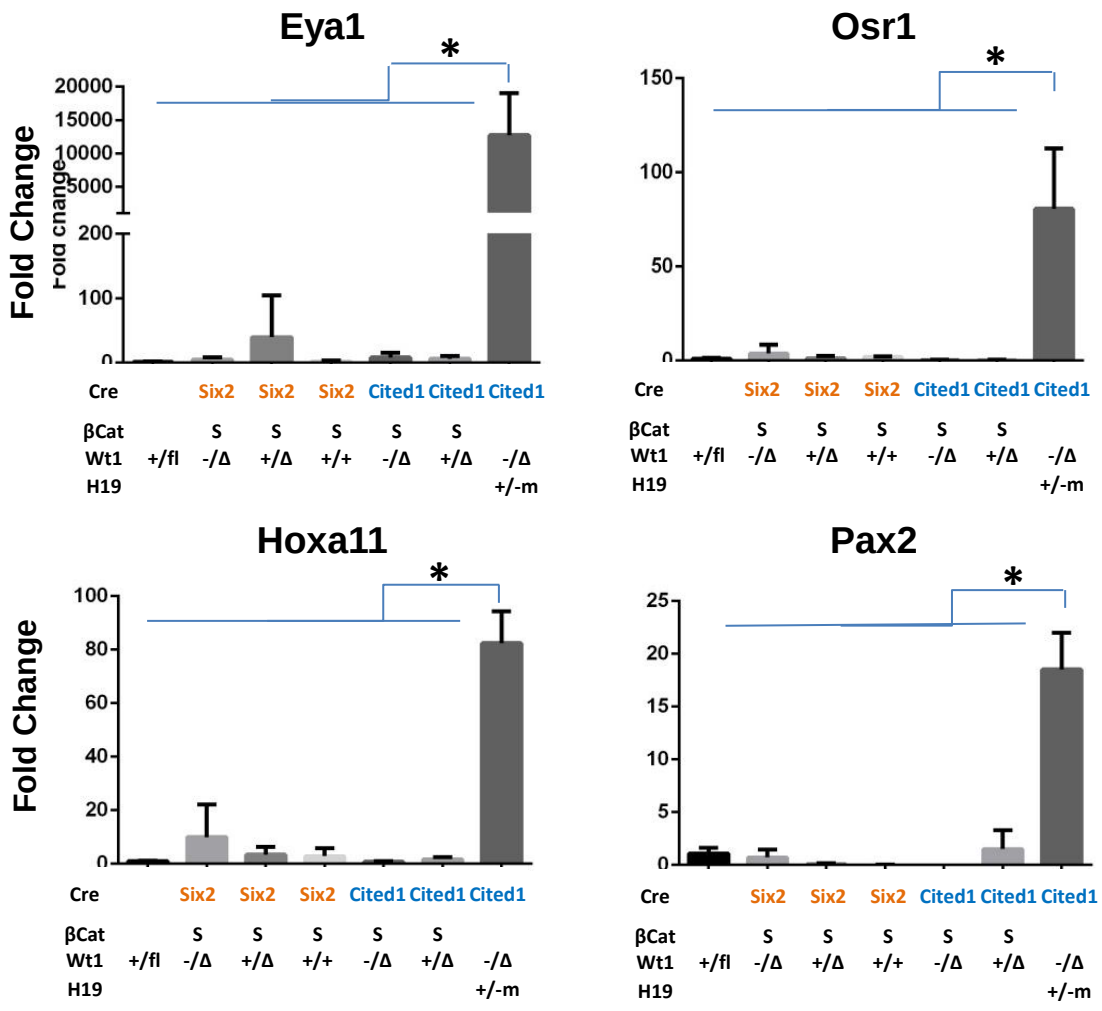

Figure 3.9 Comparison of gene expression of early mesenchyme markers in WTs of Six2^{GCE} and Cited1^{Cre} mutant mice.

qPCR analysis of intermediate mesenchyme and early metanephric mesenchyme markers in mouse tumors showed very low expression of these markers in S/C-Wt1-β-cat^{S} and S-β-cat^{S} tumors, and a significant higher expression in C-Wt1-Igf2 tumors.

Intermediate epithelial differentiation markers were also analyzed, such as *Wnt4* and *CyclinD1*, which are specifically expressed in the renal vesicle, and Jag1, a marker in proximal tubule epithelium which is more differentiated than the renal vesicle. The qRT-PCR results showed that the *S/C-Wt1-β-cat*^{S} and *S-β-cat*^{S} tumors had low expression of Wnt4 and *CyclinD1*, while *C-Wt1-Igf2* tumors had a significantly increased expression of these precursor epithelial markers (Fig. 3.10). The *S/C-Wt1-β-cat*^{S} and *S-β-cat*^{S} tumors had lower expression of *Jag1* than *C-Wt1-Igf2* tumors, but the difference was not statistically significant (Fig. 3.10). In contrast, there was no difference in the mRNA expression level of E-cadherin between S/*C-Wt1-β-cat*^{S}, *S-β-cat*^{S} and *C-Wt1-Igf2* tumors (Fig. 3.10).

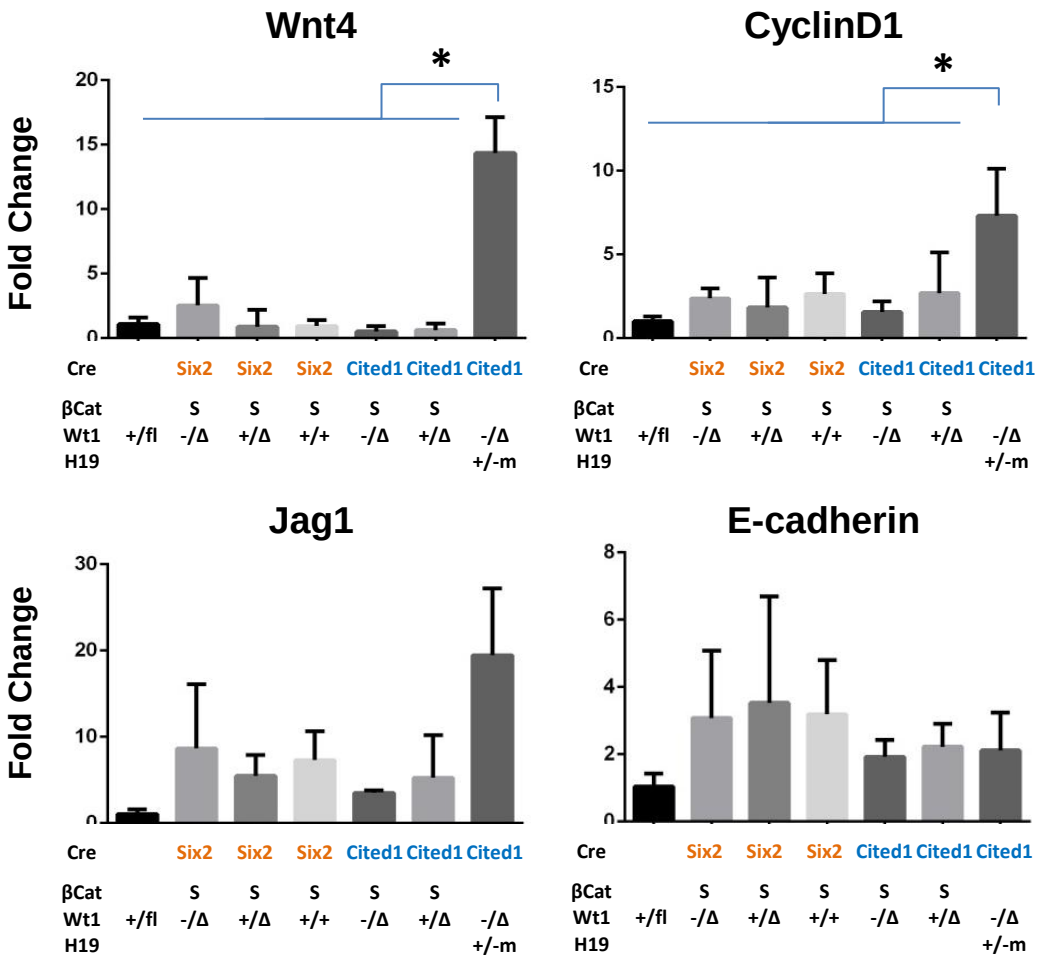

Figure 3.10 Comparison of gene expression of epithelia precursor and epithelia markers in WTs of Six2^{GCE} and Cited1^{Cre} mutant mice.

qPCR analysis showed that S/C-Wt1-β-cat^{S} and S-β-cat^{S} tumors had a low level of expression of markers in post-induction renal vesicle (Wnt4 and CyclinD1) and proximal tubule (Jag1). By contrast, C-Wt1-Igf2 tumors had a significant higher expression in Wnt4 and CyclinD1, increased but not significant higher expression of Jag1. There was no difference in RNA expression of terminal epithelial differentiation marker E-cadherin between these tumors.

3.10 *Wt1-β-cat*^{S} and *Wt1-Igf2* tumors showed slightly increased expression of muscle differentiation genes when compared to expression in normal kidneys

Histologic examination of human Wilms tumors with *WT1* mutation have shown ectopic muscle elements in the tumors, and genes involved in muscle differentiation were found up-regulated in Wilm tumors with *Wt1* mutations or *Wnt/β-catenin* activation (Fukuzawa et al., 2004). Therefore, we checked gene expression of the muscle differentiation markers in mouse tumors. qRT-PCR analysis showed that, compared to normal kidneys, the S/*C-Wt1-β-cat*^{S}, *S-β-cat*^{S} and *C-Wt1-Igf2* tumors had a slightly increased expression of myogenesis markers, eg. *Titin* and *Actin-α1*, but the differences were not significant (Fig. 3.11).

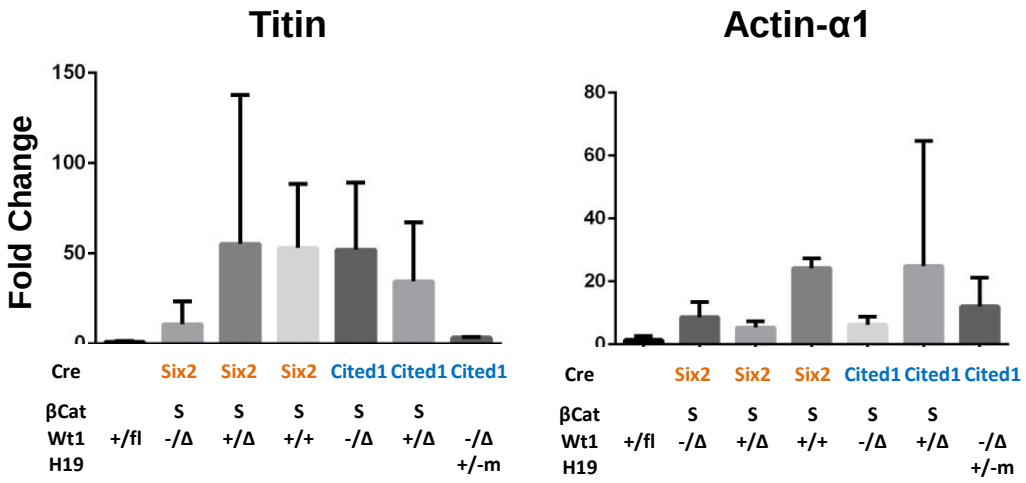

Figure 3.11 qPCR analysis of gene expression of muscle cell differentiation markers in WTs of Six2^{GCE} and Cited1^{Cre} mutant mice.

The S/C-Wt1-β-cat^{S}, S-β-cat^{S} and C-Wt1-Igf2 tumors had a slightly higher expression of markers in myogenesis, Titin and Actin-α1, than the normal adult kidneys.

3.11 *S/C-Wt1-β-cat*^{S} and *C-Wt1-Igf2* tumors showed different protein expression pattern of differentiation markers

Examination of protein expression level and subcellular localization of lineage markers by IHC staining showed that the *S-Wt1-β-cat*^{S} and *C-Wt1-β-cat*^{S} tumors expressed nephron progenitor cell markers, *Cited1* and *Six2*, in their epithelial elements (Fig. 3.12). These tumors also expressed *Dlk1* in the epithelial cells and some stromal cells (Fig. 3.12). *Dlk1* is a stem cell marker and is highly expressed in blastemal component in human Wilms tumors with myogenesis (Fukuzawa et al., 2005). However, the tumors did not express *Pax2* which was robustly expressed in the undifferentiated metanephric mesenchyme (Fig. 3.12 and 3.22). In the *S-Wt1-β-cat*^{S} and *C-Wt1-β-cat*^{S} tumors, very few epithelial cells expressed CYCLIND1, a protein specifically expressed in the renal vesicle (Fig. 3.13). However, the tumor epithelial cells expressed *E-cadherin*, a terminally differentiated epithelial marker (Fig. 3.13). These results suggested that the *S-Wt1-β-cat*^{S} and *C-Wt1-β-cat*^{S} tumors preserved expression of nephron progenitor markers but also expressed markers of a later stage of epithelial differentiation.

In comparison, *C-Wt1-Igf2* tumors expressed progenitor makers, *Cited1* and *Six2*, and mesenchyme markers, *Dlk1* and *Pax2*, in the blastemal and epithelial cells (Fig. 3.12), and the epithelial precursor marker *CyclinD1* in some of the epithelial components (Fig. 3.13). However, they did not express *E-cadherin* (Fig. 3.13). These results suggested that the *C-Wt1-Igf2* tumors were more mesenchymal than the *S/C-Wt1-β-cat*^{S} tumors and that they maintained the progenitor-like features of their tumor initiating cells.

Altogether, although *S/C-Wt1-β-cat*^{S} tumors and *C-Wt1-Igf2* tumors arose from the same cell origin of nephron progenitors, the different genetic lesions (*Wt1-β-cat*^{S} vs. *Wt1-Igf2*) in these mutant mice resulted in different types of tumors, with the *S/C-Wt1-β-cat*^{S} tumors more epithelially differentiated while the *C-Wt1-Igf2* tumors display mesenchymal elements and less differentiated epithelial elements and high expression of the mesenchyme genes.

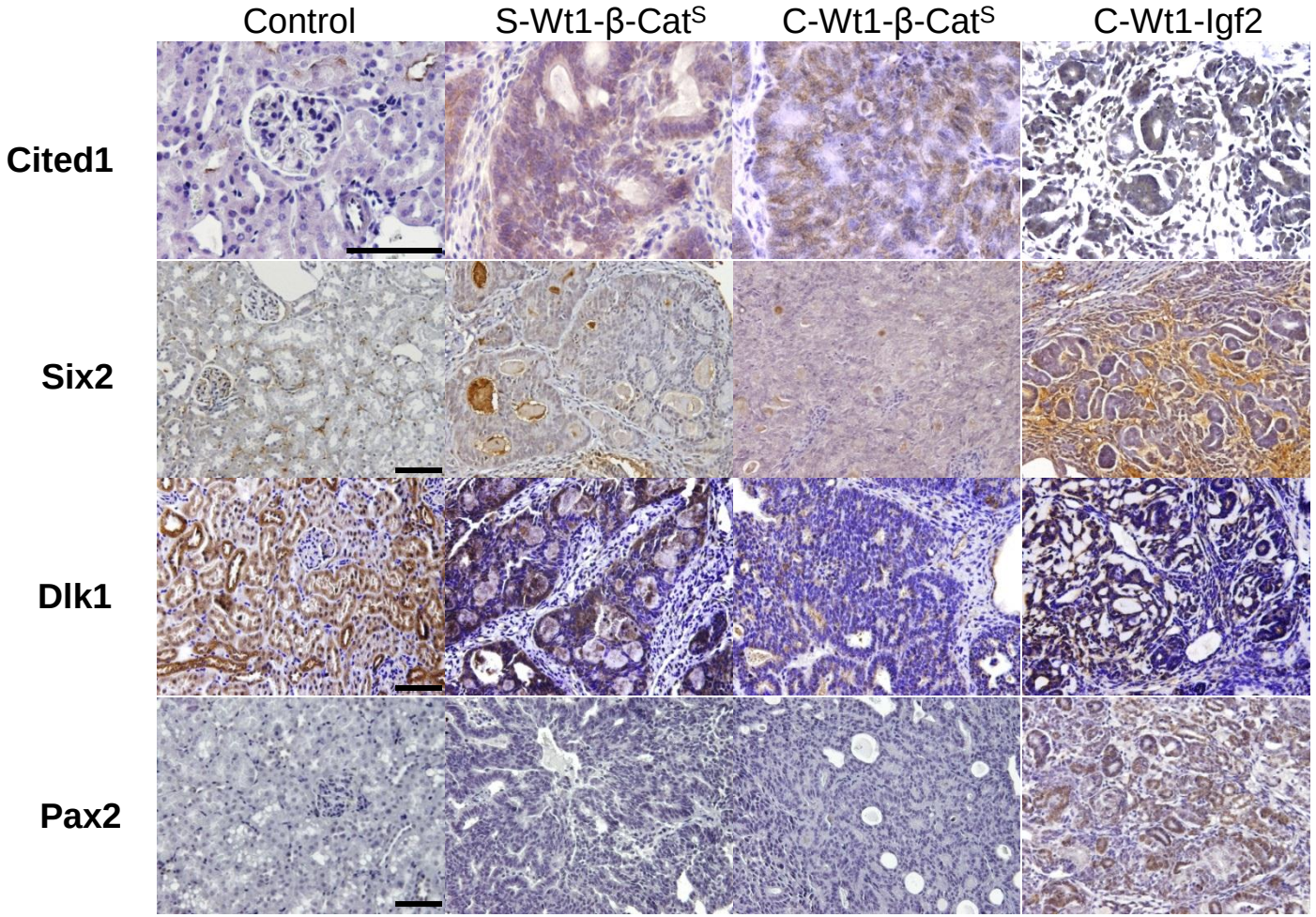

Figure 3.12 Expression of nephron progenitor markers and mesenchyme markers of WTs from Six2^{GCE} and Cited1^{Cre} mutants.

IHC staining of Cited1, Six2, Dlk1 and Pax2 on sections from normal kidneys, S-Wt1-β-cat^S tumors, C-Wt1-β-cat^S tumors and C-Wt1-Igf2 tumors. Scale bars: 100 μm.

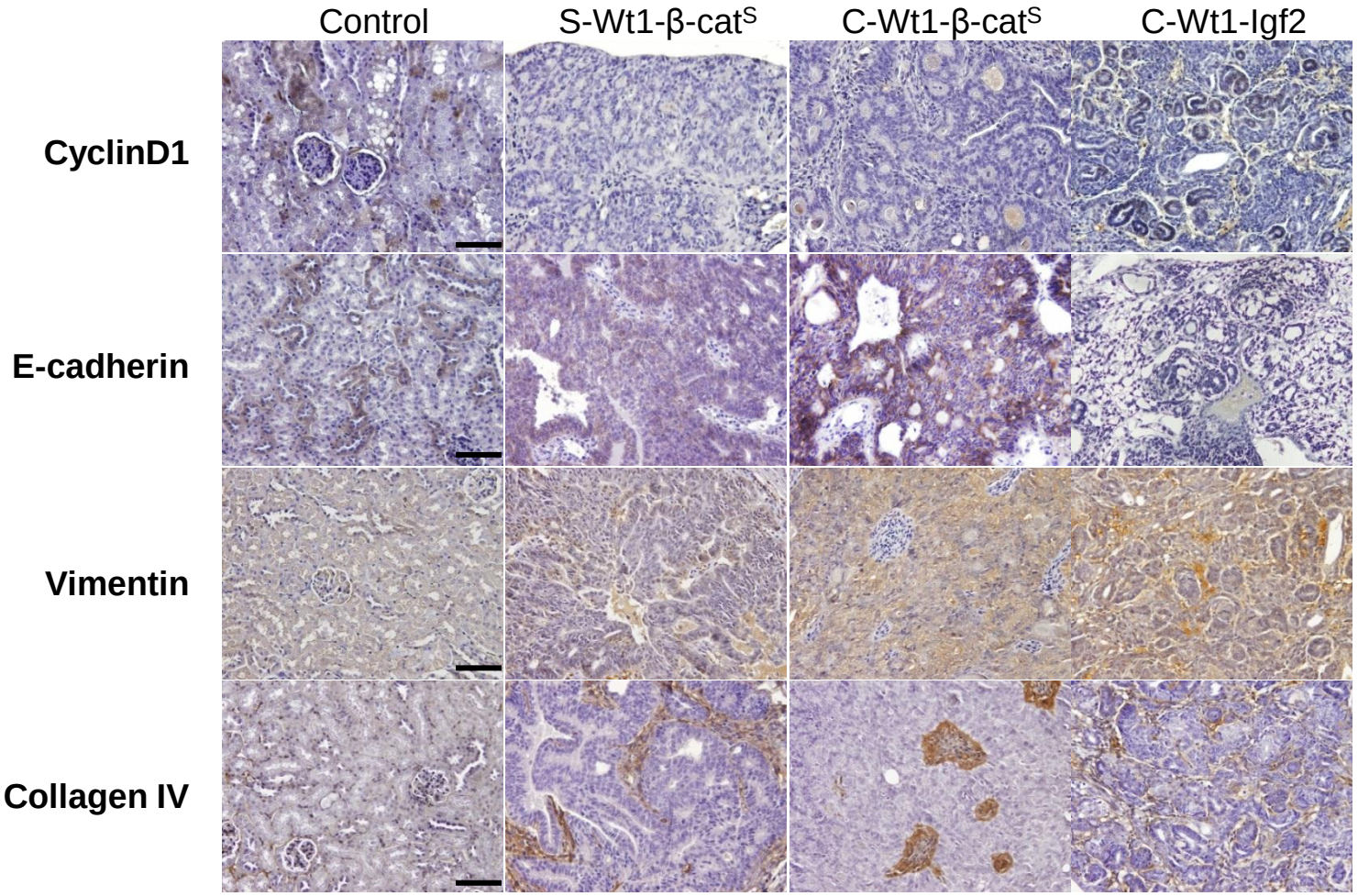

Figure 3.13 Expression of epithelia, mesenchyme and cell matrix markers in WTs of Six2^{GCE} and Cited1^{Cre} mutant mice.

IHC staining for CyclinD1, E-cadherin, Vimentin, and Collagen IV of sections from normal kidneys, S-Wt1-β-cat^{S} tumors, C-Wt1-β-cat^{S} tumors and C-Wt1-Igf2 tumors. Scale bars: 100 μm.

3.12 Expression of human WT blastemal marker and cellular matrix markers in *S/C-Wt1-β-cat^S* and *C-Wt1-Igf2* tumors

Vimentin expression is observed in the blatemal and stromal components of human Wilms tumors. Interestingly, the *S-Wt1-β-cat^S* and *C-Wt1-β-cat^S* tumors expressed *Vimentin* in tumor epithelial cells (Fig 3.13). The *C-Wt1-Igf2* tumors expressed *Vimentin* in blastemal, epithelial and stromal components in a diffuse manner (Fig. 3.13).

IHC staining of cellular matrix marker on tumor sections showed positive staining for COLLAGEN IV in the extracellular matrix of the stromal cells in the *S-Wt1-β-cat^S* tumors, *C-Wt1-β-cat^S* tumors and *C-Wt1-Igf2* tumors (Fig. 3.13).

3.13 β-catenin signaling and Wt1 target gene expression in mouse tumors

In the mutant mice, *β-catenin* stabilization or *Wt1* ablation was introduced. To determine whether their downstream signaling or expression of target genes was affected by the genetic alterations, we examined the activity of the *Wnt/β-catenin* pathway and the expression of *Wt1* transcriptional targets in the mouse tumors.

3.13.1 Nuclear accumulation of β-CATENIN protein in *S/C-Wt1-β-cat^S* tumors and increased cytoplasmic expression of β-CATENIN in *C-Wt1-Igf2* tumors

IHC staining of β-CATENIN showed that the *S/C-Wt1-β-cat^S* tumors and the *C-Wt1-Igf2* tumors had dramatically increased expression of β-CATENIN protein when compared to normal kidneys (Fig. 3.14). The *S/C-Wt1-β-cat^S* tumors showed a high level of β-CATENIN expression in the epithelial elements, and a large portion of these cells had β-CATENIN nuclear accumulation, confirming the stabilization of β-CATENIN in the *β-cat^S* tumor cells (Fig. 3.14). In comparison, β-CATENIN was expressed mainly in the cytoplasm of blastemal, epithelial and stromal components in the *C-Wt1-Igf2* tumors (Fig. 3.14).

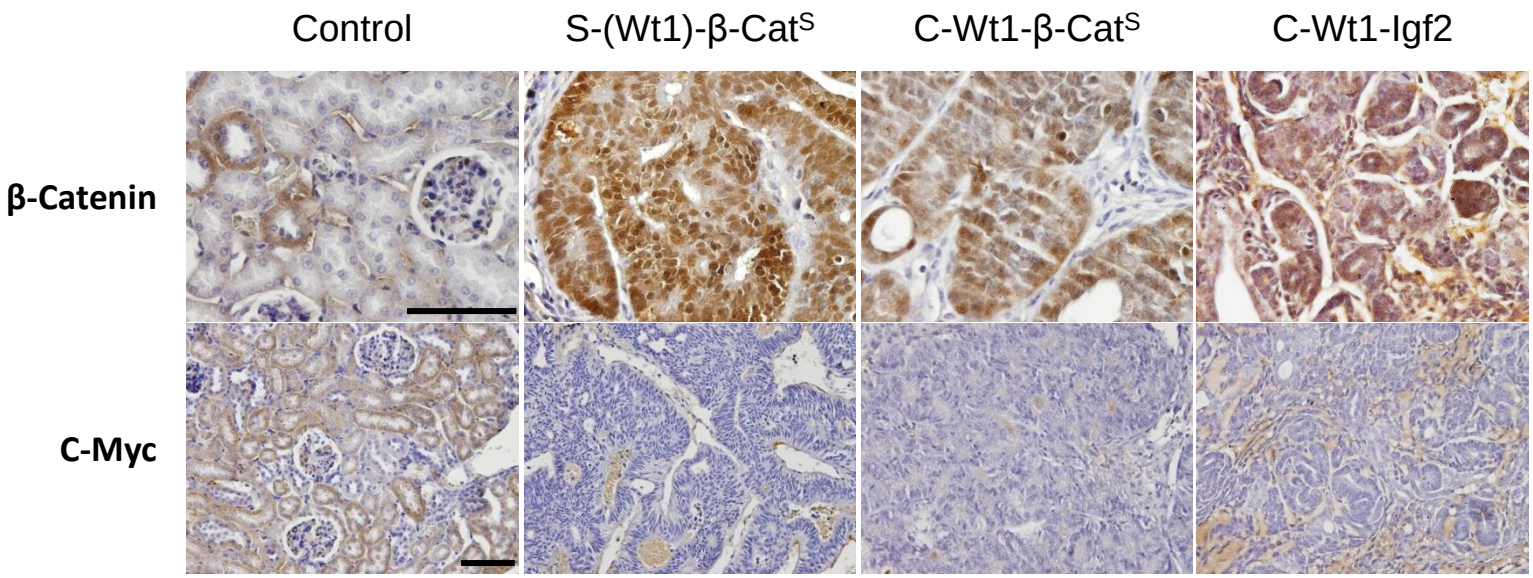

Figure 3.14 β-catenin signaling activity in WTs from Six2^{GCE} and Cited1^{Cre} mutant mice.

IHC staining of β-catenin and downstream target C-myc of sections from normal kidneys, S-Wt1-β-cat^{S} tumors, C-Wt1-β-cat^{S} tumors and C-Wt1-Igf2 tumors. Scale bars: 100 μm.

3.13.2 WNT/β-CATENIN signaling in mouse tumors

The RNA of β-CATENIN direct target *Axin2* was expressed in both *S/C-Wt1-β-cat*^{S} tumors and *C-Wt1-Igf2* tumors, compared to the very low expression of *Axin2* in control kidneys. The *S/C-Wt1-β-cat*^{S} tumors showed a slightly higher expression of *Axin2* than the *C-Wt1-Igf2* tumors (Fig. 3.15). This result is in agreement with the stabilization and nuclear accumulation of β-CATENIN protein in *S/C-Wt1-β-cat*^{S} tumors (Fig. 3.14). WNT/β-CATENIN inhibitor *Wif1* was also elevated in *S/C-Wt1-β-cat*^{S} tumors and *C-Wt1-Igf2* tumors compared to control kidneys (Fig. 3.15). The *S/C-Wt1-β-cat*^{S} tumors, however, had a much higher expression of *Wif1* than did the *C-Wt1-Igf2* tumors, suggesting a negative feedback loop responding to the stabilized β-CATENIN. Therefore, both *S/C-Wt1-β-cat*^{S} and *C-Wt1-Igf2* tumors displayed increased WNT/β-CATENIN activity, but the activity was higher in *S/C-Wt1-β-cat*^{S} tumors than *C-Wt1-Igf2* tumors. However, *S/C-Wt1-β-cat*^{S} tumors had low expression of other canonical targets of the β-CATENIN pathway, e.g., protein expression of C-MYC and transcription of *Cxxc4* (Fig. 3.14 & 3.15). Thus, we propose that β-CATENIN signaling promotes tumor growth through different sets of targets or acts through non-canonical cell-cell adhesion pathways.

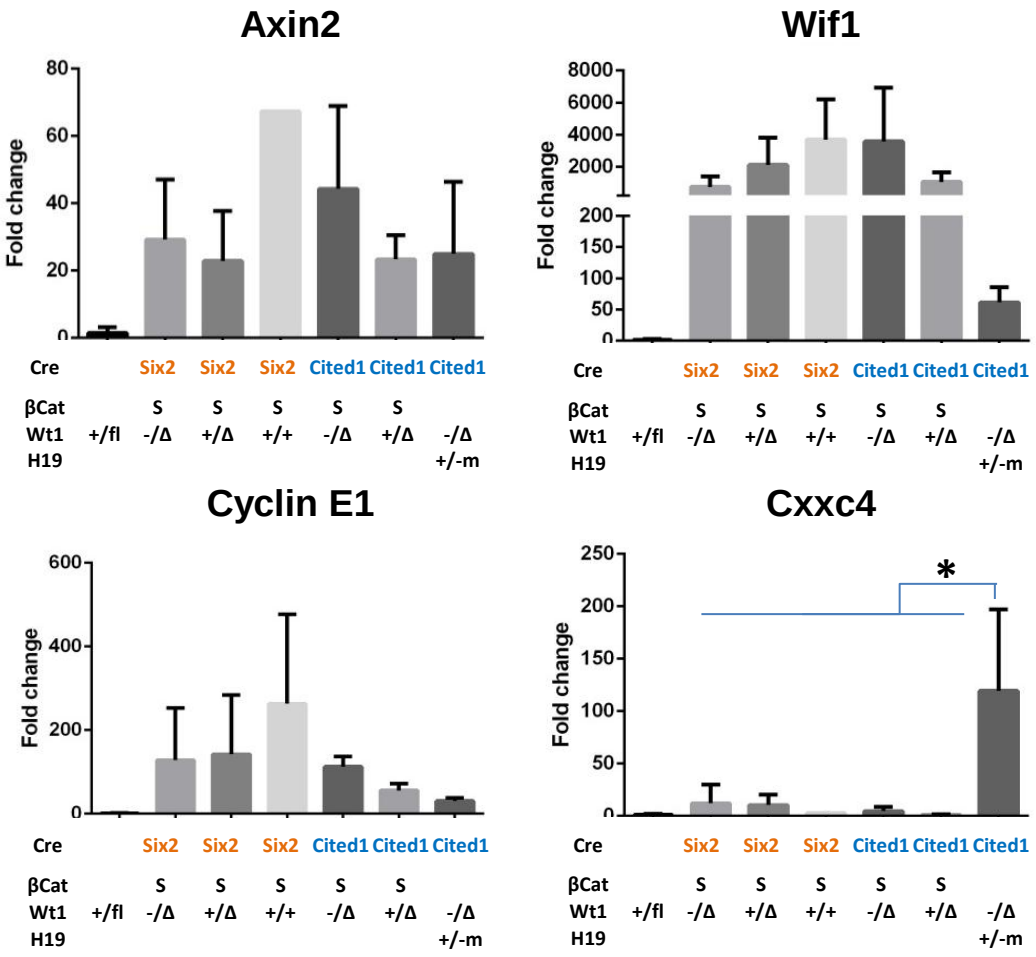

Figure 3.15 qPCR analysis of β-Catenin signaling and Wt1 target expression in WTs from Six2^{GCE} and Cited1^{Cre} mutant mice.

qPCR results showed that compared to normal kidneys, β-catenin pathway targets Axin2 and Cyclin E1 and Wnt/β-catenin inhibitors Wif1 were increased in S-Wt1-β-cat^{S} tumors, and Wt1 targets CXXC4 and Cyclin E1 were upregulated in C-Wt1-Igf2 tumors.

3.13.3 *Wt1* targets in mouse tumors

Cyclin E is a target of *β-catenin* transcriptional activation and *Wt1* transcriptional repression (Loeb et al., 2002). RNA expression of *Cyclin E* was increased in *S/C-Wt1-β-cat*^{S} tumors and *C-Wt1-Igf2* tumors compared to control kidneys (Fig. 3.15). *CXXC4* upregulation was found in *WT1* mutated human Wilms tumors (unpublished data in our lab). We therefore measured the transcription of *Cxxc4* and observed that *Cxxc4* was significantly increased in *C-Wt1-Igf2* tumors in comparison to *S/C-Wt1-β-cat*^{S} tumors and control kidneys (Fig. 3.15).

3.14 *S/C-Wt1-β-cat*^{S} and *C-Wt1-Igf2* tumors did not have increased pERK and pAKT expression

The MAPK/ERK signal transduction pathway has been shown to be activated in mouse Wilms tumor models (Clark et al., 2011; Hu et al., 2010). To test whether this pathway was altered in our mouse tumors, we performed IHC staining of the effectors in MAPK/ERK signaling. However, we did not detect positive staining for pERK and pAKT in *S/C-Wt1-β-cat*^{S} tumors and *C-Wt1-Igf2* tumors by IHC (Fig. 3.16).

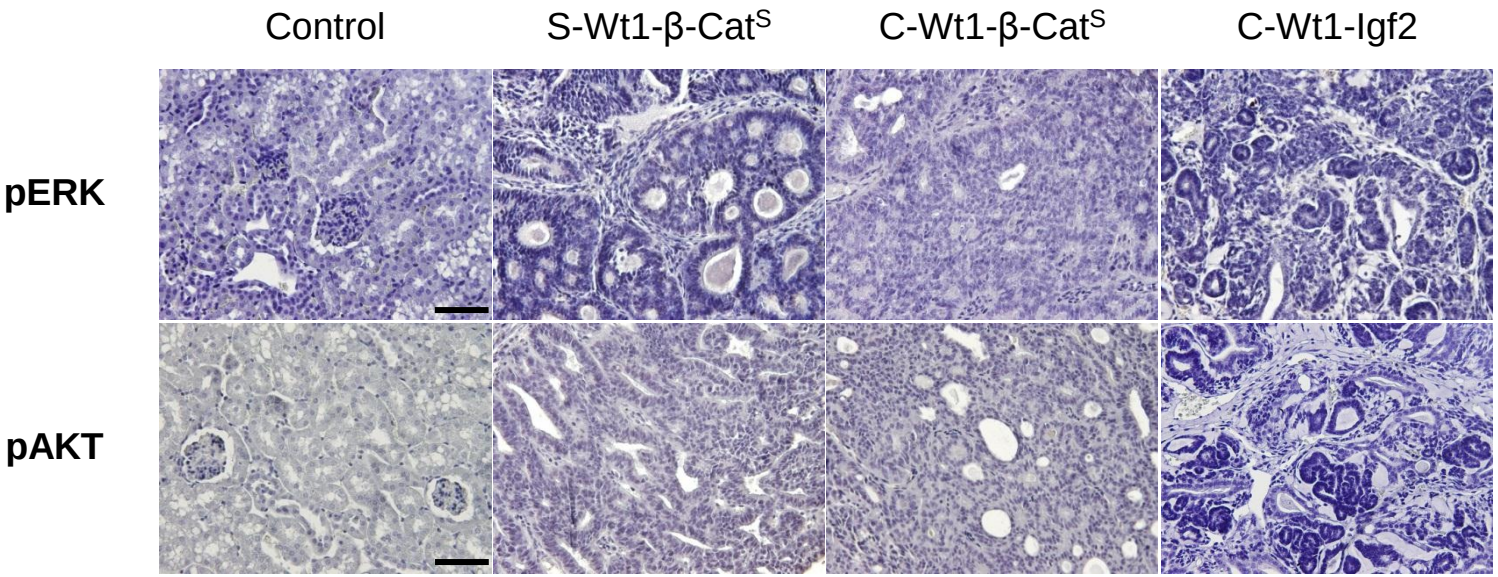

Figure 3.16 Expression of pERK and pAKT in WTs from Six2^{GCE} and Cited1^{Cre} mutant mice.

IHC staining of sections from normal kidneys, S-Wt1-β-cat^S tumors, C-Wt1-β-cat^S tumors and C-Wt1-Igf2 tumors showed negative staining of pERK and pAKT in tumors. Scale bars: 100 μm.

3.15 Proteomic analysis of *S/C-Wt1-β-cat^S* and *C-Wt1-Igf2* tumors

To identify cancer cell signaling pathways dysregulated in *S/C-Wt1-β-cat^S* and *C-Wt1-Igf2* tumors and pathways contributing to the differences in the differentiation status between *S/C-Wt1-β-cat^S* and *C-Wt1-Igf2* tumors, we carried out RPPA analysis. RPPA is a high-throughput proteomic assay which employs probing of a protein array with a panel of antibodies. The results of this assay demonstrated that the *S-Wt1-β-cat^S* tumors, the *C-Wt1-β-cat^S* tumors and the *C-Wt1-Igf2* tumors had a very similar protein expression profile (Fig. 3.17). Tumors targeted by *Six2^{GCE}* and *Cited1^{Cre}* were therefore similar in their protein expression, and *β-cat^S* tumors with differential gene dose of Wt1 were also very similar in their protein expression.

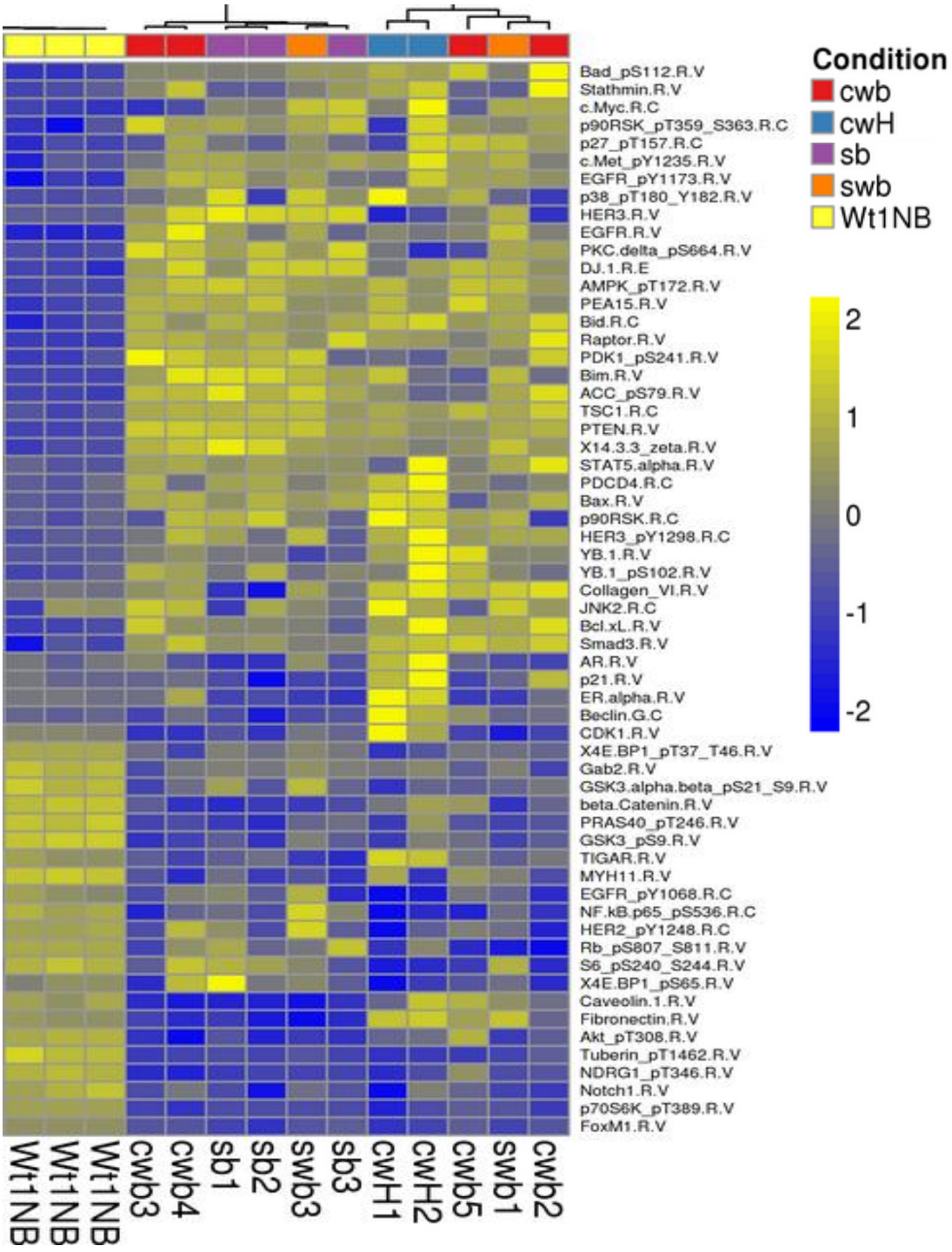

Figure 3.17 Heat map of the results of RPPA analysis of gene expression among mouse Wilms tumors.

Clustering with proteins differing among the groups from RPPA analysis showed similar protein expressions among mouse tumors. Cwb, C-Wt1$^{-/fl}$-β-cat^{S} tumors; cwH, C-Wt1-Igf2 tumors; sb, S-Wt1$^{-/fl}$-β-cat^{S} tumors; swb, S-Wt1$^{+/fl}$-β-cat^{S} tumors; Wt1NB, control new born kidneys.

3.16 Correlation of mouse *S/C-Wt1-β-cat*^{S} and *C-Wt1-Igf2* tumors to human WT subsets by gene expression analysis

A previous study has identified different subsets of human Wilms tumors by global gene expression profile (Gadd et al., 2012). Subset 1 (S1) was identified as epithelial predominant tumors with gene expression signatures correlated with late differentiation stage, while Subset 2-5 (S2-5) showed a signature of gene expression associated with early metanephric mesenchyme and a triphasic histology (Gadd et al., 2012). The differences in histology and gene expression between S1 and S2-5 were very similar to that between the mouse *S/C-Wt1-β-cat*^{S} and *C-Wt1-Igf2* tumors. Therefore, to find out whether *S/C-Wt1-β-cat*^{S} tumors expressed genes whose expression characterized S1 tumors and whether *C-Wt1-Igf2* tumors expressed genes whose expression characterized a certain subset among subsets S2-5 tumors, we examined the gene expression pattern in mouse tumors with selected genes that differentiated the S1 and S2-5 subsets. The qRT-PCR analysis demonstrated a similar pattern in expression of some genes assessed between human subsets and our mouse models. For example, the expression of genes *Hoxa11*, *HMGA2* and *Dlk1* were lower in *S/C-Wt1-β-cat*^{S} tumors than *C-Wt1-Igf2* tumors and also were lower in S1 than S2-5 (Fig. 3.18). The expression of other selected genes, however, did not show a clear correlation of the mouse tumors to human subsets (Fig. 3.18). Here we were limited by the numbers of genes tested and the methods used. Global gene expression analysis with micro-array and cross-species comparison and clustering approach are needed to explore the relationships between the mouse tumor models and patient tumor subsets.

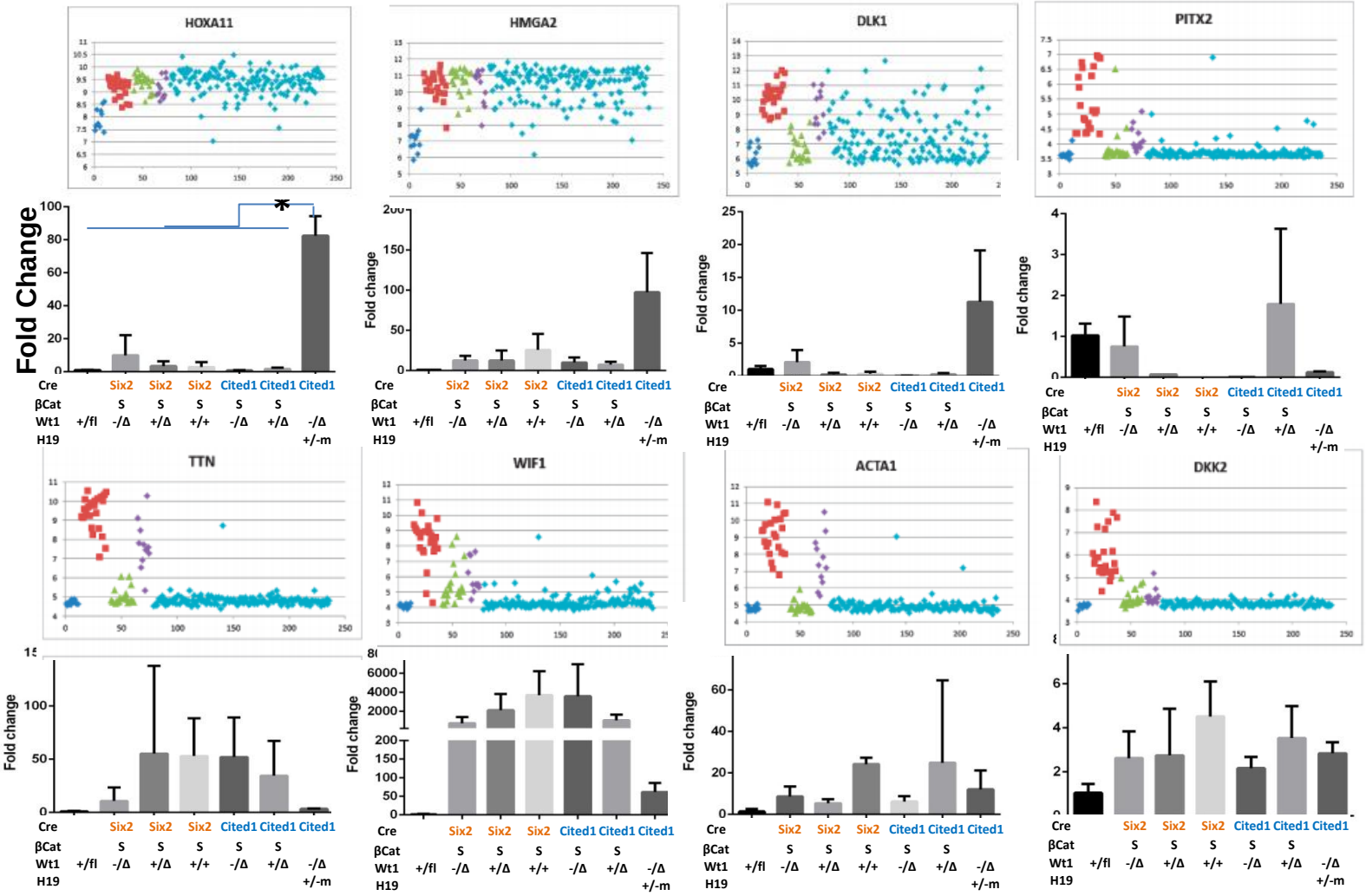

Figure 3.18 Analysis of possible correlation between mouse tumors to human WT subsets.

qRT-PCR analysis of S/C-Wt1-β-cat^{S} and C-Wt1-Igf2 tumors with genes differentiating human WT subsets.

Images are from Gadd, S., Huff, V., Huang, C.C., Ruteshouser, E.C., Dome, J.S., Grundy, P.E., Breslow, N., Jennings, L., Green, D.M., Beckwith, J.B., *et al.* (2012). Clinically relevant subsets identified by gene expression patterns support a revised ontogenic model of Wilms tumor: a Children's Oncology Group Study. Neoplasia *14*, 742-756.

Part II: *Wt1* function in kidney progenitors during development

Wt1 mutations predispose to Wilms tumor development, but the mechanisms by which *Wt1* mutations in the undifferentiated mesenchyme contribute to the cell transformation have still not been identified. Therefore, we investigated the *in vivo* function of *Wt1* specifically in kidney stromal and nephron progenitors by somatically deleting *Wt1* early during kidney development.

3.17 *Wt1* ablation in stromal progenitors did not affect kidney development

During kidney development, WT1 is expressed in the stromal progenitors and nephron progenitors in the undifferentiated metanephric mesenchyme (MM). It plays a critical role in cell survival and apoptosis of MM and MET during kidney development. With the progenitor-specific *Cre* to conditionally delete *Wt1*, we could test the biological functions of *Wt1* in each progenitor cell population. We applied a high dose of tamoxifen (6 mg/40 g bw) intraperitoneally to pregnant mice at E11.5 to ablate *Wt1* in a high proportion of progenitors (Foxd1^{+} or Six2^{+}).

The *Foxd1*$^{GCE/+}$*, Wt1* $^{-/fl}$ (*F-Wt1*) kidneys with *Wt1* ablation in stromal progenitors were examined at E19.5 and did not show a difference in morphology and histology compared to the controls (Fig. 3.19). The H&E staining showed that the mutant kidneys had the normal formation of mature nephrons, collecting ducts and stromal cells as in control kidneys (Fig. 3.19). IHC with WT1 staining showed that the *F-Wt1* mutant kidneys had normal development of metanephric mesenchyme, renal vesicles, comma-shaped bodies, S-shaped bodies and glomeruli, similar to that observed in control kidneys (Fig. 3.19).

To confirm that *Wt1* ablation did not affect the differentiation and function of stromal progenitors, we used *β-gal* as a reporter to track the *Wt1*-ablated progeny cells derived from stromal progenitors (*Foxd1*$^{GCE/+}$*, Wt1* $^{-/fl}$, *R26*$^{\beta gal/+}$). β-gal staining of mutant kidneys in E19.5

and 3.5 month-old mice showed that the *Wt1* ablated descendent cells from stromal progenitors retained stromal cell fates and differentiated normally into the interstitial cells, mesangial cells, pericytes and smooth muscle cells (Fig. 3.20). These results suggested that *Wt1* in stromal progenitors does not seem to play a critical role on nephrogenesis.

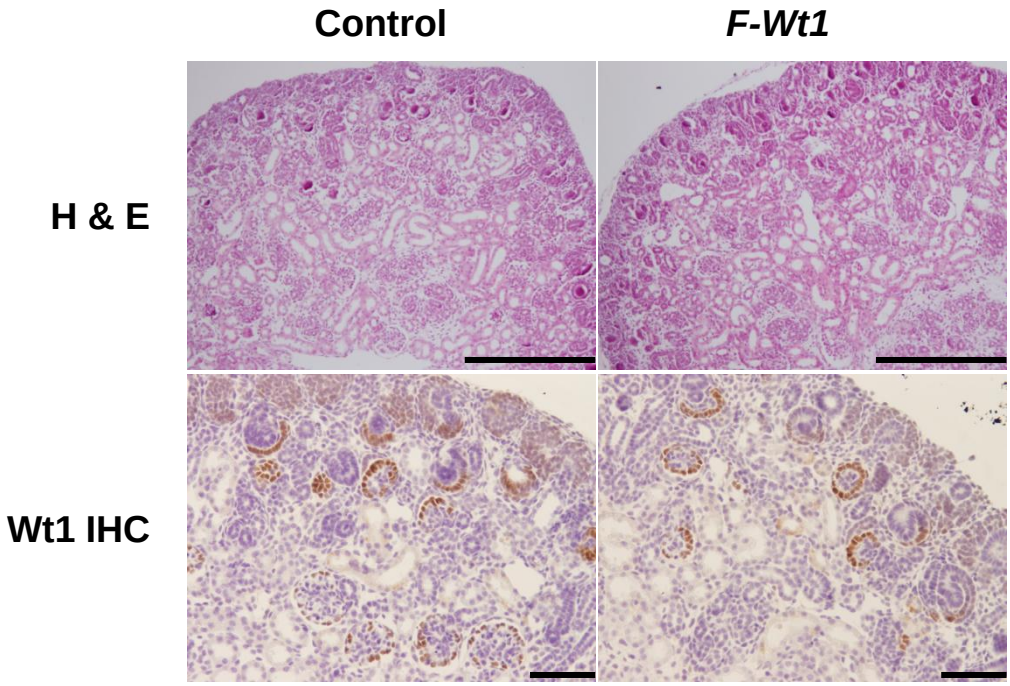

Figure 3.19 *Wt1* ablation in stromal progenitors (Foxd1^{+}) did not affect kidney development.

H&E and Wt1 IHC staining of kidney sections at E19.5 showed that the mutant F-Wt1 kidneys had normal histology and nephrogenisis shown by Wt1 positively stained normal metanephric mesenchyme, renal vesicle, comma-shaped body, S-shaped body and glomeruli as the control. Scale bars: 200 µm.

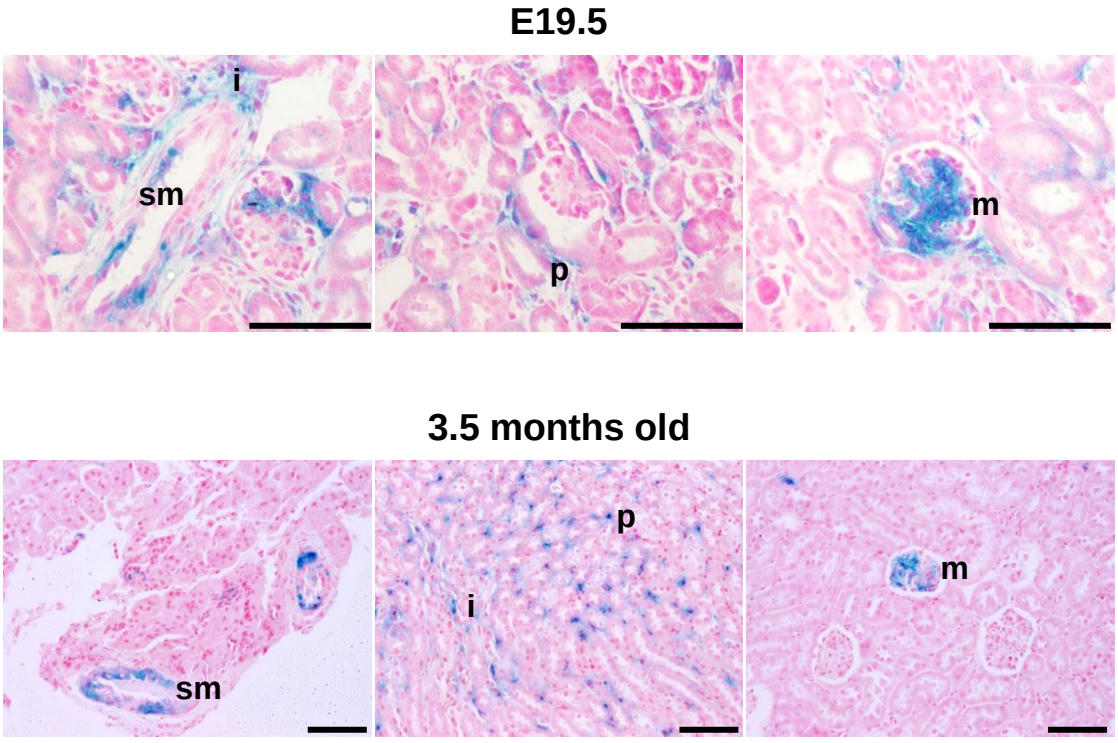

Figure 3.20 stromal progenitors with *Wt1* ablation showed normal cell differentiation.

β-gal staining of kidney sections from E19.5 and 3.5 months old F-Wt1 mutants showed that the β-gal labelled mutant cells differentiated normally into interstitial cells (i), mesangial cells (m), pericytes (p) and smooth muscle cells (sm). Scale bars: 100 μm.

3.18 *Wt1* ablation in nephron progenitors resulted in defects in nephrogenesis

In contrast, early *Wt1* ablation at E11.5 in the nephron progenitors disrupted nephrogenesis. Histological examination showed that *Six2*$^{GCE/+}$*, Wt1* $^{-/fl}$ (*S-Wt1*) mutant kidneys at E19.5 had an expanded nephrogenic zone (NZ) where the progenitors resided, reduced nephron formation, and increased number of stromal cells surrounding the epithelial structures, compared to the control kidneys (Fig. 3.21). In the control kidneys, the metanephric mesenchyme condenses to the cap mesenchyme (CM) around the tips of ureteric buds and the mesenchyme differentiates upon induction by the ureteric buds. The ureteric buds are usually surrounded by 2-3 layers of CM cells (CITED1+, WT1+ and PAX2+). However, when *Wt1* was ablated in the nephron progenitors, there were increased layers of CM cells (3-5 layers) around the ureteric buds in *S-Wt1* mutants (Fig. 3.21 and 3.22). The cells in the expanded NZ remained proliferative (Ki67^{+}) and maintained the expression of nephron progenitor cell marker CITED1 and metanephric mesenchyme marker PAX2 (Fig. 3.22), suggesting that the accumulated CM cells retained their progenitor cell features. IF staining of WT1 showed that the *S-Wt1* kidneys had marked reduction of comma-shaped bodies, S-shaped bodies and glomeruli (Fig. 3.23). IF staining of E-CADHERIN also showed the decreased formation of epithelial structures in the *S-Wt1* kidneys (Fig. 3.23). Moreover, the ureteric buds (DBA+) were slightly dilated in the *S-Wt1* kidneys, compared to the control (Fig. 3.23).

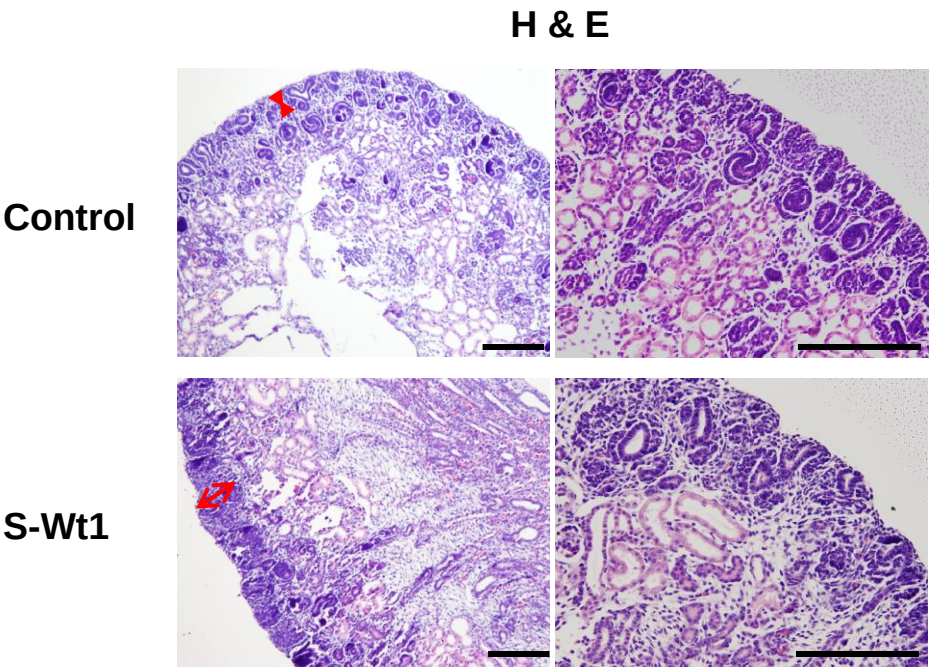

Figure 3.21 *Wt1* ablation in nephron progenitors resulted in the mesenchyme expansion and reduced nephrogenesis.

H&E staining of kidney sections at E19.5 showed that the mutant kidneys had an expanded nephrogenic zone (depth indicated by red arrows) and decreased formation of nephrons, compared to the control kidneys. Scale bars: 200 μm.

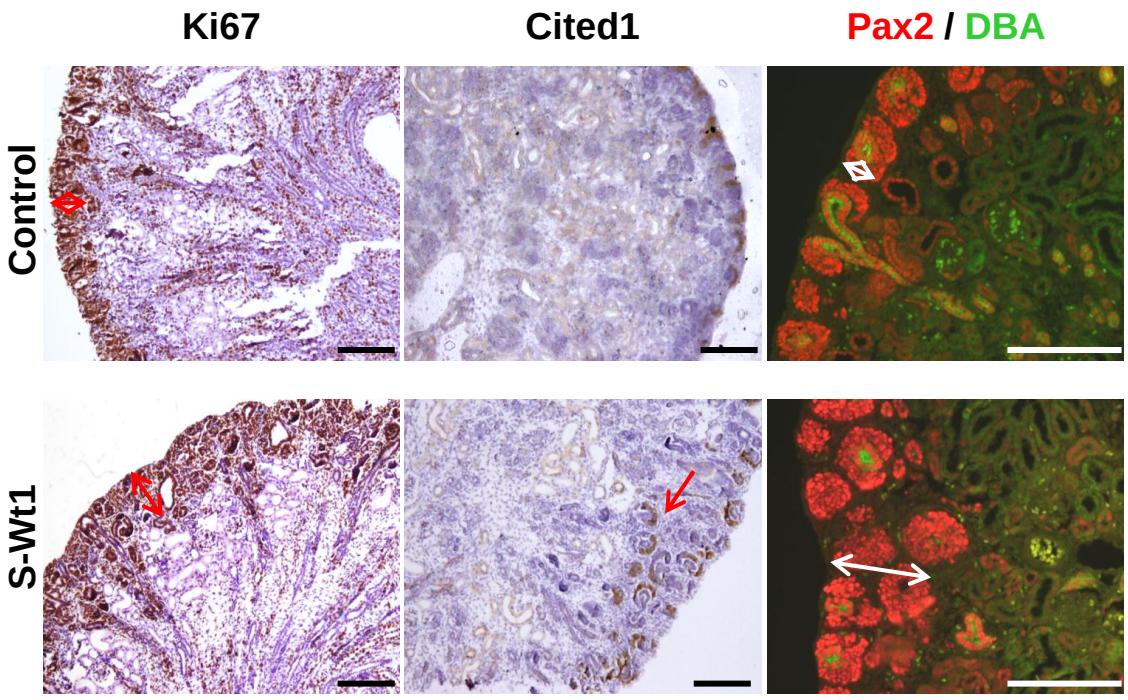

Figure 3.22 Nephron progenitors with Wt1 ablation remained proliferative and maintained progenitor marker expressions.

IF staining of kidney sections at E19.5 with proliferation marker Ki67 and progenitor markers Cited1 and Pax2. With Wt1 ablation, nephron progenitors in the expanded NZ were Ki67 positive and maintained the expression of Cited1 and Pax2. Pax2 was expressed in both progenitors and ureteric bud, so DBA was used here as a ureteric bud marker to indicate the Pax2+DBA- cap mesenchyme cells. Scale bars: 200 µm.

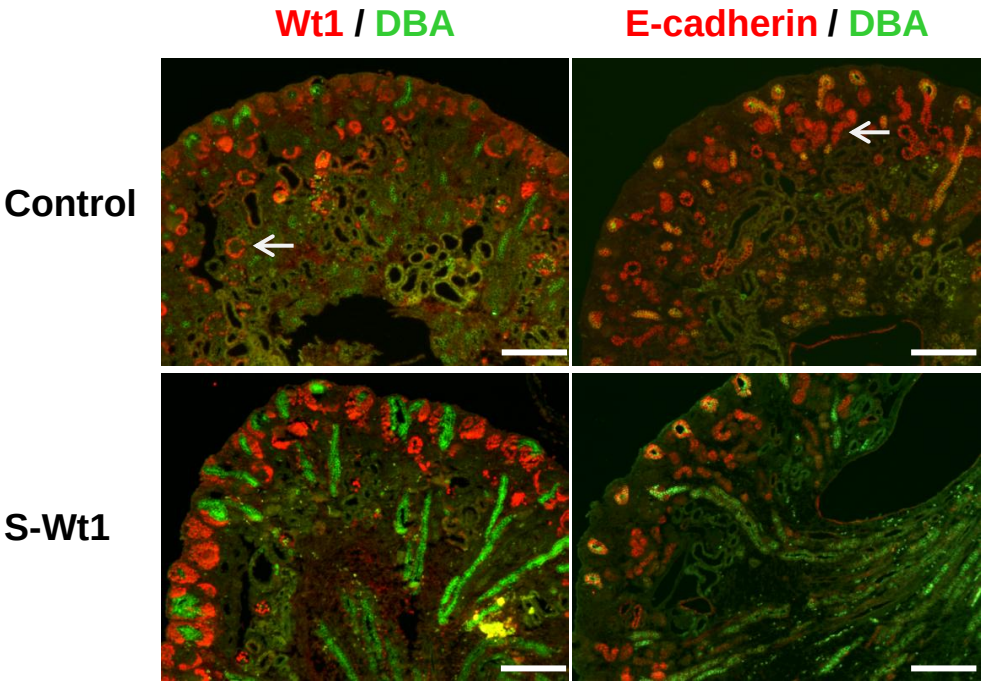

Figure 3.23 *Wt1* ablation in nephron progenitors resulted in decreased epithelial differentiation.

IF staining of kidney sections at E19.5 showing that the S-Wt1 mutant kidneys had a remarkable decrease in Wt1expressing comma-shaped bodies, S-shaped bodies and glomeruli. E-cadherin staining confirmed the reduced formation of epithelial structures caused by Wt1 ablation in nephron progenitors. DBA staining showing that the ureteric buds were slightly dilated in mutant kidneys compared to the control. (Arrow heads point to epithelial structures) Scale bars: 200 μm.

To check whether the phenotype observed in *S-Wt1* kidneys at E19.5 was evident at an earlier stage, we examined kidneys at E15.5. *S-Wt1* kidneys at E15.5 also showed an expansion of the NZ (Fig. 3.24). In the expanded NZ, there were increased cells in the CM (Fig. 3.24). Cells in the NZ of *S-Wt1* kidneys were proliferative ($Ki67^{+}$) and expressed CITED1 as shown by IHC staining (Fig. 3.25). Compared to control kidneys, the *S-Wt1* kidneys showed decreased formation of K-CADHERIN expressing early epithelial structures such as renal vesicle, comma-shaped bodies and S-shaped bodies (Fig. 3.25).

In all, these results suggested that *Wt1* ablation in the nephron progenitors prevented cells from differentiating but these cells maintained their progenitor cell state in terms of proliferation and expression the nephron progenitor markers.

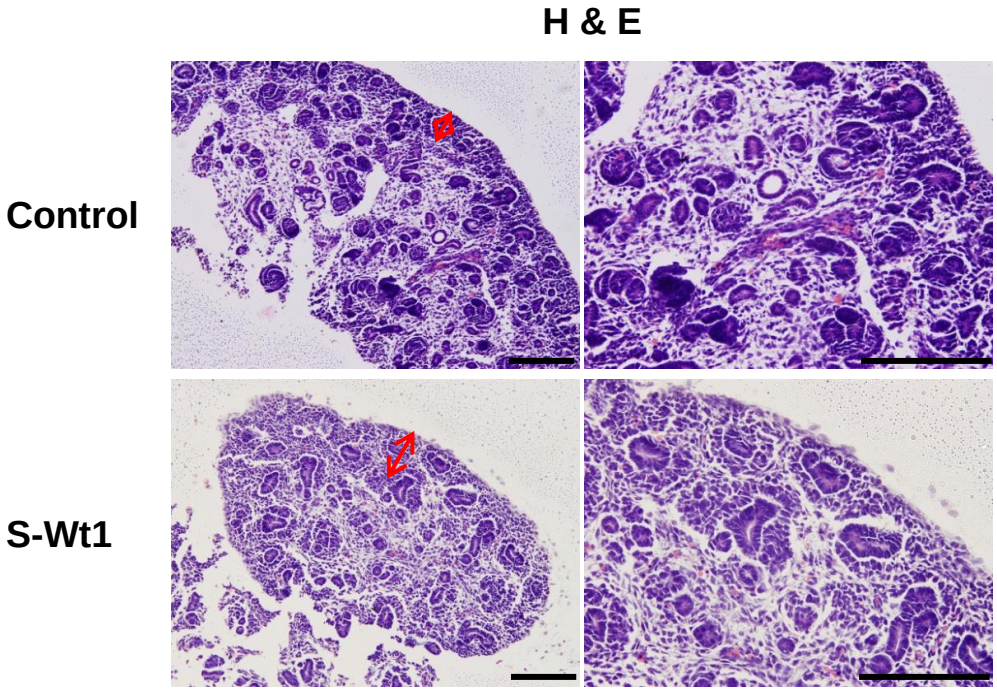

Figure 3.24 S-Wt1 mutants showed defects in nephrogenesis as early as at E15.5.

H&E staining of kidney sections from controls and S-Wt1 mutants at E15.5. The phenotypes of expanded NZ and disturbed epithelial differentiation were observed as early as E15.5 in mutant kidneys. Scale bars: 200 μm.

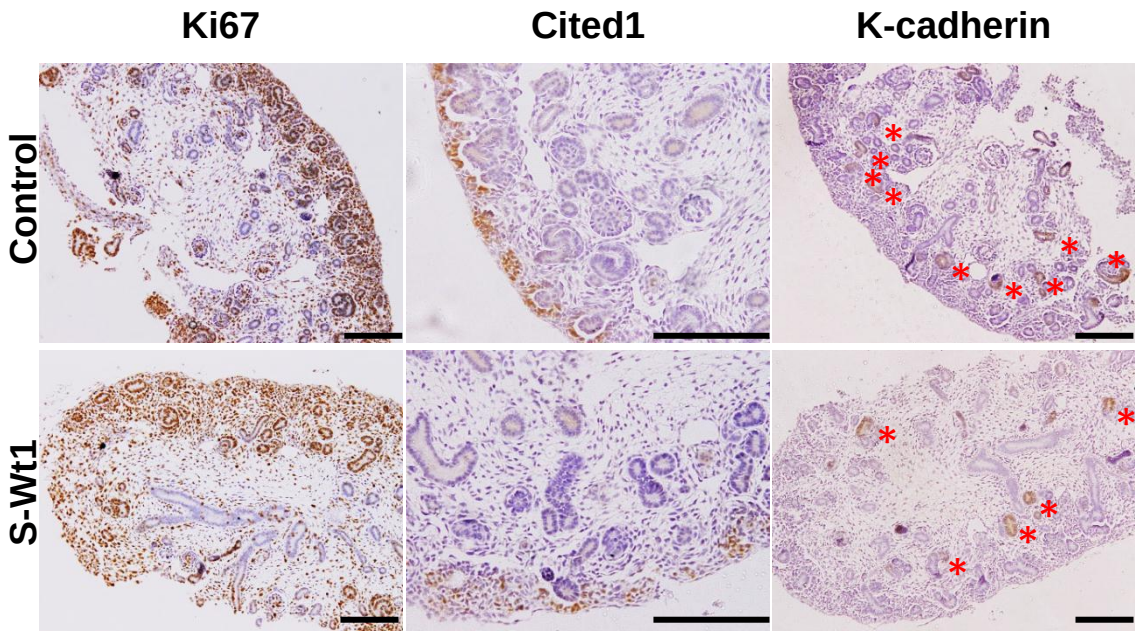

Figure 3.25 Marker expressions of S-Wt1 mutant kidneys at E15.5.

Ki67 staining showed that in S-Wt1 kidneys the expanded NZ was proliferative. The cells in the expanded NZ expressed progenitor marker Cited1. Compared to the controls, the mutant kidneys had fewer K-cadherin expressing early epithelial structures (*) such as renal vesicle, comma-shaped body and S-shaped body. Scale bars: 200 µm.

3.19 Lineage tracing of *Wt1* ablated nephron progenitors *in vivo*

To study the fate of *Wt1*-ablated nephron progenitors, we used *β-gal* or *tdTomato* as reporters to track the mutant cells in *S-Wt1* kidneys (*Six2*$^{GCE/+}$, *Wt1*$^{-/fl}$, *R26*$^{\beta gal/+}$ or *Six2*$^{GCE/+}$, *Wt1*$^{-/fl}$, *R26*$^{tdTomato/+}$). β-gal staining of mutant kidneys at E15.5 and E19.5 showed that most of the CM cells were labeled with β-gal, which suggested that the *Wt1* ablated progenitors retained their capacity for self-renewal. Moreover, β-gal was expressed in disorganized epithelial-like structures with closed lumen compared to normal tubule formation in the control kidneys (Fig. 3.26). This phenotype may result from abnormal differentiation of the *Wt1* ablated progenitors and possibly disrupted polarization in the cells. Very interestingly, the mutant kidneys had a few β-gal^{+} cells present in the kidney stromal, which was not detected in the control kidneys (Fig. 3.26). Whether this is due to mislocation of *Wt1* ablated cells in the stromal or a trans-differentiation of mutant cells from nephron progenitor cell origin to a stromal cell fate is not known.

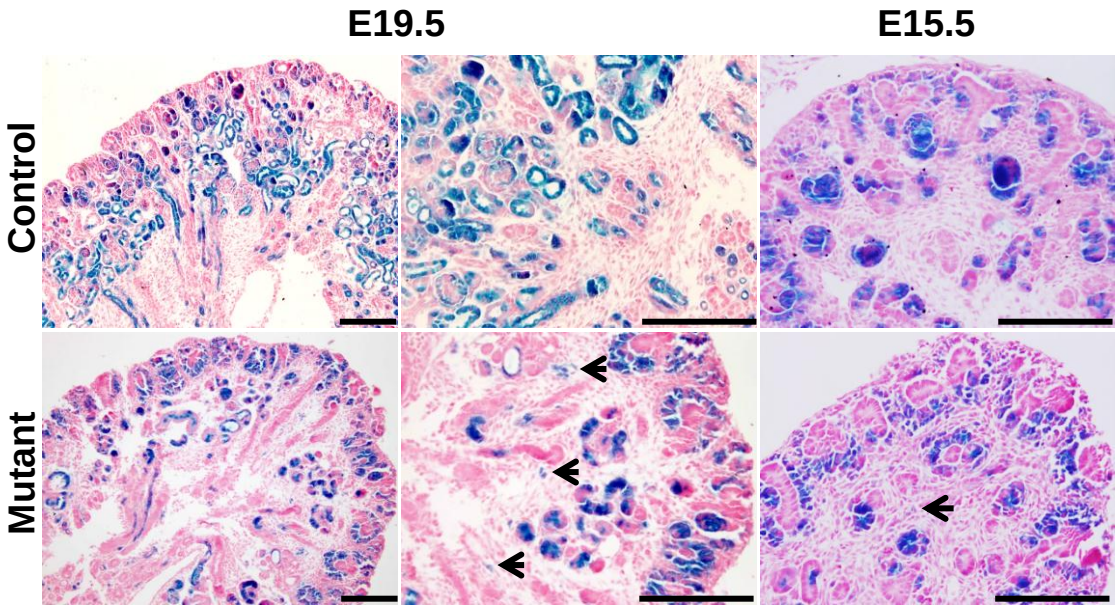

Figure 3.26 β-gal reporter tracing of *Wt1* ablated cells from nephron progenitor origin.

β-gal was expressed in the self-renewing progenitors in CM, in abnormally differentiated epithelial structures with closed lumen, and rarely but aberrantly in the the kidney stromal (arrow heads). Scale bars: 200 μm.

3.20 Tracing *Wt1* ablated cells from nephron progenitors with tdTOMATO reporter

To monitor the behavior of the cells from *Wt1* ablated nephron progenitors in real-time, we used a kidney rudiment culture system to visualize the rudiment growth by imaging cultures every 30 minutes for 3-4 days to generate time-lapse movies. tdTOMATO reporter was used to track the mutant cells.

Pregnant mice were injected with 6mg/40g BW tamoxifen at E11.5, then at E13.5 mutant kidneys *Six2*$^{GCE/+}$*, Wt1*$^{-/fl}$*, R26*$^{tdTomato/+}$ (*S-Wt1-tdTomato*) and littermate controls *Six2*$^{GCE/+}$*, Wt1*$^{+/fl}$*, R26*$^{tdTomato/+}$ (*S-tdTomato* with a wild type *Wt1*) were dissected out and cultured on filters with media supplied with tamoxifen so that the floxed allele of *Wt1* and *R26*^{tdTomato} were recombined in a very high efficiency. The rudiments were placed inside an incubator equipped with a fluorescent microscope. Live images and tdTOMATO fluorescence images of the whole kidney rudiment were taken during culture.

Representative images at the 15th and 51st hours of the rudiment culture showed that the wild type rudiments expressed tdTOMATO reporter robustly in the CM and clusters of differentiating epithelial cells (Fig. 3.27). However, the mutant rudiment had extended and elongated CM and lacked formation of epithelial structures (Fig. 3.27). PCR of isolated tdTOMATO expressing cells showed highly efficient *Wt1* ablation in tdTOMATO marked cells derived from nephron progenitors (Fig. 3.27).

To confirm the phenotype of impaired epithelial differentiation of mutant nephron progenitors, we characterized the expression of epithelial markers in the rudiments harvested after 3-day culture with immunofluorescence staining (IF). IF staining showed WT1 was expressed in cap mesenchyme and epithelial clusters in the control kidneys, while in the mutant the WT1 expressing cap mesenchyme was expanded, and very few WT1 expressing epithelial clusters were observed (Fig. 3.27). K-CADHERIN staining confirmed a remarkable decrease of epithelial structure formation in the mutant rudiments (Fig. 3.27).

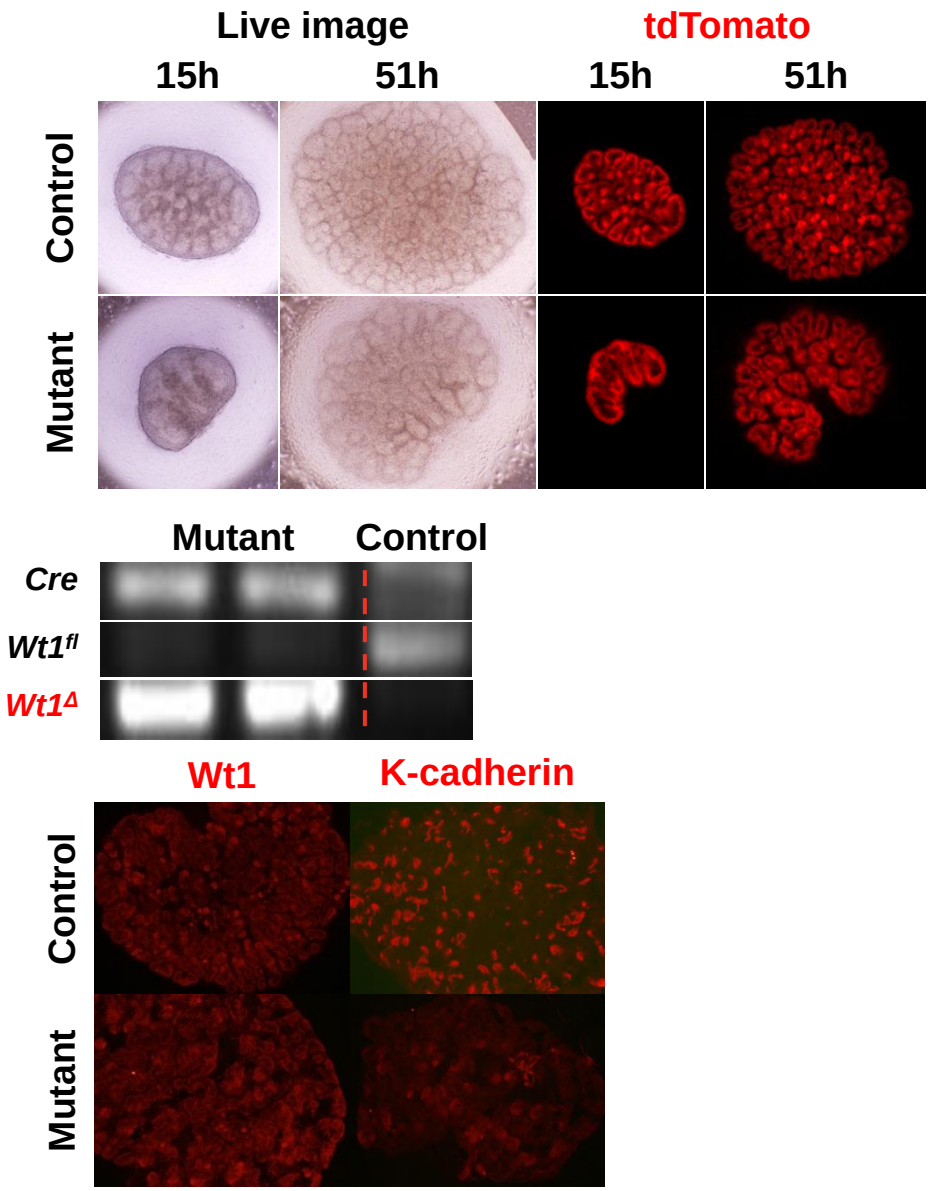

Figure 3.27 Tracking and monitoring Wt1 ablated cells from Six2^{GCE} with tdTomato reporter in kidney rudiment culture

Live field images and tdTomato images of rudiments during culture. PCR of isolated tdTOMATO^{+} cells confirmed efficient Wt1 ablation in nephron progenitor derived cells. IF staining of Wt1 showed mutant cells in cap mesenchyme were arrested in the MET. K-cadherin staining of the cultured rudiments confirmed the impaired formation of K-cadherin expressing epithelial structures.

To examine whether ureteric bud branching was affected by the differentiation arrested mesenchyme with *Wt1* ablation, we did IF staining of the rudiment with LAMININ, a ureteric bud marker. We calculated the branching efficiency based on how many branches developed from the trunk to the bud ends. Branching efficiency of the ureteric bud in the mutant (*Six2*$^{GCE/+}$*; Wt1*$^{-/fl}$) was slightly lower than the control with *Wt1* haploinsufficiency (*Six2*$^{GCE/+}$*; Wt1*$^{+/fl}$) and the control of *Wt1* wild type (*Wt1*$^{+/fl}$) (p-value=0.03) (Fig. 3.28).

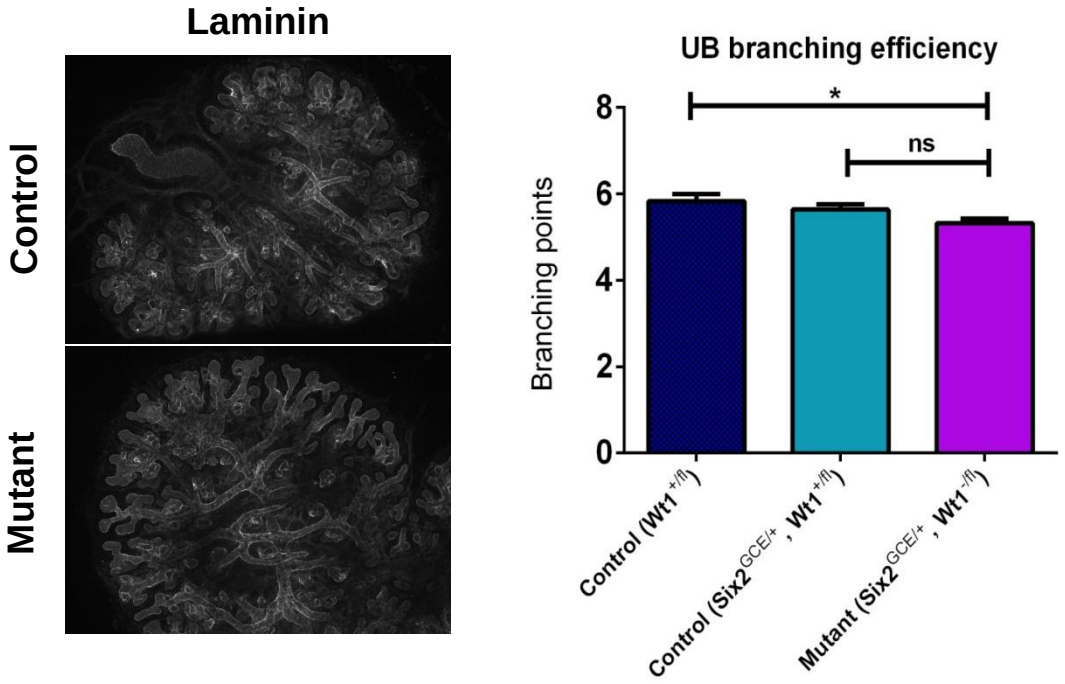

Figure 3.28 Mutant kidneys showed slightly decreased branching efficiency.

Laminin staining was used to visualize and highlight the ureteric buds for the calculation of the branching efficiency. After 3 day culture with tamoxifen, the mutant kidneys showed slightly less efficient in ureteric bud branching and slight dilation at the tips of the ureteric buds. Quantification of the ureteric bud branching efficiency showed that the mutant was not significantly different from the control *Six2*$^{GCE/+}$*; Wt1*$^{+/fl}$ with Wt1 haploinsufficiency, but was significantly less efficient in branching than the control *Wt1*$^{+/fl}$ with wild type Wt1.

3.21 Gene expression analysis of kidneys with *Wt1* ablation in nephron progenitors

To investigate what potential targets or signaling pathways were affected by WT1 loss of function in nephron progenitors, we performed qPCR analysis of the mutant and control kidneys at E19.5. Pregnant mice were injected with tamoxifen at E11.5 to ablate *Wt1* with *Six2*$^{GCE/+}$ at E11.5 and kidneys were dissected out and RNA isolated for qRT-PCR analysis. We tested genes which were identified as markers in human WTs, effectors in Wnt/β-CATENIN canonical and non-canonical Ca^{2+} pathway, differentiation markers in early mesenchyme and stromal and epithelial differentiation (Fig. 3.29). Among all the genes tested, two genes showed significant increase in mRNA expression of the mutants compared to the control (Fig. 3.29): *Axin2*, a Wnt/β-CATENIN direct target, and, *Osr1*, an early mesenchyme marker (Fig. 3.29). These results suggested that *Wt1* ablation in nephron progenitors resulted in increased the Wnt/β-CATENIN signaling, in agreement with a previous study that showed that *Wt1* was a repressor for the Wnt/β-CATENIN pathway (Chang et al., 2008). The results of *Osr1* up-regulation in *S-Wt1* kidneys and the presence of *S-Wt1* cells in kidney stromal suggested that *Wt1* ablation in the nephron progenitors may help cells to acquire long-term self-renewal and differentiation plasticity to an earlier lineage, and potentially prepare the cells to be transformed to a tumor cell.

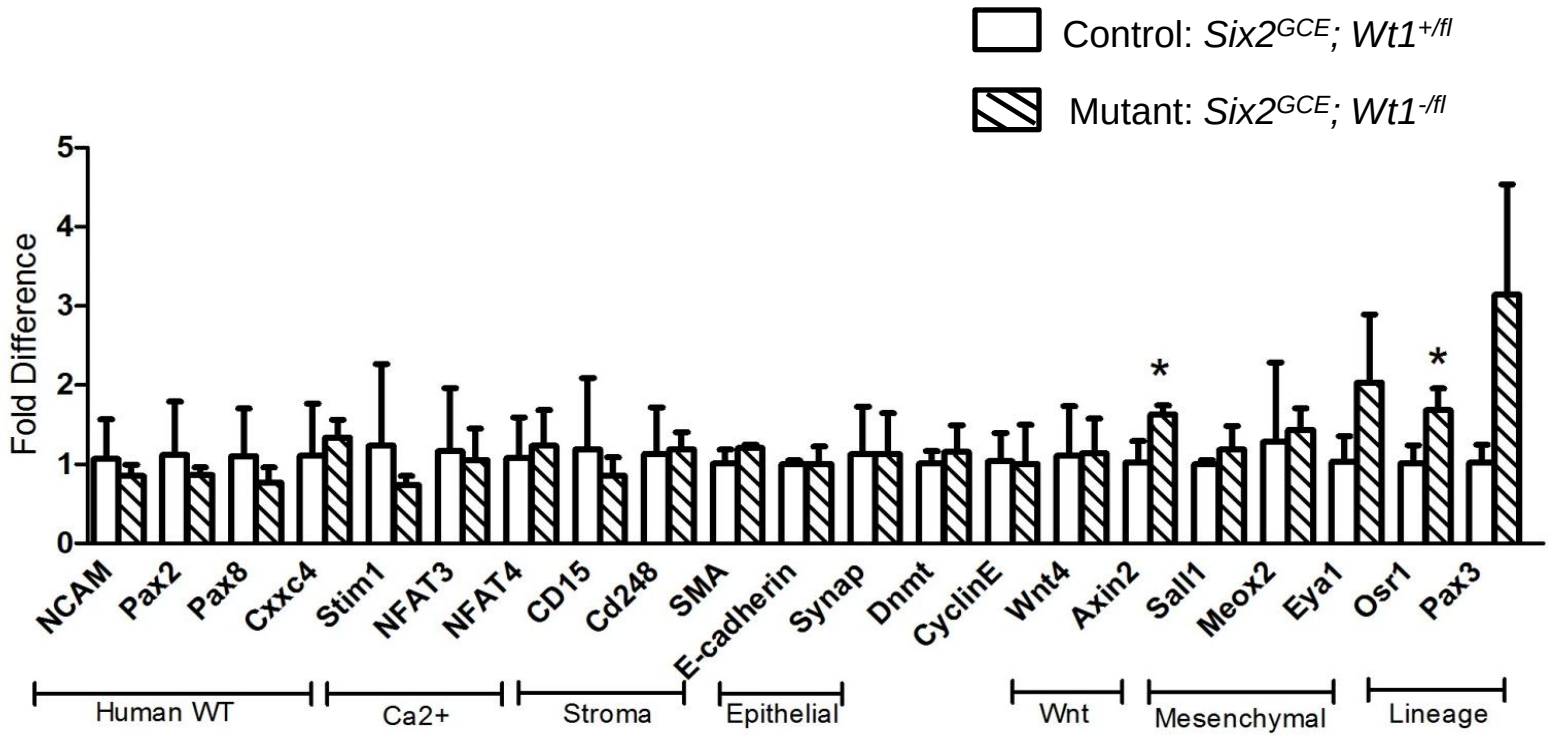

Figure 3.29 Gene expression analysis of S-Wt1 mutant kidneys and control kidneys at E19.5.

qPCR analysis of the S-Wt1 mutant and control kidneys at E19.5 with genes in Human WTs, Wnt/β-Catenin canonical and non-canonical pathways and differentiation markers.

3.22 *Wt1* ablation in nephron progenitors resulted in fibrosis in adult kidneys

To assess the longer term effects of *Wt1* ablation in nephron progenitors, we examined adult kidneys in 2 month-old mice. The mutant kidneys displayed a thinner cortex and multiple lesions with tubule dilation (Fig. 3.29). To check whether the cells in the lesion came from *S-Wt1* mutant cells, we used β-gal to track the cells with *Wt1* ablation. In the adult mutants, β-gal reporter was expressed in the tubule cells but not in the cells in the lesion (Fig. 3.30). This indicated that the lesions may not directly come from *Wt1* ablated nephron progenitors, but they were caused by a secondary response to the *Wt1* ablated cells. Alternatively, negative staining of β-gal in lesions could be due to technical difficulties in visualizing β-gal staining in lesional cells with little cytoplasm. The cells in the lesions were positive for Ki67 staining, suggesting they were proliferative (Fig. 3.30). To identify what type of cells constituted the lesions, we did IHC and IF staining with protein markers. The cells in these lesions did not express CITED1, SIX2 and K-CADHERIN (Fig. 3.30), which confirmed that these cells were not persisting nephron progenitor cells. To determine whether the lesion cells were inflammatory cells, we stained kidney sections with F4/80 (macrophage marker) IF staining. The cells in the lesions were not F4/80 expressing macrophages (Fig. 3.31). However, these lesion cells were positively stained for VIMENTIN, suggesting a fibrotic nature of the lesions. PAS positive staining and extensive deposition of Type IV Collagen in the lesions in the mutant kidneys further confirmed that the lesions were fibrotic tissues (Fig. 3.31). Therefore, early *Wt1* ablation in the nephron progenitors led to the formation of fibrosis in the adult kidneys, but it is not clear how the fibrotic tissues were formed.

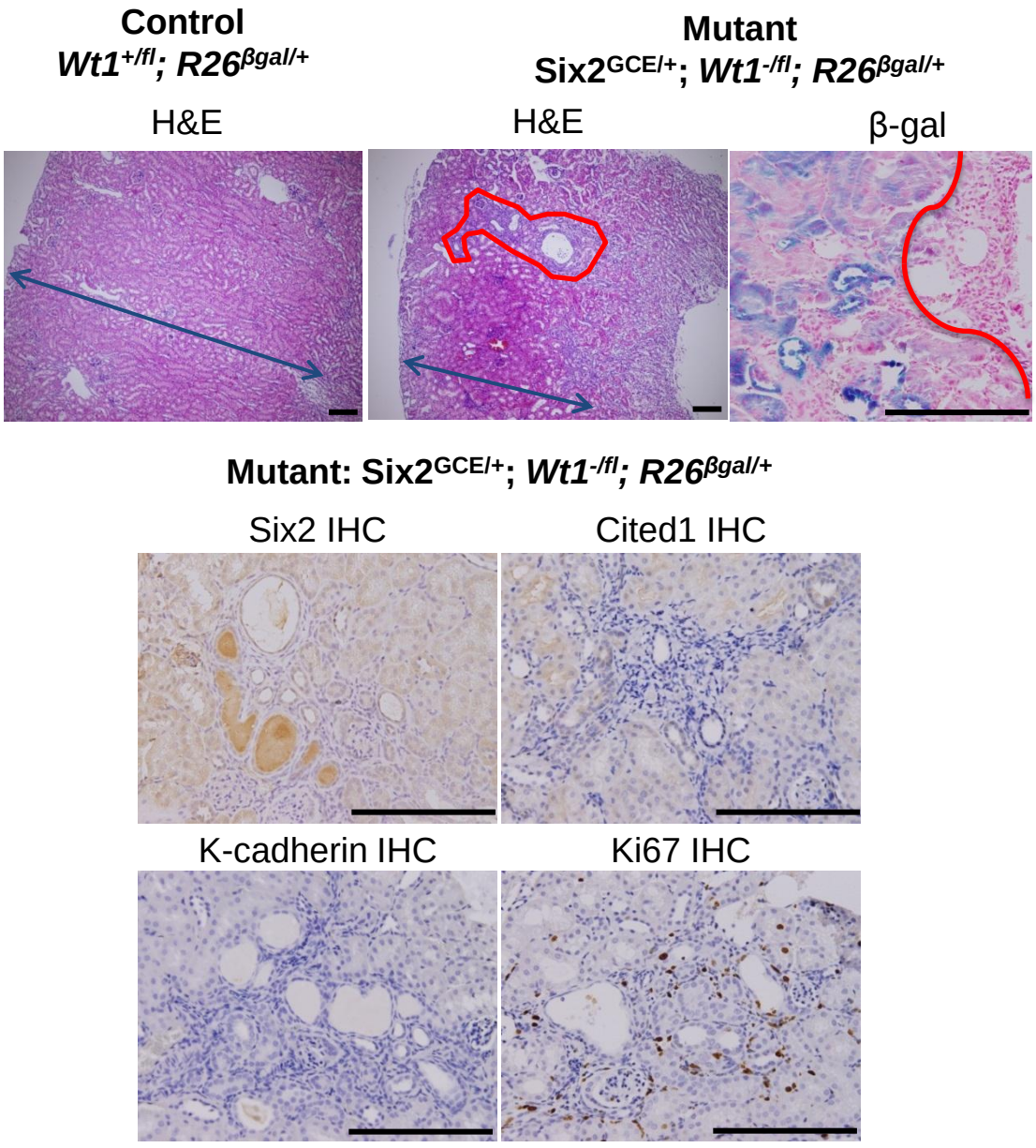

Figure 3.30 *Wt1* ablation in nephron progenitors results in lesion formation in adult kidneys

H&E staining of kidney sections from S-Wt1 mutant and control kidneys at 2 months old. Mutants showed a thinner cortex and lesion formation highlighted by red line. β-gal staining of kidney sections from S-Wt1-β-gal mutant kidneys showed that the lesions did not express β-gal. IHC staining of kidney sections showed that cells in the lesions did not express Six2, Cited1 and K-cadherin, but Ki67. Scale bars: 250 µm.

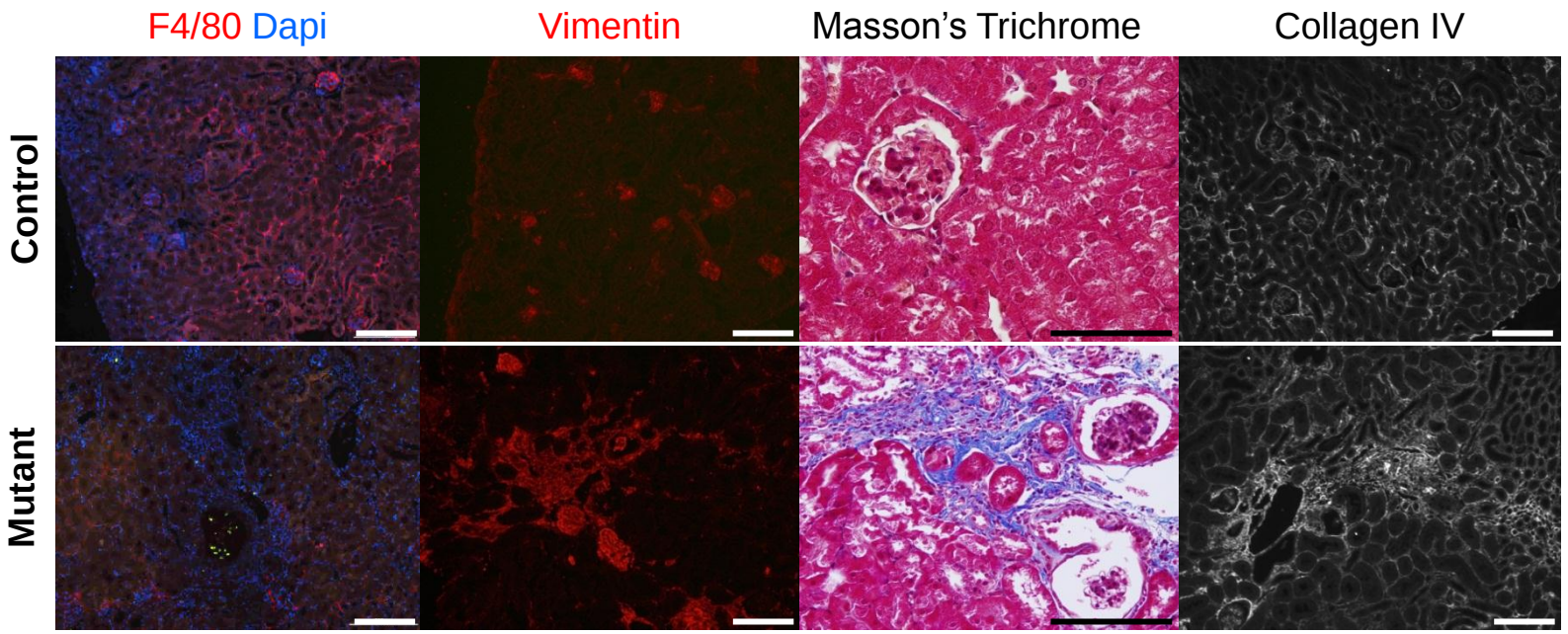

Figure 3.31 Lesions in *Wt1* ablated adult mutants were fibrotic.

IF staining of adult kidney sections with macrophage marker F4/80 and fibrosis markers Vimentin, Collagen IV, and Masson's Trichorme staining. Lesions in the mutants were negative for F4/80 staining but positively stained for Vimetnin, Masson's Trichrome and Collagen IV. Scale bars: 200 µm.

Chapter 4: Discussion

4.1 Cell origin of Wilms tumors in metanephric mesenchyme

Wilms tumor is an embryonal tumor of the kidney. Typically it has a triphasic histology and is thought to be a malignancy derived from transformed fetal metanephric mesenchyme, which can variably differentiate and clonally expand to generate the bulk of the tumor. However, it is not clear yet what type(s) of cells in the undifferentiated metanephric mesenchyme are the origins of the tumors. Recent global expression analysis of a large panel of WT patients has identified different subsets of WTs that are distinct in their clinical outcomes and gene expression profiles. These subsets variably express specific genes that correspond to early renal mesenchyme or fully differentiated epithelium. These results suggest that different subsets of WTs may arise from cells transformed at different stages of differentiation and that the stage of differentiation at which a tumor arises is a major factor in determining tumor biology and clinical outcomes.

To investigate the malignant potential of different types of cells in the undifferentiated metanephric mesenchyme, we generated cohorts of mice by using cell-type-specific tamoxifen-inducible *Cre* to somatically and mosaically introduce genetic lesions into specific progenitor cell populations including stromal progenitors (by $Foxd1^{GCE}$) and nephron progenitors (by $Six2^{GCE}$ or $Cited1^{Cre}$). The gene alterations introduced into the mice are frequently observed in tumors from WT patients and affect genes which are expressed in the metanephric mesenchyme and play essential roles in kidney development. Using the *Cre-Loxp* system, we somatically and mosaically ablated *Wt1* in the background of *Igf2* up-regulation (*Wt1-Igf2*) or stabilized *β-catenin* with or without *Wt1* ablation (*Wt1-β-catenin*).

With the gene alterations we introduced, the nephron progenitors but not the stromal progenitors gave rise to Wilms tumors. During early kidney development, the stromal progenitors and nephron progenitors are derived from the $OSR1^{+}$ cells in the metanephros

and the stromal progenitors and nephron progenitors are fated exclusively (Mugford et al., 2008b). Based on previous findings that tumor cells retain features of progenitor cellular origin in brain tumors (Schuller et al., 2008), we initially speculated that targeting the stromal progenitor would result in the stromal predominant type of Wilms tumors, whereas targeting the nephron progenitor would lead to the blastemal or epithelial predominant type of Wilms tumors. We found that targeting the stromal progenitors with either group of gene mutations, *Wt1-Igf2* or *Wt1-β-catenin*, did not lead to Wilms tumors, suggesting that the stromal progenitors were refractory to the oncogenic stimulation of *Wt1-Igf2* or *Wt1-β-catenin* genetic alterations. However, both combinations of gene alterations introduced into the nephron progenitors resulted in Wilms tumor development, suggesting that the nephron progenitors are the tumor initiating cells. Moreover, the transformed nephron progenitors were able to aberrantly differentiate to the different cell types in the tumors such as blastemal, epithelial, and stromal elements. Altogether, the stromal progenitors and nephron progenitors with different lineages showed different tumorigenic potentials. This was also the case in studies of the cell origin of pediatric brain tumors, in which different progenitors exhibited different susceptibility for tumor transformation and progenitors with different lineage commitments generated different types of tumors (Swartling et al., 2012). As development proceeds, progenitors exit the cell cycle and differentiate; however, with oncogenic stimulation, progenitors acquire the ability to self-renew long-term and remain proliferative and eventually comprise the bulk of tumors (Yang et al., 2008). The *Patched* deletion medulloblastoma model also suggested that the granule lineage is specifically sensitive to the oncogenic stress of hedgehog signaling, though the multipotent neural stem cells were targeted (Yang et al., 2008).

4.2 Stromal progenitors are not at risk of Wilms tumor development

One possible reason for the absence of tumor development from the stromal progenitor is the intrinsic property of the progenitor itself. Transcriptionally and epigenetically, the stromal progenitors and nephron progenitors are programmed differently. When stromal progenitors were targeted with genetic lesions, they may undergo apoptosis or may function normally with the mutations. We did not test in this study whether stromal progenitors with mutations underwent apoptosis. However, the resistance of stromal progenitors to oncogenic stimulation is consistent with our observation from the developmental study that when stromal progenitors were targeted with *Wt1* ablation only, stromal progenitor-derived cells differentiated normally and kidneys appeared normal. When *β-catenin* was deleted in stromal progenitors by using constitutive *Foxd1-Cre*, the phenotype of the stromal progenitor derived cells, nephron induction and ureteric bud branching, was normal except for a slightly thicker cortex and lack of medulla development (Yu et al., 2009). Therefore, although WT1 and β-CATENIN are expressed in the stromal progenitors, normal expression of these genes may not be important for the stromal progenitors to survive, self-renew, proliferate and differentiate. In other words, the stromal progenitors are not sensitive to the genetic manipulations we used here for transformation. More work is required to test whether additional gene mutations, for example *p53* mutations, are needed for cell transformation of the stromal progenitors. On the other hand, the microenvironment of the tumor initiating cells is also critical for tumor development. The niche of the stromal progenitor, resulting from the local paracrine signaling, extracellular cell matrix, angiogenesis and inflammatory cells, may not favor cell transformation.

4.3 Nephron progenitors are competent to generate Wilms tumors

Gene expression and IHC analysis of human Wilms tumors showed that tumors had a profile of marker gene expression similar to that of the nephron lineage, including

expression of SIX2, CITED1 (Murphy et al., 2012), PAX2 and PAX8 (Eccles et al., 1995). This suggested that the nephron progenitor is a more promising target as the tumor initiating cell than the stromal progenitor. The genes we genetically engineered have been shown to be critical in functions of the nephron progenitors. *Wt1* is essential for MET of the nephron progenitor, thus when *Wt1* is ablated, the progenitor can not go through MET but maintains a progenitor status of self-renewing and proliferating. When *Igf2* is simultaneously over-expressed, which promotes the metanephric mesenchymal cell to proliferate, the nephron progenitor becomes fully transformed. *β-catenin* regulates the nephron progenitors in cell survival, self-renewal, proliferation and differentiation (Schmidt-Ott and Barasch, 2008). When the balances between these functions are disrupted by β-CATENIN stabilization, the nephron progenitor cells are transformed. However, we can not rule out the possibility that the nephron progenitor cells are partially transformed when they are targeted with the genetic alterations and that the mutated cells persist. They become completely tumorigenic until a later stage when they gain further epigenetic alterations or when they are affected by microenvironment changes.

4.4 Wilms tumors with the nephron progenitor origin targeted with *Six2^{GCE}* or *Cited1^{Cre}*

We targeted the nephron progenitor by using two *Cre* lines, *Six2^{GCE}* and *Cited1^{Cre}*. CITED1 is expressed in the uninduced nephron progenitor that has the capability of self-renewal and resistance to differentiation. SIX2 is expressed in the uninduced nephron progenitor and also the induced nephron progenitor that responds to WNT9b-β-CATENIN signaling and starts to undergo MET. A subset of SIX2-expressing cells also expresses CITED1. Both *Cited1* and *Six2* are markers for the multipotent and self-renewing nephron progenitors, but *Cited1* is not essential for nephrogenesis because *Cited1* deletion in mice does not affect kidney development (Boyle et al., 2007). *Six2* is required for the

maintenance of self-renewal of nephron progenitors (Self et al., 2006). We took advantage of the availability of *Cited1*^{Cre} and *Six2*^{GCE} mouse lines and incorporated a *flox* allele of the gene of interest to target mutations to the nephron progenitors.

The difference between the *Cited1*^{Cre} and *Six2*^{GCE} *Cre*s is that the *Cited1*^{Cre} is a transgene while *Cited1* and *Six2* genes are wild type, whereas *Six2*^{GCE} is a knock-in allele, resulting in *Six2* is haploinsufficiency. When we targeted *Wt1* ablation into the nephron progenitors with *Cited1*^{Cre} (*C-Wt1-Igf2*), triphasic Wilms tumors developed, but tumors did not develop in *S-Wt1-Igf2* mutants. The difference between the *Cited1*^{Cre}+ cells and the *Six2*^{GCE}+ cells is that they have different gene dosages of *Six2*. *Six2* has been shown to be essential for the self-renewal of nephron progenitors (Kobayashi et al., 2008). Moreover, in human Wilms tumors, SIX2 is expressed in blastemal elements of tumors (Murphy et al., 2012), and overexpression of *SIX2* in a human Wilms tumor cell line enhanced cell survival, proliferation and migration of tumor cells (Pierce et al., 2014; Senanayake et al., 2013). Overexpression of *Six2* repressed differentiation directed by *Tcf/Lef* dependent *Wnt* signaling and promoted the stemness facilitated by *Survivin* dependent *Wnt* signaling (Pierce et al., 2014). It is possible that in the genetic context of *Wt1-Igf2*, wild type *Six2* expression and *Wt1* ablation synergistically contributed to cell transformation, and haploinsufficiency of *Six2* in *Six2*^{GCE}+ cells prevented cells from being tumorigenic. Thus, the *Six2*^{GCE}+ cells were not as sensitive as the *Cited1*^{Cre}+ cells were to the oncogenic effects of *Wt1* ablation.

However, both *Cited1*^{Cre}+ cells and *Six2*^{GCE}+ cells were able to give rise to Wilms tumors when β-CATENIN was stabilized. This indicates that in the case of β-CATENIN stabilization, *Six2* gene dosage (Wild type in *Cited1*^{Cre}+ cells or haploinsufficient in *Six2*^{GCE}+ cells) did not affect the malignant competency of nephron progenitors. Moreover, phenotypically, molecularly, and immunohistochemically, tumors targeted by both *Cre allele*s, *Cited1*^{Cre} or *Six2*^{GCE}, are very similar. Both the *Cited1*^{Cre} and *Six2*^{GCE} tumors histologically showed a

primitive epithelial type of Wilms tumor and were associated with kidney cyst phenotype. qRT-PCR and IHC analysis showed the *Cited1*^{Cre} and *Six2*^{GCE} tumors had a similar expression profile of differentiation markers. The unsupervised clustering of RPPA results with *Cited1*^{Cre} and *Six2*^{GCE} tumors did not show a difference in the protein expression level of the oncoproteins and tumor suppressors in the canonical cancer signaling pathway that were included in the RPPA assay. Since both *Cited1*^{Cre} and *Six2*^{GCE} targeted the nephron progenitors, it is not surprising that they resulted in similar type of Wilms tumors.

4.5 *Wt1* is not required for tumor development once β-CATENIN is stabilized in nephron progenitors

When β-CATENIN stabilization was targeted into the nephron progenitors with either *Six2*^{GCE} or *Cited1*^{Cre}, tumors developed, despite the fact that these tumor mice carried different genotypes of *Wt1*, eg. *Wt1*$^{-/fl}$, *Wt1*$^{+/fl}$, or *Wt1*$^{+/+}$. Moreover, in nephron progenitors with *β-cat*^{S}, the *Wt1* floxed allele was either completely or partially recombined, suggesting that *Wt1* status is not relevant in tumorigenesis when *β-catenin* is stabilized in nephron progenitors. In particular, the mutant mice with *Wt1*$^{+/+}$ developed tumors and all these tumors had *β-cat*^{S}, confirming that β-catenin stabilization is sufficient to transform nephron progenitors. Furthermore, qPCR, IHC and RPPA analysis of the tumors with differential gene dosage of *Wt1* showed very similar histology and expression profiles of marker genes and cancer signaling proteins between these tumors. However, in human Wilms tumors, *β-CATENIN* stabilization mutations are exclusively associated with *WT1* loss of function mutations, and *WT1* mutations and *β-CATENIN* mutations occurred in sequence during tumor progression (Maiti et al., 2000) (Fukuzawa et al., 2007). It is because of these findings that we initially designed the experiments by combining *Wt1* ablation together with *β-catenin* stabilization and engineered them genetically into mouse embryo kidney cells. The different

roles of *Wt1* in tumor development between mice and humans could be explained by the differences in the developmental process between mice and humans.

4.6 Within the nephron progenitor cell origin, different genetic lesions generated different tumor types

With the nephron progenitor cell origin, we found that different sets of mutations (*Wt1-β-cat*^{S} and *Wt1-Igf2*) generated different types of Wilms tumors. *Wt1-β-cat*^{S} tumors and *Wt1-Igf2* tumors had a similar tumor onset, penetrance of tumor occurrence and tumor proliferation profile. But *Wt1-Igf2* tumors did not have the cystic kidney phenotype that we observed in *Wt1-β-cat*^{S} tumors. Expression analysis of differentiation markers showed that *Wt1-β-cat*^{S} tumors were more epithelially differentiated, while the *Wt1-Igf2* tumors were more mesenchymal.

Wt1-β-cat^S tumors were characterized by a differentiated epithelial histology, composed mainly of epithelial cells forming tubule-like structures surrounded by stromal cells. These tumor epithelial cells expressed the epithelial differentiation marker E-CADHERIN, which was not expressed in the *Wt1-Igf2* tumors. Interestingly, these epithelial tumor cells also showed expression of the nephron progenitor markers CITED1 and SIX2 and the mesenchymal stem cell marker DLK1, suggesting that these cells were abnormally differentiated and retained features of their progenitor cell origin. In addition, *Wt1-β-cat*^{S} tumors expressed muscle differentiation markers, suggesting that a muscle cell differentiation program was likely activated by β-CATENIN stabilization. However, they did not express intermediate mesenchyme markers (*Eya1*, *Hoxa11* and *Osr1*), renal mesenchyme markers (*Pax2* and *NCAM*) and precursor epithelial markers for renal vesicle (*Wnt4*, *CyclinD1* and *Jag1*) as *Wt1-Igf2* tumors did.

By contrast, *Wt1-Igf2* tumors displayed a triphasic histology, comprised dominantly of undifferentiated blastemal cells, differentiated epithelial cells and stromal cells. *Wt1-Igf2* tumors showed high expression of genes upregulated in nephron progenitor (*Cited1*, *Six2* and *Pax2*) and in renal vesicle (*Wnt4*, *CyclinD1* and *Jag1*). This expression profile correlates with the histology of blastemal and differentiating epithelial elements in the tumors. Moreover, genes corresponding to intermediate mesenchyme (*Eya1*, *Hoxa11* and *Osr1*) were highly expressed in *Wt1-Igf2* tumors. Overexpression of the transcription factors *Six2*, *Eya1*, *Hoxa11*, *Osr1* and *Snail2* in differentiated proximal tubule cells was sufficient to reprogram cells to nephron progenitor cells (Hendry et al., 2013). Thus, we propose that the transformed cells in *Wt1-Igf2* tumors may have undergone dedifferentiation and acquired in*cre*ased ability of self-renewal and multipotency. Furthermore, *Wt1-Igf2* tumors showed elevated expression of genes involved in muscle differentiation such as *Ttn* and *Actin-a1*, demonstrating an enhanced plasticity in differentiation capabilities in tumor cells like in the intermediate mesenchyme.

The molecular and immunohistochemical analysis of mouse tumors indicated that the differentiation program of the tumor-initiating cells was influenced by the genetic lesions of *Wt1-Igf2* or *Wt1-β-catenin*, which is likely related to the functions of the genes in nephron progenitors for normal renal development.

4.7 Gene mutations impact dominantly on the formation of different types of mouse WTs

Wt1 and *β-catenin* are both critical in regulating the functions and differentiation of the nephron progenitors. When one or more of them are deregulated, the resulting signaling can become oncogenic and facilitate cell transformation, and at the same time, it can affect the

cell differentiation program by either directing cells to dedifferentiate or to differentiate ectopically.

Wt1 is required for MET (Hu et al., 2010). *Wt1* deletion prevented the nephron progenitor cells from differentiating, but preserved progenitor cells in a self-renewing and stem-like state. A very recent study found that at E11.5 and E15.5, at the periphery of the CM, there were rarely cells expressing both SIX2 and FOXD1 and that these few cells with dual identities could be fated toward either the stromal or epithelial cell types (Brunskill et al., 2014). Therefore, it is possible that the *Wt1-Igf2* mutant nephron progenitor cells could dedifferentiate to an earlier lineage such as the SIX2-FOXD1 dual identity state or even an earlier state, such as intermediate mesenchyme. In addition to the partial transformation resulting from *Wt1* deletion, the *Igf2* overexpression that promoted cell proliferation caused the progenitor cells to fully transform into tumor cells with a broad differentiation potential.

Wnt/β-catenin signaling has been shown to be essential for nephron progenitors to survive, proliferate, and self-renew (Park et al., 2007). WNT9b signaling from the ureteric bud induces the undifferentiated and uninduced nephron progenitor cells to differentiate via activation of the canonical β-CATENIN signaling pathway (Schmidt-Ott and Barasch, 2008). However, when the cells further differentiate, β-CATENIN signaling activity must be reduced for full epithelialization (Kuure et al., 2007). Our study demonstrated that constant activation of *β-catenin* signaling was not only sufficient to transform nephron progenitor cells but also biased the tumorigenic cells towards epithelial differentiation, thus generating the primitive epithelial type of WTs. Moreover, we observed a strong association of kidney cyst formation with the epithelial tumors and we speculated that β-CATENIN stabilization may disrupt cell adhesion formation or cilia formation and in*cre*ase the cytokinesis of the tumor cells.

4.8 Comparison of tumor models in this study and published mouse WT models

The first Wilms tumor mouse model was generated by using a ubiquitous tamoxifen-inducible *Cre* to somatically and mosaically ablate *Wt1* together with systematic over-expression of *Igf2* (*Ub^{Cre}-Wt1-Igf2*). In this model, about 64% of mutants developed tumors by the age of 19 weeks (Hu et al., 2010). The *Ub^{Cre}-Wt1-Igf2* tumors had triphasic histology and showed activated extracellular signal-regulated kinase (ERK) signaling. In our *C-Wt1-Igf2* mouse model targeted by *Cited1^{Cre}*, the tumors developed at 70 weeks old with a frequency of 50% of the mutant mice. The *C-Wt1-Igf2* tumors also had a triphasic histology similar to the *Ub^{Cre}-Wt1-Igf2* tumors. The differences in tumor latency between the *Ub^{Cre}-Wt1-Igf2* mutants and the *C-Wt1-Igf2* mutants may result from the different targeting strategies with *Cre* expression driven by different promoters. In the *Ub^{Cre}-Wt1-Igf2* model, kidney cells were targeted at E11.5. At E11.5, *Wt1* is expressed in the metanephric mesenchyme mainly composed of the nephron progenitors, stromal progenitors, and possibly some other un-identified progenitor cell types (Mugford et al., 2009). Thus, all these cell types could serve as candidate targets for tumor cell transformation. However, in our *C-Wt1-Igf2* model, only the uninduced nephron progenitors were targeted at E14.5. We speculated that in the *Ub^{Cre}-Wt1-Igf2* model, a cell population at an earlier lineage than the nephron progenitor was targeted by the ubiquitous *Cre*. This stem cell population had a higher capacity of proliferation and self-renewal than the nephron progenitor and led to faster expansion of the transformed cells and thus an earlier tumor onset in *Ub^{Cre}-Wt1-Igf2* mice. There was a higher content of blastemal cells and a lower content of epithelial cells in the histology of *Ub^{Cre}-Wt1-Igf2* tumors than that in the *C-Wt1-Igf2* tumors. This observation may also reflect our speculated stem cell origin of the *Ub^{Cre}-Wt1-Igf2* tumors versus the lineage restricted nephron progenitor cell origin of the *C-Wt1-Igf2* tumors. Cells targeted by the *Ub^{Cre}* could include the CITED1^{+} nephron progenitors, so the tumor spectrum of *Ub^{Cre}-Wt1-Igf2* tumors should include tumors like the *C-Wt1-Igf2* tumors. Indeed, we observed that

some of the *Ub^{Cre}-Wt1-Igf2* tumors histologically appeared very similar to the *C-Wt1-Igf2* tumors.

Later, another mouse model was reported in which mini-primitive epithelial WTs developed with the use of *Cited1^{Cre}* to stabilize β-CATENIN with or without *Kras* activation postnatally (*C-β-cat^{S}-Kras*) (Clark et al., 2011). In this model, a proximal tubule specific *γGT-Cre* was also used to stabilize β-CATENIN and activate *Kras* (*γGT^{Cre}-β-cat^{S}-Kras*) and the development of the same epithelial WTs was detected as was the case with the *C-β-cat^{S}-Kras* tumors. The *C-β-cat^{S}-Kras* and *γGT^{Cre}-β-cat^{S}-Kras* tumors looked histologically very similar to our *S/C-Wt1*-β-cat^{S} and *S-β-cat^{S}* tumors. However, our mouse tumors had a cystic kidney phenotype that was absent in *C-β-cat^{S}-Kras* and *γGT^{Cre}-β-cat^{S}-Kras* tumors. In our mouse models, the *Six2^{GCE}* or *Cited1^{Cre}* was activated by tamoxifen at an early stage of kidney development (E14.5 or E17.5) to target the nephron progenitors, which was different from the *C-β-cat^{S}-Kras* and *γGT^{Cre}-β-cat^{S}-Kras* models where cells were targeted at the post-natal stage, when CITED1^{+} nephron progenitor cells were depleted and γGT^{+} cells were fully differentiated. It was likely that the γGT^{+} tubule cells underwent dedifferentiation when they had *β-catenin* and *Kras* activation during the cell transformation process. Altogether, with β-CATENIN stabilization, both multipotent nephron progenitors and completely differentiated proximal tubules presented the capacity to give rise to epithelial WTs, suggesting that similar type of WTs can be generated from diverse sources of cell origins.

Very recently, overexpression of a heterochronic regulator *Lin28* in primordial germ cells but not in nephron or stromal progenitors generated Wilms tumor (Urbach et al., 2014). This suggested that different types of cells at different lineages can serve the cell origins of WTs but that the malignant potentials depended on the context of the genetic alterations.

4.9 Comparison of tumor models with human WT subsets

To correlate the mouse tumors with the identified 5 subsets of human WTs (Gadd et al., 2012), we selected a few significant genes differentiating the human tumor subsets. We compared the expression patterns of these genes in the different mouse tumor types with the intent of determining whether these expression patterns were consistent with any of the human tumor subsets.

S1 tumors are characterized by epithelial tubular differentiated histology without muscle differentiation. S1 tumors had low expression of genes in early metanephric mesenchyme but expressed genes in the post-induction stage of nephron and mature epithelium. S2-S5 tumors showed triphasic histology with varying degree of skeletal muscle differentiation, and molecularly S2-S5 tumors were similar to one another. S2 tumors had loss of *Wt1* expression and *Wnt* activation, and genes enriched in S2 corresponded to the differentiation stage before mesenchyme induction (e.g. intermediate mesenchyme) and to kidney interstitium. Compared to S2 tumors, S3 also had low *Wt1* expression, but the expression of skeletal muscle differentiation genes were lower and activity of canonical signaling such as *Wnt*, *Tgfβ*, *NFAT* and *Ras* pathways was lower. S4 tumors were also very similar to S2 tumors in gene expression pattern, but showed less evidence of *Wt1* loss of expression and *Wnt* activation. S5 tumors expressed genes corresponding to early metanephric mesenchyme.

The epithelial histology of *S/C-Wt1-β-cat^S* and *S-β-cat^S* tumors were like the S1 tumors except that there are no *β-catenin* mutations in S1. However, the *C-Wt1-Igf2* tumors showed triphasic histology, which mimicked S2-S5 tumors histologically.

The genes that we checked in mouse tumors included genes in intermediate mesenchyme before nephron induction, muscle differentiation and *Wnt* signaling. The mesenchymal marker genes (*Hoxa11*, *HMGA2* and *Dlk1*) that were expressed significantly

lower in *β-cat*^{S} mouse tumors than the *C-Wt1-Igf2* tumors were also expressed lower in S1 tumors than other subtypes. Therefore we thought that *β-cat*^{S} tumors may mimic S1 not only histologically but also in gene expression, and that *C-Wt1-Igf2* tumors may correlate to certain subset among S1-S5. For the genes involved in muscle differentiation such as *Pitx2*, *Ttn* and *Actin-a1*, the *β-cat*^{S} tumors and the *C-Wt1-Igf2* tumors had similar expression level, which was also observed between S1, S3 and S5. S3 tumors had low expression of *Wt1*, less *Wnt* activation and high expression of *Igf2*, so we speculated that *C-Wt1-Igf2* tumors could be more related to S3 tumors. For the expression of *Wnt/β-catenin* inhibitor *Wif1*, *β-cat*^{S} tumors had higher expression than the *Wt1-Igf2* tumors, which was not the case between S1 and the other subsets, probably due to the lack of *β-catenin* mutations in S1 tumors. Together, based on these very preliminary data, we speculated that the *β-cat*^{S} tumors may correspond to S1, while *C-Wt1-Igf2* tumors may be related to S3. However, further analysis such as microarray, cross-species comparison and clustering will be required to define the correlation between the mouse models and the human tumor subsets.

4.10 *Wt1* function in kidney development

Functional mutations of *WT1* have been found in 20% of Wilms tumor patients. To understand the mechanisms by which *WT1* loss of function predisposes to malignant transformation, it is important to understand *WT1* function in kidney development. *Wt1* is expressed in the metanephric mesenchyme, mainly containing stromal and nephron progenitors at an early stage of kidney development. Therefore, we used a high dose of tamoxifen to ablate *Wt1* in a high proportion of progenitor cells to study the effects of *Wt1* ablation on nephrogenesis.

We found that *Wt1* ablation in stromal progenitors (FOXD1$^+$) did not seem to affect kidney development. The *F-Wt1* mutant kidneys appeared normal phenotypically and

histologically. Cell tracking with a β-gal reporter showed that the stromal progenitor derived cells with *Wt1* ablation could differentiate and persisted in the adult kidney. A previous study showed that FOXD1$^+$ stromal progenitors gave rise to FLK1$^+$ endothelial progenitors and contributed partially to the vasculature patterning of the kidney (Sims-Lucas et al., 2013). An *in vitro* culture study showed, at the periphery of embryonic kidney where the stromal progenitors reside, FLK1+ angioblast mesenchyme expressed *Wt1* and *Wt1*-stimulated *Vegfa* signaling was essential to initially induce but not required to sustain the differentiation of the MM and the outgrowth and branching of the ureteric bud (Gao et al., 2005). These studies suggested that *Wt1* in stromal progenitors could regulate the mesenchyme-ureteric bud interaction. However, our *in vivo* mouse model with *Wt1* ablation in stromal progenitors did not show a defect in nephrogenesis. The different outcomes between our findings and the previous study of *Wt1* in angioblasts could be due to the differences in using an *in vivo* genetic model in our study versus using the *in vitro* culture method employed in the previous study, or because we ablated *Wt1* at a stage which has passed the time for the requirement of angioblast-mesenchyme for initial induction of nephrogenesis.

When *Wt1* was ablated in nephron progenitors (SIX2+), the nephrogenic zone (NZ), where the progenitors reside, was expanded with increased numbers of cells condensing and surrounding the ureteric buds. The cells in the expanded NZ were proliferative and expressed the nephron progenitor markers (CITED1 and PAX2), confirming their nephron progenitor identity. The mutant kidneys expressed significantly higher levels of the marker for intermediate mesenchyme, *Osr1*, than did the normal kidneys, suggesting that *Wt1* ablation may have reprogramed nephron progenitors to an OSR1$^+$ cell state which is an earlier lineage than the nephron progenitor. This could explain the presence of ectopic skeletal elements in the human tumors with loss of *Wt1* function mutations, which may result from the gained differentiation plasticity of the tumor cells. The gained multipotency and

long-term self-renewal caused the *Wt1*-ablated mutant cells to become partially transformed and be good candidates for transformation once another oncogenic event occurred.

Furthermore, in the *S-Wt1* mutant kidneys, nephrogenesis was blocked. The disrupted nephrogenesis phenotype appeared as early as at E15.5 in the mutant kidneys. The results with *S-Wt1* mutant kidneys indicated that *Wt1* ablation in the nephron progenitors prevented the cells from differentiating but sustained the undifferentiated state of the nephron progenitor. This result was consistent with the findings of previous studies. When *Wt1* was ablated at E11.5 using a ubiquitous *Cre*, the metanephric mesenchyme did not condense and the MET process was blocked (Hu et al., 2010). Knock-down of *Wt1* using siRNA in mouse embryonic kidney rudiment *in vitro* also showed abnormal cell proliferation and disrupted cell epithelial differentiation (Davies et al., 2004).

Deletion of another Wilms tumor suppressor, *Wtx,* also presented a similar phenotype in neonatal kidneys (Moisan et al., 2011). Although $Wtx^{-/-}$ kidneys showed normal nephrogenesis, they had expanded pools of aggregates of $SIX2^{+}$ cells and altered cell fate commitment and delayed differentiation in mesenchymal progenitor cells (Moisan et al., 2011). The defects in cell fate determination were regulated by abnormal activation of *β-catenin* signaling (Moisan et al., 2011). Interestingly, in our *Wt1* ablated mutant kidneys, the expression of *Axin2* (the effector of WNT/β-CATENIN signaling) was significantly higher than the normal kidneys, suggesting that *β-catenin* activation may also be involved in the defects in cell differentiation of nephron progenitors that were caused by *Wt1* ablation. *Wnt4* was identified as a *Wt1* transcriptional target to promote the MET (Sim et al., 2002), but in our study *Wnt4* was not differentially expressed between the *S-Wt1* mutant kidneys and the normal kidneys.

In addition, *S-Wt1* mutant kidneys from 1 month and 2.5 months old mutant mice showed a thinner cortex and multiple fibrotic lesions. However, it was unknown whether

these fibrotic cells were derived from *Wt1* ablated nephron progenitor or whether they were a secondary response to signaling caused by *Wt1* ablated but phenotypically normal cells in the kidney. β-gal reporter tracking of *Wt1* ablated cells showed that the cells in the fibrotic lesions did not express β-gal, suggesting that the lesional cells may not come from nephron progenitors, although this result could also have been caused by the scarcity of cytoplasm in the lesion cells which was insufficient to visualize β-gal staining. Lack of the expression of nephron progenitor markers SIX2, CITED1 and precursor epithelial marker K-CADHERIN in these cells suggested these cells were not persisting progenitor cells or abnormally differentiating epithelial cells. F4/80 staining showed that these cells were not infiltrating inflammatory cells. Ubiquitous deletion of *Wt1* in adult mice also showed no systemic inflammatory response in the mutant although the mutant had acute multiple organ failure due to disturbed tissue homeostasis (Chau et al., 2011). In the adult *S-Wt1* adult mice, the cells in the lesions were proliferative. VIMENTIN and COLLAGEN IV staining showed that these cells were mesenchymal and Masson's Trichrome staining confirmed these cells were associate with fibrotic tissue. Increased COLLAGEN IV expression indicated TGFβ signaling may be involved. Further analysis of IHC and qPCR needs to be done to identify the dysregulated signaling pathway resulting in fibrosis formation.

Our study of ablating *Wt1* in nephron progenitors has shown that *Wt1* promotes the nephron progenitors to differentiate and that loss of *Wt1* sustains the long-term self-renewal capability and multipotency of the lineage-restricted nephron progenitors, making these cells good targets for cell transformation.

Conclusion and Significance

In conclusion, we investigated the cell origin of Wilms tumor and the effects of genetic mutations on formation of different tumor types by using mouse genetic models. Our study has demonstrated that during kidney development the nephron progenitors can give rise to Wilms tumors with *Wt1-Igf2* or *β-catenin* mutations but the stromal progenitors are not at risk of tumor development with these genetic alterations. With the nephron progenitor cell origin, *Wt1-β-cat*^{S} tumors and *Wt1-Igf2* tumors had similar profiles in tumor latency and tumor frequency. However, the type of gene mutations affects the differentiation program of the transformed cells, thus resulting in different types of tumors. The *Wt1-β-cat*^{S} mutations resulted in epithelial differentiated Wilms tumors, whereas the *Wt1-Igf2* alterations led to more mesenchymal Wilms tumors. Moreover, we characterized the effects of *Wt1* ablation in the stromal and nephron progenitors on kidney development in order to understand the mechanisms by which *Wt1* inactivation mutations predispose to WTs. *Wt1* does not seem to be critical in stromal progenitors, but in nephron progenitors *Wt1* is essential for the mesenchyme to epithelial transition and may regulate the dedifferentiation program of nephron progenitors.

Wilms tumor is genetically and histologically heterogeneous. Understanding the impact of the differentiation status of tumor initiating cells on resulting tumor biology and the effects of gene mutations on the formation of different tumor types can provide significant insights into the mechanisms of the tumorigenic processes. Knowledge of the functions of *Wt1* in renal progenitors will further help us to understand how *Wt1* mutations transform the progenitors to tumor cells.

Wilms tumor patients are sometimes treated with chemotherapy and radiation therapy, which can cause side effects and place them at risk for a secondary tumor later in life. Targeted therapies are needed to help reduce such side effects while providing effective

treatment. The mouse models of different types of Wilms tumors provide a useful tool for the identification of the biomarkers associated with different tumor types and tumor stages. With the development of new tumor biomarkers, we can detect tumors at an earlier stage and we also can stratify patients according to their biomarker profiles and apply specific treatment strategies to specific tumor subsets. Moreover, the mouse models can be used to identify druggable protein targets which are the key regulators in Wilms tumorigenesis and used to s*cree*n and test drugs for the best efficacy for treating tumors with minimum side effects. The preclinical models can be utilized for the development of improved therapy for the ultimate benefits of these young patients.

Future directions

A complete understanding of the tumor initiation process is important in preventing tumor development. Fluorescent protein reporter and sensitive imaging techniques are great tools to track Wilms tumor initiating cells to monitor the early stages of tumor development and tumor progression. These methods can be used to detect the presence of Wilms tumor precursor lesions and monitor when and how the lesions progress to tumors. Our mouse models have shown that tumors arising from the same nephron progenitor origin are different in histology, gene expression profile and differentiation status due to the different genetic mutations induced. Therefore it is interesting to investigate how these genetic alterations affected the formation of different types of tumors. With the tool of the reporter tracking tumorigenic cells, the pathological process can be monitored by analyzing the reporter labeled cells with the examination of histology, co-staining with antibodies for differentiation markers and cancer signaling regulators. Not only can we study how the tumor cells differentiate, but we also can investigate how the tumor cells interact with the tumor microenvironment. Moreover, tumor precursor lesions or small tumors at an early stage can be isolated with FACS of the fluorescent protein labeled mutant cells in order to allow gene expression and protein expression analysis of these cells. To examine tumor cell aggressiveness and metastatic potential, the isolated tumor cells can be injected as xenografts to test transplanted tumor growth and metastatic ability.

To understand the molecular mechanisms of the development of different types of mouse Wilms tumors, microarray of the tumors can be performed to characterize the global gene expression patterns between the types of mouse tumors. These data can be analyzed with Ingenuity Pathway Analysis (IPA) to determine genes and pathways that are significantly differentially expressed between the different types of tumors. The expression profiles of mouse models then can be compared to the expression data of human subsets

with cross-species analysis and clustering of the results can be performed to find out whether there is an association of the mouse WTs with the human subsets. Potentially, with this bioinformatics information, drug targets and the biomarkers differentiating these tumor types may be identified. Thus this will help to develop targeted therapies for patients and potentially avoid the long-term side effects from chemotherapy and radiation.

References

Armstrong, J.F., Pritchard-Jones, K., Bickmore, W.A., Hastie, N.D., and Bard, J.B. (1993). The expression of the Wilms' tumour gene, WT1, in the developing mammalian embryo. Mechanisms of development *40*, 85-97.

Barak, H., Huh, S.H., Chen, S., Jeanpierre, C., Martinovic, J., Parisot, M., Bole-Feysot, C., Nitschke, P., Salomon, R., Antignac, C., Ornitz, D.M., and Kopan, R. (2012). FGF9 and FGF20 maintain the stemness of nephron progenitors in mice and man. Developmental cell *22*, 1191-1207.

Bardeesy, N., Falkoff, D., Petruzzi, M.J., Nowak, N., Zabel, B., Adam, M., Aguiar, M.C., Grundy, P., Shows, T., and Pelletier, J. (1994). Anaplastic Wilms' tumour, a subtype displaying poor prognosis, harbours p53 gene mutations. Nature genetics *7*, 91-97.

Basta, J.M., Robbins, L., Kiefer, S.M., Dorsett, D., and Rauchman, M. (2014). Sall1 balances self-renewal and differentiation of renal progenitor cells. Development *141*, 1047-1058.

Beckwith, J.B. (1983). Wilms' tumor and other renal tumors of childhood: a selective review from the National Wilms' Tumor Study Pathology Center. Human pathology *14*, 481-492.

Beckwith, J.B. (1998). Nephrogenic rests and the pathogenesis of Wilms tumor: developmental and clinical considerations. American journal of medical genetics *79*, 268-273.

Beckwith, J.B., and Palmer, N.F. (1978). Histopathology and prognosis of Wilms tumors: results from the First National Wilms' Tumor Study. Cancer *41*, 1937-1948.

Bouchard, M., Souabni, A., Mandler, M., Neubuser, A., and Busslinger, M. (2002). Nephric lineage specification by Pax2 and Pax8. Genes & development *16*, 2958-2970.

Boyle, S., Misfeldt, A., Chandler, K.J., Deal, K.K., Southard-Smith, E.M., Mortlock, D.P., Baldwin, H.S., and de Caestecker, M. (2008). Fate mapping using Cited1-CreERT2 mice

demonstrates that the cap mesenchyme contains self-renewing progenitor cells and gives rise exclusively to nephronic epithelia. Developmental biology *313*, 234-245.

Boyle, S., Shioda, T., Perantoni, A.O., and de Caestecker, M. (2007). Cited1 and Cited2 are differentially expressed in the developing kidney but are not required for nephrogenesis. Developmental dynamics : an official publication of the American Association of Anatomists *236*, 2321-2330.

Boyle, S.C., Kim, M., Valerius, M.T., McMahon, A.P., and Kopan, R. (2011). Notch pathway activation can replace the requirement for Wnt4 and Wnt9b in mesenchymal-to-epithelial transition of nephron stem cells. Development *138*, 4245-4254.

Breslow, N., Olshan, A., Beckwith, J.B., and Green, D.M. (1993). Epidemiology of Wilms tumor. Medical and pediatric oncology *21*, 172-181.

Brodbeck, S., Besenbeck, B., and Englert, C. (2004). The transcription factor Six2 activates expression of the Gdnf gene as well as its own promoter. Mechanisms of development *121*, 1211-1222.

Brown, A.C., Muthukrishnan, S.D., Guay, J.A., Adams, D.C., Schafer, D.A., Fetting, J.L., and Oxburgh, L. (2013). Role for compartmentalization in nephron progenitor differentiation. Proceedings of the National Academy of Sciences of the United States of America *110*, 4640-4645.

Brunskill, E.W., Park, J.S., Chung, E., Chen, F., Magella, B., and Potter, S.S. (2014). Single cell dissection of early kidney development: multilineage priming. Development *141*, 3093-3101.

Call, K.M., Glaser, T., Ito, C.Y., Buckler, A.J., Pelletier, J., Haber, D.A., Rose, E.A., Kral, A., Yeger, H., Lewis, W.H., Jones, C., and Housman, D.E. (1990). Isolation and characterization of a zinc finger polypeptide gene at the human chromosome 11 Wilms' tumor locus. Cell *60*, 509-520.

Carroll, T.J., Park, J.S., Hayashi, S., Majumdar, A., and McMahon, A.P. (2005). Wnt9b plays a central role in the regulation of mesenchymal to epithelial transitions underlying organogenesis of the mammalian urogenital system. Developmental cell *9*, 283-292.

Chang, H., Gao, F., Guillou, F., Taketo, M.M., Huff, V., and Behringer, R.R. (2008). Wt1 negatively regulates beta-catenin signaling during testis development. Development *135*, 1875-1885.

Chau, Y.Y., Brownstein, D., Mjoseng, H., Lee, W.C., Buza-Vidas, N., Nerlov, C., Jacobsen, S.E., Perry, P., Berry, R., Thornburn, A., Sexton, D., Morton, N., Hohenstein, P., Freyer, E., Samuel, K., van't Hof, R., and Hastie, N. (2011). Acute multiple organ failure in adult mice deleted for the developmental regulator Wt1. PLoS genetics *7*, e1002404.

Cheng, H.T., Kim, M., Valerius, M.T., Surendran, K., Schuster-Gossler, K., Gossler, A., McMahon, A.P., and Kopan, R. (2007). Notch2, but not Notch1, is required for proximal fate acquisition in the mammalian nephron. Development *134*, 801-811.

Cho, E.A., Patterson, L.T., Brookhiser, W.T., Mah, S., Kintner, C., and Dressler, G.R. (1998). Differential expression and function of cadherin-6 during renal epithelium development. Development *125*, 803-812.

Clark, P.E., Polosukhina, D., Love, H., Correa, H., Coffin, C., Perlman, E.J., de Caestecker, M., Moses, H.L., and Zent, R. (2011). β-Catenin and K-RAS Synergize to Form Primitive Renal Epithelial Tumors with Features of Epithelial Wilms' Tumors. The American journal of pathology *179*, 3045-3055.

Das, A., Tanigawa, S., Karner, C.M., Xin, M., Lum, L., Chen, C., Olson, E.N., Perantoni, A.O., and Carroll, T.J. (2013). Stromal-epithelial crosstalk regulates kidney progenitor cell differentiation. Nature cell biology *15*, 1035-1044.

Davidson, A.J. (2008). Mouse kidney development. In StemBook (Cambridge (MA)).

Davies, J.A., Ladomery, M., Hohenstein, P., Michael, L., Shafe, A., Spraggon, L., and Hastie, N. (2004). Development of an siRNA-based method for repressing specific genes in

renal organ culture and its use to show that the Wt1 tumour suppressor is required for nephron differentiation. Human molecular genetics *13*, 235-246.

Discenza, M.T., and Pelletier, J. (2004). Insights into the physiological role of WT1 from studies of genetically modified mice. Physiological genomics *16*, 287-300.

Drummond, I.A., Madden, S.L., Rohwer-Nutter, P., Bell, G.I., Sukhatme, V.P., and Rauscher, F.J., 3rd (1992). Repression of the insulin-like growth factor II gene by the Wilms tumor suppressor WT1. Science *257*, 674-678.

Eccles, M.R., Yun, K., Reeve, A.E., and Fidler, A.E. (1995). Comparative in situ hybridization analysis of PAX2, PAX8, and WT1 gene transcription in human fetal kidney and Wilms' tumors. The American journal of pathology *146*, 40-45.

Elizabeth, P. (2014). Wilms Tumors. In Cancer genomics: from bench to personalized medicine, pp. 397-413.

Englert, C., Hou, X., Maheswaran, S., Bennett, P., Ngwu, C., Re, G.G., Garvin, A.J., Rosner, M.R., and Haber, D.A. (1995). WT1 suppresses synthesis of the epidermal growth factor receptor and induces apoptosis. The EMBO journal *14*, 4662-4675.

Fetting, J.L., Guay, J.A., Karolak, M.J., Iozzo, R.V., Adams, D.C., Maridas, D.E., Brown, A.C., and Oxburgh, L. (2014). FOXD1 promotes nephron progenitor differentiation by repressing decorin in the embryonic kidney. Development *141*, 17-27.

Fukuzawa, R., Anaka, M.R., Weeks, R.J., Morison, I.M., and Reeve, A.E. (2009). Canonical WNT signalling determines lineage specificity in Wilms tumour. Oncogene *28*, 1063-1075.

Fukuzawa, R., Heathcott, R.W., More, H.E., and Reeve, A.E. (2007). Sequential WT1 and CTNNB1 mutations and alterations of beta-catenin localisation in intralobar nephrogenic rests and associated Wilms tumours: two case studies. Journal of clinical pathology *60*, 1013-1016.

Fukuzawa, R., Heathcott, R.W., Morison, I.M., and Reeve, A.E. (2005). Imprinting, expression, and localisation of DLK1 in Wilms tumours. Journal of clinical pathology *58*, 145-150.

Fukuzawa, R., Heathcott, R.W., Sano, M., Morison, I.M., Yun, K., and Reeve, A.E. (2004). Myogenesis in Wilms' tumors is associated with mutations of the WT1 gene and activation of Bcl-2 and the Wnt signaling pathway. Pediatric and developmental pathology : the official journal of the Society for Pediatric Pathology and the Paediatric Pathology Society *7*, 125-137.

Gadd, S., Huff, V., Huang, C.C., Ruteshouser, E.C., Dome, J.S., Grundy, P.E., Breslow, N., Jennings, L., Green, D.M., Beckwith, J.B., and Perlman, E.J. (2012). Clinically relevant subsets identified by gene expression patterns support a revised ontogenic model of Wilms tumor: a Children's Oncology Group Study. Neoplasia *14*, 742-756.

Gao, F., Maiti, S., Alam, N., Zhang, Z., Deng, J.M., Behringer, R.R., Lecureuil, C., Guillou, F., and Huff, V. (2006). The Wilms tumor gene, Wt1, is required for Sox9 expression and maintenance of tubular architecture in the developing testis. Proceedings of the National Academy of Sciences of the United States of America *103*, 11987-11992.

Gao, X., Chen, X., Taglienti, M., Rumballe, B., Little, M.H., and Kreidberg, J.A. (2005). Angioblast-mesenchyme induction of early kidney development is mediated by Wt1 and Vegfa. Development *132*, 5437-5449.

Gong, K.Q., Yallowitz, A.R., Sun, H., Dressler, G.R., and Wellik, D.M. (2007). A Hox-Eya-Pax complex regulates early kidney developmental gene expression. Molecular and cellular biology *27*, 7661-7668.

Goss, A.M., Tian, Y., Tsukiyama, T., Cohen, E.D., Zhou, D., Lu, M.M., Yamaguchi, T.P., and Morrisey, E.E. (2009). Wnt2/2b and beta-catenin signaling are necessary and sufficient to specify lung progenitors in the foregut. Developmental cell *17*, 290-298.

Grubb, G.R., Yun, K., Williams, B.R., Eccles, M.R., and Reeve, A.E. (1994). Expression of WT1 protein in fetal kidneys and Wilms tumors. Laboratory investigation; a journal of technical methods and pathology *71*, 472-479.

Guertl, B., Leuschner, I., Harms, D., and Hoefler, G. (2006). Genetic clonality is a feature unifying nephroblastomas regardless of the variety of morphological subtypes. Virchows Archiv : an international journal of pathology *449*, 171-174.

Guo, J.K., Menke, A.L., Gubler, M.C., Clarke, A.R., Harrison, D., Hammes, A., Hastie, N.D., and Schedl, A. (2002). WT1 is a key regulator of podocyte function: reduced expression levels cause crescentic glomerulonephritis and mesangial sclerosis. Human molecular genetics *11*, 651-659.

Harada, N., Tamai, Y., Ishikawa, T., Sauer, B., Takaku, K., Oshima, M., and Taketo, M.M. (1999). Intestinal polyposis in mice with a dominant stable mutation of the beta-catenin gene. The EMBO journal *18*, 5931-5942.

Hartwig, S., Ho, J., Pandey, P., Macisaac, K., Taglienti, M., Xiang, M., Alterovitz, G., Ramoni, M., Fraenkel, E., and Kreidberg, J.A. (2010). Genomic characterization of Wilms' tumor suppressor 1 targets in nephron progenitor cells during kidney development. Development *137*, 1189-1203.

Hatini, V., Huh, S.O., Herzlinger, D., Soares, V.C., and Lai, E. (1996). Essential role of stromal mesenchyme in kidney morphogenesis revealed by targeted disruption of Winged Helix transcription factor BF-2. Genes & development *10*, 1467-1478.

Hayashi, S., and McMahon, A.P. (2002). Efficient recombination in diverse tissues by a tamoxifen-inducible form of Cre: a tool for temporally regulated gene activation/inactivation in the mouse. Developmental biology *244*, 305-318.

Hendry, C., Rumballe, B., Moritz, K., and Little, M.H. (2011). Defining and redefining the nephron progenitor population. Pediatric nephrology *26*, 1395-1406.

Hendry, C.E., Vanslambrouck, J.M., Ineson, J., Suhaimi, N., Takasato, M., Rae, F., and Little, M.H. (2013). Direct transcriptional reprogramming of adult cells to embryonic nephron progenitors. Journal of the American Society of Nephrology : JASN *24*, 1424-1434.

Hohenstein, P., and Hastie, N.D. (2006). The many facets of the Wilms' tumour gene, WT1. Human molecular genetics *15 Spec No 2*, R196-201.

Hu, Q., Gao, F., Tian, W., Ruteshouse, E.C., Wang, Y., Lazar, A., Stewart, J., Strong, L.C., Behringer, R.R., and Huff, V. (2010). Wt1 ablation and Igf2 up-regulation in mice results in Wilms Tumors with activated pERK1/2. The Journal of Clinical Investigation, in press.

Huff, V. (2007). Wilms tumor genetics: a new, UnX-pected twist to the story. Cancer cell *11*, 105-107.

Hum, S., Rymer, C., Schaefer, C., Bushnell, D., and Sims-Lucas, S. (2014). Ablation of the renal stroma defines its critical role in nephron progenitor and vasculature patterning. PloS one *9*, e88400.

Humphreys, B.D., Lin, S.L., Kobayashi, A., Hudson, T.E., Nowlin, B.T., Bonventre, J.V., Valerius, M.T., McMahon, A.P., and Duffield, J.S. (2010). Fate tracing reveals the pericyte and not epithelial origin of myofibroblasts in kidney fibrosis. The American journal of pathology *176*, 85-97.

Karner, C.M., Das, A., Ma, Z., Self, M., Chen, C., Lum, L., Oliver, G., and Carroll, T.J. (2011). Canonical Wnt9b signaling balances progenitor cell expansion and differentiation during kidney development. Development *138*, 1247-1257.

Kobayashi, A., Mugford, J.W., Krautzberger, A.M., Naiman, N., Liao, J., and McMahon, A.P. (2014). Identification of a Multipotent Self-Renewing Stromal Progenitor Population during Mammalian Kidney Organogenesis. Stem cell reports *3*, 650-662.

Kobayashi, A., Valerius, M.T., Mugford, J.W., Carroll, T.J., Self, M., Oliver, G., and McMahon, A.P. (2008). Six2 defines and regulates a multipotent self-renewing nephron

progenitor population throughout mammalian kidney development. Cell Stem Cell *3*, 169-181.

Komiya, Y., and Habas, R. (2008). Wnt signal transduction pathways. Organogenesis *4*, 68-75.

Kreidberg, J.A., Sariola, H., Loring, J.M., Maeda, M., Pelletier, J., Housman, D., and Jaenisch, R. (1993). WT-1 is required for early kidney development. Cell *74*, 679-691.

Kuure, S., Popsueva, A., Jakobson, M., Sainio, K., and Sariola, H. (2007). Glycogen synthase kinase-3 inactivation and stabilization of beta-catenin induce nephron differentiation in isolated mouse and rat kidney mesenchymes. Journal of the American Society of Nephrology *18*, 1130-1139.

Lee, S.B., Huang, K., Palmer, R., Truong, V.B., Herzlinger, D., Kolquist, K.A., Wong, J., Paulding, C., Yoon, S.K., Gerald, W., Oliner, J.D., and Haber, D.A. (1999). The Wilms tumor suppressor WT1 encodes a transcriptional activator of amphiregulin. Cell *98*, 663-673.

Leighton, P.A., Ingram, R.S., Eggenschwiler, J., Efstratiadis, A., and Tilghman, S.M. (1995). Disruption of imprinting caused by deletion of the H19 gene region in mice. Nature *375*, 34-39.

Li, C.M., Guo, M., Borczuk, A., Powell, C.A., Wei, M., Thaker, H.M., Friedman, R., Klein, U., and Tycko, B. (2002). Gene expression in Wilms' tumor mimics the earliest committed stage in the metanephric mesenchymal-epithelial transition. The American journal of pathology *160*, 2181-2190.

Li, C.M., Kim, C.E., Margolin, A.A., Guo, M., Zhu, J., Mason, J.M., Hensle, T.W., Murty, V.V., Grundy, P.E., Fearon, E.R., D'Agati, V., Licht, J.D., and Tycko, B. (2004). CTNNB1 mutations and overexpression of Wnt/beta-catenin target genes in WT1-mutant Wilms' tumors. The American journal of pathology *165*, 1943-1953.

Little, M.H., and McMahon, A.P. (2012). Mammalian kidney development: principles, progress, and projections. Cold Spring Harbor perspectives in biology *4*.

Loeb, D.M., Korz, D., Katsnelson, M., Burwell, E.A., Friedman, A.D., and Sukumar, S. (2002). Cyclin E is a target of WT1 transcriptional repression. The Journal of biological chemistry *277*, 19627-19632.

MacDonald, B.T., Tamai, K., and He, X. (2009). Wnt/beta-catenin signaling: components, mechanisms, and diseases. Developmental cell *17*, 9-26.

Maiti, S., Alam, R., Amos, C.I., and Huff, V. (2000). Frequent association of beta-catenin and WT1 mutations in Wilms tumors. Cancer research *60*, 6288-6292.

Major, M.B., Camp, N.D., Berndt, J.D., Yi, X., Goldenberg, S.J., Hubbert, C., Biechele, T.L., Gingras, A.C., Zheng, N., Maccoss, M.J., Angers, S., and Moon, R.T. (2007). Wilms tumor suppressor WTX negatively regulates WNT/beta-catenin signaling. Science *316*, 1043-1046.

Maschietto, M., de Camargo, B., Brentani, H., Grundy, P., Sredni, S.T., Torres, C., Mota, L.D., Cunha, I.W., Patrao, D.F., Costa, C.M., Soares, F.A., Brentani, R.R., and Carraro, D.M. (2008). Molecular profiling of isolated histological components of wilms tumor implicates a common role for the Wnt signaling pathway in kidney and tumor development. Oncology *75*, 81-91.

mdanderson.org RPPA Core Facility - Functional Proteomics.

Miyoshi, Y., Ando, A., Egawa, C., Taguchi, T., Tamaki, Y., Tamaki, H., Sugiyama, H., and Noguchi, S. (2002). High expression of Wilms' tumor suppressor gene predicts poor prognosis in breast cancer patients. Clinical cancer research : an official journal of the American Association for Cancer Research *8*, 1167-1171.

Moisan, A., Rivera, M.N., Lotinun, S., Akhavanfard, S., Coffman, E.J., Cook, E.B., Stoykova, S., Mukherjee, S., Schoonmaker, J.A., Burger, A., Kim, W.J., Kronenberg, H.M., Baron, R., Haber, D.A., and Bardeesy, N. (2011). The WTX tumor suppressor regulates mesenchymal progenitor cell fate specification. Developmental cell *20*, 583-596.

Mokkapati, S., Niopek, K., Huang, L., Cunniff, K.J., Ruteshouser, E.C., deCaestecker, M., Finegold, M.J., and Huff, V. (2014). beta-catenin activation in a novel liver progenitor cell

type is sufficient to cause hepatocellular carcinoma and hepatoblastoma. Cancer research *74*, 4515-4525.

Mori, K., Yang, J., and Barasch, J. (2003). Ureteric bud controls multiple steps in the conversion of mesenchyme to epithelia. Seminars in cell & developmental biology *14*, 209-216.

Mrowka, C., and Schedl, A. (2000). Wilms' tumor suppressor gene WT1: from structure to renal pathophysiologic features. Journal of the American Society of Nephrology : JASN *11 Suppl 16*, S106-115.

Mugford, J.W., Sipila, P., Kobayashi, A., Behringer, R.R., and McMahon, A.P. (2008a). Hoxd11 specifies a program of metanephric kidney development within the intermediate mesoderm of the mouse embryo. Developmental biology *319*, 396-405.

Mugford, J.W., Sipila, P., McMahon, J.A., and McMahon, A.P. (2008b). Osr1 expression demarcates a multi-potent population of intermediate mesoderm that undergoes progressive restriction to an Osr1-dependent nephron progenitor compartment within the mammalian kidney. Developmental biology *324*, 88-98.

Mugford, J.W., Yu, J., Kobayashi, A., and McMahon, A.P. (2009). High-resolution gene expression analysis of the developing mouse kidney defines novel cellular compartments within the nephron progenitor population. Developmental biology *333*, 312-323.

Murphy, A.J., Pierce, J., de Caestecker, C., Taylor, C., Anderson, J.R., Perantoni, A.O., de Caestecker, M.P., and Lovvorn, H.N., 3rd (2012). SIX2 and CITED1, markers of nephronic progenitor self-renewal, remain active in primitive elements of Wilms' tumor. Journal of pediatric surgery *47*, 1239-1249.

NLM, N.a. (2015). Wilms Tumor and Other Childhood Kidney Tumors Treatment (PDQ®).

Ogawa, O., Becroft, D.M., Morison, I.M., Eccles, M.R., Skeen, J.E., Mauger, D.C., and Reeve, A.E. (1993). Constitutional relaxation of insulin-like growth factor II gene imprinting associated with Wilms' tumour and gigantism. Nature genetics *5*, 408-412.

Park, J.S., Ma, W., O'Brien, L.L., Chung, E., Guo, J.J., Cheng, J.G., Valerius, M.T., McMahon, J.A., Wong, W.H., and McMahon, A.P. (2012). Six2 and Wnt regulate self-renewal and commitment of nephron progenitors through shared gene regulatory networks. Developmental cell *23*, 637-651.

Park, J.S., Valerius, M.T., and McMahon, A.P. (2007). Wnt/beta-catenin signaling regulates nephron induction during mouse kidney development. Development *134*, 2533-2539.

Patel, S.R., and Dressler, G.R. (2013). The genetics and epigenetics of kidney development. Seminars in nephrology *33*, 314-326.

Pierce, J., Murphy, A.J., Panzer, A., de Caestecker, C., Ayers, G.D., Neblett, D., Saito-Diaz, K., de Caestecker, M., and Lovvorn, H.N., 3rd (2014). SIX2 Effects on Wilms Tumor Biology. Translational oncology *7*, 800-811.

Reidy, K.J., and Rosenblum, N.D. (2009). Cell and molecular biology of kidney development. Seminars in nephrology *29*, 321-337.

Rosenfeld, C., Cheever, M.A., and Gaiger, A. (2003). WT1 in acute leukemia, chronic myelogenous leukemia and myelodysplastic syndrome: therapeutic potential of WT1 targeted therapies. Leukemia *17*, 1301-1312.

Ruteshouser, E.C., Robinson, S.M., and Huff, V. (2008). Wilms tumor genetics: mutations in WT1, WTX, and CTNNB1 account for only about one-third of tumors. Genes, chromosomes & cancer *47*, 461-470.

Ryan, G., Steele-Perkins, V., Morris, J.F., Rauscher, F.J., 3rd, and Dressler, G.R. (1995). Repression of Pax-2 by WT1 during normal kidney development. Development *121*, 867-875.

Sajithlal, G., Zou, D., Silvius, D., and Xu, P.X. (2005). Eya 1 acts as a critical regulator for specifying the metanephric mesenchyme. Developmental biology *284*, 323-336.

Schmidt-Ott, K.M., and Barasch, J. (2008). WNT/beta-catenin signaling in nephron progenitors and their epithelial progeny. Kidney International *74*, 1004-1008.

Schuchardt, A., D'Agati, V., Larsson-Blomberg, L., Costantini, F., and Pachnis, V. (1994). Defects in the kidney and enteric nervous system of mice lacking the tyrosine kinase receptor Ret. Nature *367*, 380-383.

Schuller, U., Heine, V.M., Mao, J., Kho, A.T., Dillon, A.K., Han, Y.G., Huillard, E., Sun, T., Ligon, A.H., Qian, Y., Ma, Q., Alvarez-Buylla, A., McMahon, A.P., Rowitch, D.H., and Ligon, K.L. (2008). Acquisition of granule neuron precursor identity is a critical determinant of progenitor cell competence to form Shh-induced medulloblastoma. Cancer cell *14*, 123-134.

Self, M., Lagutin, O.V., Bowling, B., Hendrix, J., Cai, Y., Dressler, G.R., and Oliver, G. (2006). Six2 is required for suppression of nephrogenesis and progenitor renewal in the developing kidney. The EMBO journal *25*, 5214-5228.

Senanayake, U., Koller, K., Pichler, M., Leuschner, I., Strohmaier, H., Hadler, U., Das, S., Hoefler, G., and Guertl, B. (2013). The pluripotent renal stem cell regulator SIX2 is activated in renal neoplasms and influences cellular proliferation and migration. Human pathology *44*, 336-345.

Shimazui, T., Oosterwijk-Wakka, J., Akaza, H., Bringuier, P.P., Ruijter, E., Debruyne, F.M., Schalken, J.A., and Oosterwijk, E. (2000). Alterations in expression of cadherin-6 and E-cadherin during kidney development and in renal cell carcinoma. European urology *38*, 331-338.

Sim, E.U., Smith, A., Szilagi, E., Rae, F., Ioannou, P., Lindsay, M.H., and Little, M.H. (2002). Wnt-4 regulation by the Wilms' tumour suppressor gene, WT1. Oncogene *21*, 2948-2960.

Sims-Lucas, S., Schaefer, C., Bushnell, D., Ho, J., Logar, A., Prochownik, E., Gittes, G., and Bates, C.M. (2013). Endothelial Progenitors Exist within the Kidney and Lung Mesenchyme. PloS one *8*, e65993.

Smith, M.A., Altekruse, S.F., Adamson, P.C., Reaman, G.H., and Seibel, N.L. (2014). Declining childhood and adolescent cancer mortality. Cancer *120*, 2497-2506.

Spandidos, A., Wang, X., Wang, H., and Seed, B. (2010). PrimerBank: a resource of human and mouse PCR primer pairs for gene expression detection and quantification. Nucleic acids research *38*, D792-799.

Steenman, M.J., Rainier, S., Dobry, C.J., Grundy, P., Horon, I.L., and Feinberg, A.P. (1994). Loss of imprinting of IGF2 is linked to reduced expression and abnormal methylation of H19 in Wilms' tumour. Nature genetics *7*, 433-439.

Swartling, F.J., Savov, V., Persson, A.I., Chen, J., Hackett, C.S., Northcott, P.A., Grimmer, M.R., Lau, J., Chesler, L., Perry, A., Phillips, J.J., Taylor, M.D., and Weiss, W.A. (2012). Distinct neural stem cell populations give rise to disparate brain tumors in response to N-MYC. Cancer cell *21*, 601-613.

Tang, M.J., Cai, Y., Tsai, S.J., Wang, Y.K., and Dressler, G.R. (2002). Ureteric bud outgrowth in response to RET activation is mediated by phosphatidylinositol 3-kinase. Developmental biology *243*, 128-136.

Tang, M.J., Worley, D., Sanicola, M., and Dressler, G.R. (1998). The RET-glial cell-derived neurotrophic factor (GDNF) pathway stimulates migration and chemoattraction of epithelial cells. The Journal of cell biology *142*, 1337-1345.

Torban, E., Dziarmaga, A., Iglesias, D., Chu, L.L., Vassilieva, T., Little, M., Eccles, M., Discenza, M., Pelletier, J., and Goodyer, P. (2006). PAX2 activates WNT4 expression during mammalian kidney development. The Journal of biological chemistry *281*, 12705-12712.

Torres, M., Gomez-Pardo, E., Dressler, G.R., and Gruss, P. (1995). Pax-2 controls multiple steps of urogenital development. Development *121*, 4057-4065.

Torrezan, G.T., Ferreira, E.N., Nakahata, A.M., Barros, B.D., Castro, M.T., Correa, B.R., Krepischi, A.C., Olivieri, E.H., Cunha, I.W., Tabori, U., Grundy, P.E., Costa, C.M., de Camargo, B., Galante, P.A., and Carraro, D.M. (2014). Recurrent somatic mutation in DROSHA induces microRNA profile changes in Wilms tumour. Nature communications *5*, 4039.

Urbach, A., Yermalovich, A., Zhang, J., Spina, C.S., Zhu, H., Perez-Atayde, A.R., Shukrun, R., Charlton, J., Sebire, N., Mifsud, W., Dekel, B., Pritchard-Jones, K., and Daley, G.Q. (2014). Lin28 sustains early renal progenitors and induces Wilms tumor. Genes & development *28*, 971-982.

Voronkov, A., and Krauss, S. (2013). Wnt/beta-catenin signaling and small molecule inhibitors. Current pharmaceutical design *19*, 634-664.

Wang, Q., Lan, Y., Cho, E.S., Maltby, K.M., and Jiang, R. (2005). Odd-skipped related 1 (Odd 1) is an essential regulator of heart and urogenital development. Developmental biology *288*, 582-594.

Wellik, D.M., Hawkes, P.J., and Capecchi, M.R. (2002). Hox11 paralogous genes are essential for metanephric kidney induction. Genes & development *16*, 1423-1432.

Wu, M.K., Sabbaghian, N., Xu, B., Addidou-Kalucki, S., Bernard, C., Zou, D., Reeve, A.E., Eccles, M.R., Cole, C., Choong, C.S., Charles, A., Tan, T.Y., Iglesias, D.M., Goodyer, P.R., and Foulkes, W.D. (2013). Biallelic DICER1 mutations occur in Wilms tumours. The Journal of pathology *230*, 154-164.

Xu, J., Liu, H., Park, J.S., Lan, Y., and Jiang, R. (2014a). Osr1 acts downstream of and interacts synergistically with Six2 to maintain nephron progenitor cells during kidney organogenesis. Development *141*, 1442-1452.

Xu, J., Wong, E.Y., Cheng, C., Li, J., Sharkar, M.T., Xu, C.Y., Chen, B., Sun, J., Jing, D., and Xu, P.X. (2014b). Eya1 Interacts with Six2 and Myc to Regulate Expansion of the Nephron Progenitor Pool during Nephrogenesis. Developmental cell *31*, 434-447.

Xu, P.X., Adams, J., Peters, H., Brown, M.C., Heaney, S., and Maas, R. (1999). Eya1-deficient mice lack ears and kidneys and show abnormal apoptosis of organ primordia. Nature genetics *23*, 113-117.

Yang, Z.J., Ellis, T., Markant, S.L., Read, T.A., Kessler, J.D., Bourboulas, M., Schuller, U., Machold, R., Fishell, G., Rowitch, D.H., Wainwright, B.J., and Wechsler-Reya, R.J. (2008).

Medulloblastoma can be initiated by deletion of Patched in lineage-restricted progenitors or stem cells. Cancer cell *14*, 135-145.

Yu, J., Carroll, T.J., Rajagopal, J., Kobayashi, A., Ren, Q., and McMahon, A.P. (2009). A Wnt7b-dependent pathway regulates the orientation of epithelial cell division and establishes the cortico-medullary axis of the mammalian kidney. Development *136*, 161-171.

Zhang, H., Palmer, R., Gao, X., Kreidberg, J., Gerald, W., Hsiao, L., Jensen, R.V., Gullans, S.R., and Haber, D.A. (2003). Transcriptional activation of placental growth factor by the forkhead/winged helix transcription factor FoxD1. Current biology : CB *13*, 1625-1629.

Zhuang, Z., Merino, M.J., Vortmeyer, A.O., Bryant, B., Lash, A.E., Wang, C., Deavers, M.T., Shelton, W.F., Kapur, S., and Chandra, R.S. (1997). Identical genetic changes in different histologic components of Wilms' tumors. Journal of the National Cancer Institute *89*, 1148-1152.

Zirn, B., Samans, B., Wittmann, S., Pietsch, T., Leuschner, I., Graf, N., and Gessler, M. (2006). Target genes of the WNT/beta-catenin pathway in Wilms tumors. Genes, chromosomes & cancer *45*, 565-574.

Vita

Le Huang was born in Changsha, Hunan, China, on October 26, 1983, the daughter of Xizhen Jiang and Yongming Huang. After graduating from Changsha No.6 High School, (Changsha, Hunan, China) in 2001, she entered Hunan Normal University in Changsha, Hunan where she received her Bachelor of Science with a major in Biotechnology in June 2005. In August 2005, she attended Technical University of Denmark, and in May 2008, she earned a Master of Science in Biotechnology. In August of 2008, she entered the Ph.D. graduate program at the The University of Texas Graduate School of Biomedical Sciences at Houston. In 2009, she joined the lab of Dr. Vicki Huff at the Department of Genetics at the University of Texas MD Anderson Cancer Center.

Permanent address:

208, Building 2, District M, Postal Residence, Guhancheng

Changsha, Hunan, China 410016